Modelling of Tropospheric Ozone

Annual Report 2010

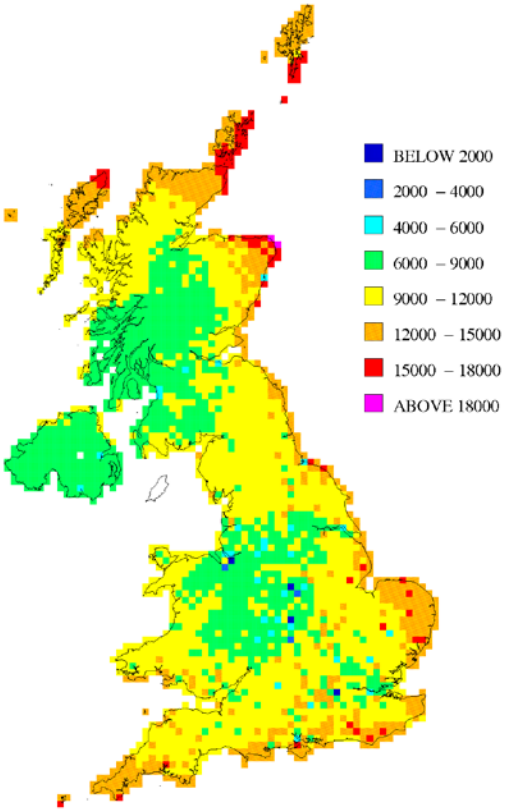

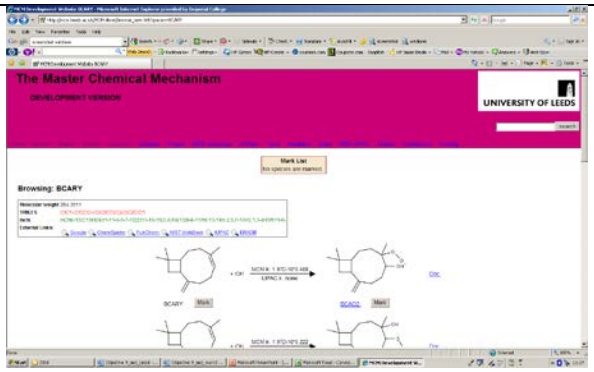

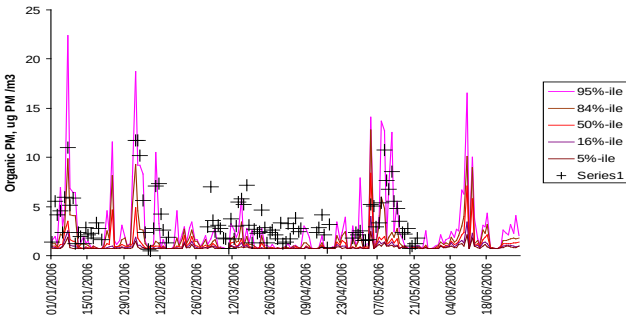

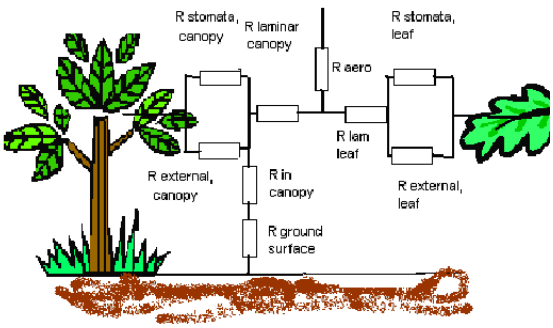

Report for Defra

Unrestricted
ED47546
Issue Number 1
AEAT/ENV/R/3134
Date 11/02/2011

Customer:

The Department for Environment, Food and Rural Affairs, Welsh Assembly Government, the Scottish Executive and the Department of the Environment for Northern Ireland

Customer reference:

AQ0704

Confidentiality, copyright & reproduction:

AEA reference:

ED47546- Issue Number 1

Contact:

Tim Murrells
AEA Technology plc
Gemini Building, Harwell International Business Centre, Didcot, OX11 0QR
t: 0870 190 6539
f: 0870 190 6318
e: tim.p.murrells@aeat.co.uk
AEA is a business name of AEA Technology plc
AEA is certificated to ISO9001 and ISO14001

Author:

Tim Murrells
Sally Cooke
John Abbott
Andrea Fraser
Prof Dick Derwent (rdscientific)
Mike Jenkin (Atmospheric Chemistry Services)
Andrew Rickard (University of Leeds)
Jenny Young (University of Leeds)

Approved By:

Geoff Dollard

Date:

11 February 2011

Signed:

Executive summary

The concentrations of ground-level ozone, a pollutant that affects human health, ecosystems and materials, widely exceed environmental quality standards across the UK and Europe. Ozone is not emitted directly into the atmosphere, but is a secondary photochemical pollutant formed in the lower atmosphere from the sunlight-initiated oxidation of volatile organic compounds (VOCs) in the presence of nitrogen oxides (NO_x). Elevated concentrations of ozone over the UK are especially generated when slow-moving or stagnant high pressure (anticyclonic) weather systems occurring in the spring or summer bring in photochemically reacting air masses from mainland Europe.

The non-linear nature of ground-level ozone production requires the use of sophisticated chemical transport models to understand the factors affecting its production and subsequent control on a wide spatial scale.

This report describes the work undertaken during 2010 in the second phase of the project "*Modelling of Tropospheric Ozone*" funded by the Department for Environment, Food and Rural Affairs (Defra) and the Devolved Administrations (the Scottish Executive, the Welsh Assembly Government and the Department of the Environment for Northern Ireland). The project is due for completion in December 2011.

The overall purpose of the project is to maintain, develop, and apply tools for modelling tropospheric ozone formation and distribution over a range of spatial scales (global, regional and national). The modelling is used to support and guide Defra's policy on emission reductions and objectives for pollutants that influence ozone and to verify compliance with UK policy and with European directives on ground-level ozone. The project scope has been extended to include secondary organic aerosols (SOA), another secondary air pollutant formed in the atmosphere from emitted VOCs requiring similar modelling approaches to predict their concentrations.

The work programme consists of four main objectives to meet the overall aims of the project. The report describes the work programme and presents a summary and conclusions for each objective. These are fully amalgamated in the report's Conclusions chapter 8. A brief synopsis of the summary and conclusions is as follows.

Improvement to Photochemical Reaction Schemes

- **A new chemical reaction scheme has been developed and successfully tested describing the atmospheric degradation of a highly reactive volatile organic compound (VOC) from natural biogenic sources, β–caryophyllene. The new mechanism expands the coverage and extends the reactivity range of biogenic VOCs in models.**
- **The reactivity and mechanisms involved in degrading halogenated VOCs emitted from solvent use has been assessed. This has shown how reactivity decreases with increasing halogen substitution at certain parts of the VOC**
- **A hypothesis has been developed to explain the poorly understood mechanisms for atmospheric degradation of VOCs under conditions of low NO_x leading to OH radical recycling.**

Modelling the UK Ozone Climate in 2008

- **The Ozone Source Receptor Model (OSRM) was used to model the UK's ozone climate in 2008 at 10x10km resolution. Compared with results from monitoring data, the model tended to underestimate some ozone concentration metrics, but overestimated others.**

Modelling Support for Policy Development and Implementation

- **The OSRM was used to forecasts the UK's ground-level ozone climate in 2020 based on current projections of ozone precursor emissions. Ozone concentrations are predicted to be higher in 2020 than in 2007. The results will be used as the benchmark for further analysis of future 2020 emission scenarios.**
- **The Photochemical Trajectory Model (PTM) was used for a probabilistic uncertainty analysis of modelled ozone episodes and of the model's response to reductions in precursor emissions. For conditions leading to peak ozone concentrations observed in the West Midlands in 1999, the assessment showed that there was less than 10% probability that 30% reductions in NO_x or VOC emissions would bring predicted peak ozone concentrations to below 120 µg m^{-3}.**

Specific Modelling and Assessments for Policy Development on SOA

- **The PTM has also been used to model SOA and the results compared with observations at a site in Birmingham during 2006. The model was able to account for organic carbon episodes observed at this site, but overall tended to underpredict concentrations.**
- **The contribution of natural biogenic and anthropogenic emission sources to SOA was evaluated and the spatial distribution and seasonal cycle in SOA concentrations in the UK assessed. The results showed that the contributions of natural and anthropogenic sources were comparable at many locations, but biogenic sources tended to dominate, especially at sites in Scotland. Seasonal cycles in SOA were found to be highly variable at different sites, but the contribution from biogenic sources shows a strong maximum in May. Model runs predict a decline in anthropogenic contributions to SOA between 2008 and 2020, whereas SOA from biogenic sources is predicted to increase illustrating how SOA components respond differently to NO_x and VOC emission controls.**

Assessments of Background and Urban-Scale Oxidant

- **A method based on the analysis of ambient data on O_3, NO_2 and NO_x has been developed to characterise the geographical variation in annual mean background oxidant ($O_3 + NO_2$) concentrations over the UK at 1x1km resolution. Optimised maps of annual mean background oxidant concentrations were developed for each year between 2001 and 2009.**
- **The background oxidant maps and parameterisations developed in this work are being used to inform and improve NO_2 and O_3 empirical modelling activities in Defra's UK Ambient Air Quality Assessments programme (UKAAQA) for air quality directive reporting and further Defra policy analysis.**

Development of the Surface Ozone Flux Model

- **New stomatal flux algorithms developed by Stockholm Environment Institute, University of York, have been implemented into the Surface Ozone Flux Model to improve the estimation of ozone fluxes to different ecosystem types and the damage to crop yield. The model was used in conjunction with the OSRM to**

model accumulated stomatal flux conditions in the UK during 2006.

- **The model predicted that growth of wheat across the whole of the UK was affected by ozone deposition in 2006. Ozone deposition was associated with at least a 5% loss in yield across the whole of the UK, but losses were variable in different parts of the country.**
- **The results from this study will be combined with those from other studies and the results and conclusions will be presented in a publication for external peer review.**

Table of contents

1 Introduction

The concentrations of ground-level ozone, a pollutant that affects human health, ecosystems and materials, widely exceed environmental quality standards across the UK and Europe. Ozone is not emitted directly into the atmosphere, but is a secondary photochemical pollutant formed in the lower atmosphere from the sunlight-initiated oxidation of volatile organic compounds (VOCs) in the presence of nitrogen oxides (NO_x). Elevated concentrations of ozone over the UK are especially generated when slow-moving or stagnant high pressure (anticyclonic) weather systems occurring in the spring or summer bring in photochemically reacting air masses from mainland Europe.

Under conditions characteristic of photochemical pollution episodes, the formation and transport of ozone and other secondary air pollutants can occur over hundreds of kilometres, with concentrations at a given location influenced by the history of the airmass over a period of up to several days. In addition to this, the increasing levels of ozone in the free troposphere on a global scale also influences regional scale photochemical processes by providing an increasing background ozone level upon which the regional and national scale formation is superimposed. This effect has to be considered when assessing whether proposed air quality standards for ozone are likely to be achieved.

The non-linear nature of ground-level ozone production requires the use of sophisticated chemical transport models to understand the factors affecting its production and subsequent control on a wide spatial scale. The Department for Environment, Food and Rural Affairs (Defra) and the Devolved Administrations (DAs, the Welsh Assembly Government, the Scottish Executive and the Department of the Environment for Northern Ireland) have funded the development of ozone modelling tools over the years and the application of the scientific understanding that underpins the models. Defra and the DAs have a need to further develop, maintain and refine the models as further evidence emerges on factors influencing ozone levels on different spatial sales and timescales. They also have a need to apply the models in order to establish the effectiveness of policies changing precursor emissions in the UK and the rest of Europe and how these will affect ozone concentrations in the future in the context of current and future air quality target values and objectives for ozone.

The current "*Modelling of Tropospheric Ozone*" contract started in January 2007 and runs until December 2011. The overall aims of the project are to maintain, develop, and apply tools for modelling tropospheric ozone and other secondary air pollutant formation and distribution over a range of spatial scales (global, regional and national). The first phase of the project completed in August 2009 met a number of key objectives and was summarised in the report by Murrells et al (2009a). The objectives involved:

- the maintenance and application of the Ozone Source Receptor Model (OSRM) and Photochemical Trajectory Model (PTM) to support Defra's ozone policy.
- a programme of improvements to the Master Chemical Mechanism (MCM), a near-explicit and comprehensive photochemical reaction scheme describing the atmospheric processes forming ozone in the troposphere from emitted VOCs and NO_x, following a comprehensive review of the MCM
- detailed assessments of ambient data to understand the local-scale coupling between NO_x and ozone in urban environments in order to improve the prediction of ozone and NO_2 in other national and local scale models used for Defra policy
- an initial screening and assessment of more complex Eulerian chemical transport models and the development of a protocol to enable a consistent, robust and transparent approach in comparing the performances of different air quality models used for Defra policy.

- The development of a methodology for assessing the wider costs, benefits and trade-offs of solvent reduction and substitution policies

As well as ozone, the model development work addressed the formation of secondary organic aerosols (SOA) for the first time, since these are also formed in the atmosphere from emitted VOCs and require similar modelling approaches to predict their concentrations and contributions to fine airborne particulate matter, PM_{10} and $PM_{2.5}$.

The current, second phase of the project started in September 2009 and builds on the achievements of the first phase through a programme of work consisting of four main objectives to meet the overall aims of the project. Continuing from the objectives of Phase 1, the current objectives are:

Objective 9: Improvement to Photochemical Reaction Schemes for Treatment of Biogenic Emissions and Emissions of Chlorinated VOCs from Solvents

Objective 10: Application of Ozone and Secondary PM Chemical Transport Models for Defra Policy

Objective 11: Assessments of Background and Urban-Scale Oxidant

Objective 12: Update of Ozone Flux Model in the OSRM

These objectives are described in more detail in Section 2. The remainder of this report then describes the work undertaken in Phase II of the project over the period up to December 2010.

2 Overview of Project Aims and Structure

The work of Phase II is divided into four main Objectives that involve the further research and development relating to the underlying chemistry behind formation of tropospheric ozone and secondary organic aerosol and factors controlling them, understanding trends in observations of ground-level ozone and other secondary air pollutants, the application of current modelling tools to support Defra ozone air quality policy and further development of components of models to address the uptake of ozone by vegetation.

Objective 9: Improvement to Photochemical Reaction Schemes for Treatment of Biogenic Emissions and Emissions of Chlorinated VOCs from Solvents

This objective involves the further improvements to photochemical reactions schemes used in models. The aim is to:

- Develop new and revised schemes for the Master Chemical Mechanism covering emissions of VOCs from natural sources (biogenic emissions) and from use of chlorinated solvents;
- Develop new reduced chemical schemes for chlorinated solvent emissions
- Revise reduced codes for Secondary Organic Aerosol formation suitable for implementation in the OSRM
- Evaluate revised MCM schemes using the Photochemical Trajectory Model (PTM)
- Maintain the MCM website

Objective 10: Application of Ozone and Secondary PM Chemical Transport Models for Defra Policy

This objective involves the application of current models in support of Defra policy on ozone and secondary PM, including:

- the modelling of UK ozone in 2008, 2009 and 2010 using the OSRM
- the use of the OSRM or PTM for modelling specific emission scenarios on an ad-hoc basis to support Defra's development and implementation of policies on ozone and secondary particulate matter (PM)
- specific modelling with the PTM to assess policy development on secondary air pollutants, by examining the spatial distribution of secondary organic aerosols across the UK and the sensitivity to meteorology, emissions and input parameters relating to climate change.

Objective 11: Assessments of Background and Urban-Scale Oxidant

This objective involves assessment of background and urban-scale oxidant through analysis of ambient data for ozone, nitrogen dioxide (NO_2) and nitrogen oxides (NO_x) to further improve local effects in air quality models used for Defra policy.

Objective 12: Update of Ozone Flux Model in OSRM Using New Formulations from SEI's DO_3SE Ozone Deposition Model

This objective involves the implementation and evaluation with the OSRM of a new ozone flux model developed by the Stockholm Environment Institute, University of York.

There are strong linkages between the different objectives as shown in Figure 2.1.

Figure 2.1: Linkages among core programme

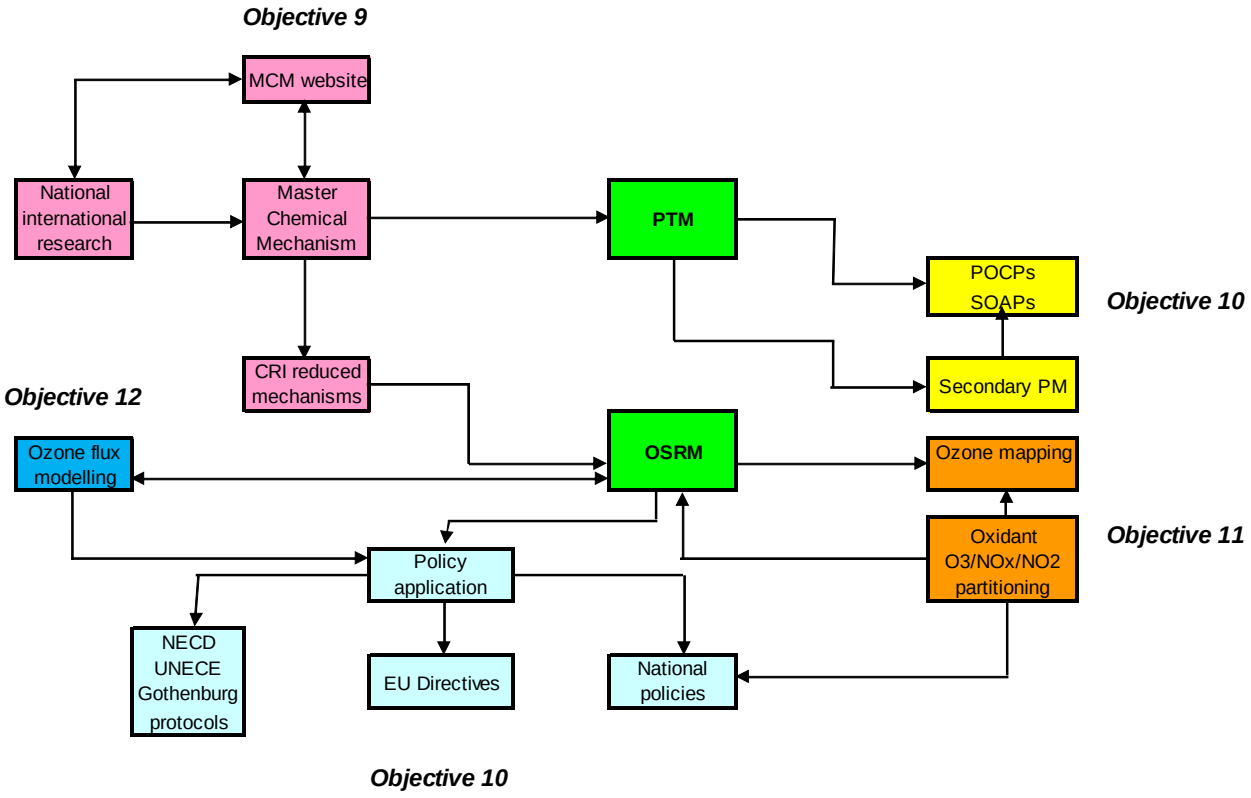

Thus the mechanism development work of Objective 9 feeds directly into the main ozone models used in this project, the OSRM and PTM, as well as other regional scale air pollution models used for Defra and EU policies. The PTM is involved in Objective 10 in evaluating models using new chemistry schemes and assessing the contribution of different sources to concentrations of ozone and secondary organic aerosols observed in the UK. The OSRM is involved in Objective 10 through describing the current and future ozone climate in the UK and modelling the impact of policies aimed at reducing precursor emissions in the UK and rest of Europe. The assessment of oxidant partitioning in Objective 11 helps to understand the spatial and temporal variability in hemispheric and regional components of background ozone and the effects of locally emitted NO_x which helps to improve the mapping of ozone concentrations and improve local effects in air quality models used for Defra policy. The work of Objective 12 improves the treatment of ozone deposition in models such as the OSRM and the quantification of ozone flux to different vegetation species which in turn will help improve assessments on the impacts of ozone on crop damage for evaluating policies on ecosystem effects.

The work programme is carried out by a consortium of groups led by **AEA**. The other consortium partners are **Professor Dick Derwent (rdscientific), Dr Mike Jenkin (Atmospheric Chemistry Services) and Dr Andrew Rickard (University of Leeds)**. Each of these partners undertakes specific tasks as shown in Table 2.1.

Table 2.1: Role of project partners

Project Member	Main activity
AEA	Project management. Modelling using the OSRM for policy support in Objective 10 and implementation of new ozone flux modelling methods in Objective 12.
rdscientific	Modelling using the PTM for policy support in Objective 10 and testing of new chemistry schemes in Objective 9
Atmospheric Chemistry Services	Development of chemistry schemes (Objective 9) and oxidant analysis (Objective 11)
University of Leeds	Development of chemistry schemes and maintenance of MCM website (Objective 9)

The project follows a schedule shown in Figure 2.2. There is some flexibility in some of the tasks to meet the policy needs of Defra, especially those relating to ad-hoc modelling and support in Objective 10. Progress is monitored through quarterly contract reports submitted to Defra and approximately 6-monthly project meetings involving all the project partners and Defra officials.

Figure 2.2: Project schedule

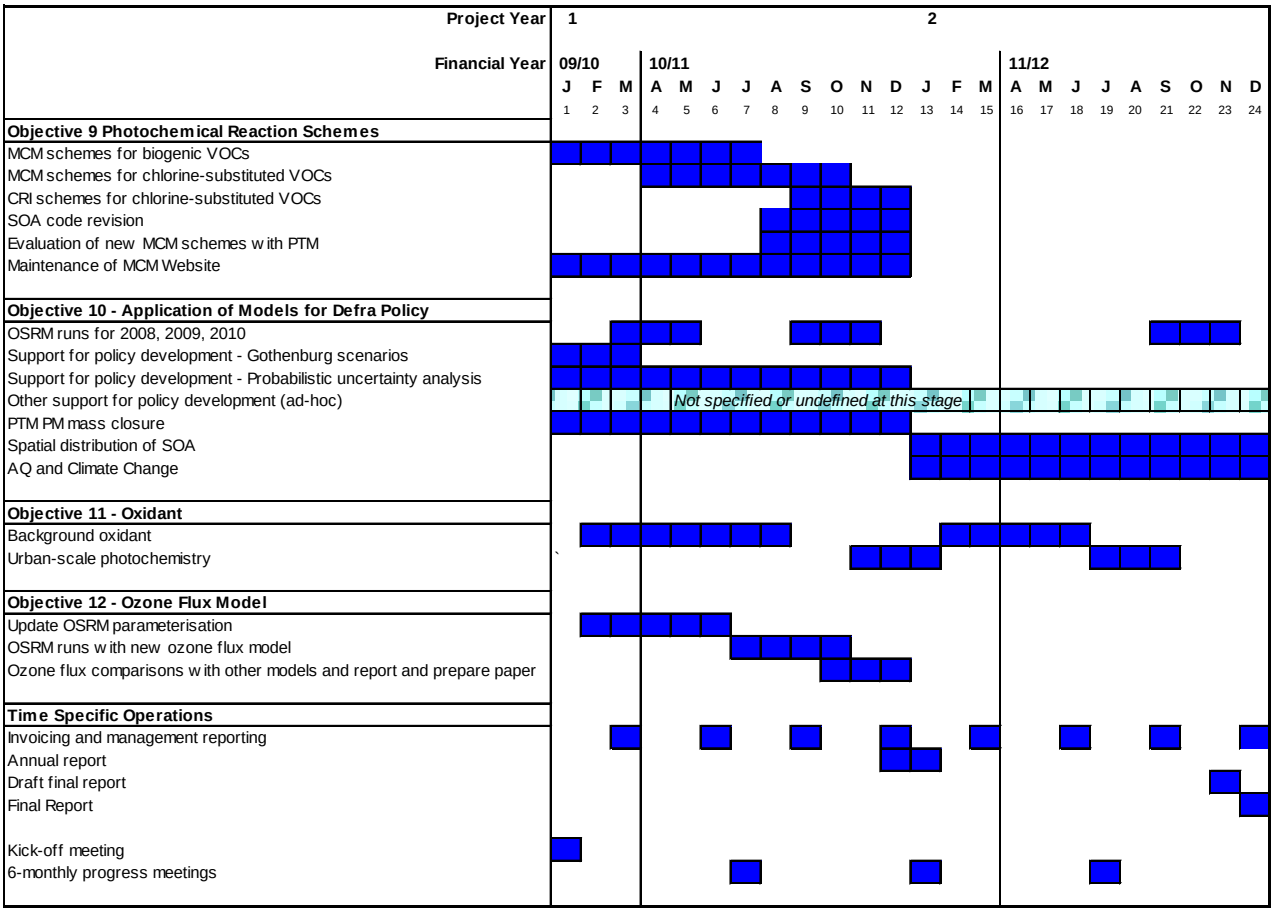

3 Improvements to Photochemical Reaction Schemes

3.1 Introduction

The **Master Chemical Mechanism (MCM)** is an internationally-recognised mechanism, describing the detailed processes involved in the formation of ozone from the degradation of a large number of emitted precursor VOCs. Because of its detail in describing the intermediate organic oxidation products formed, it is also increasingly being applied to describe and understand the formation of particulates in the form of secondary organic aerosol (SOA), through gas-to-aerosol transfer of the organic oxidation products. The mechanism is thus regularly used in the scientific community as a benchmark in mechanism intercomparison and validation exercises, and in the development of reduced mechanisms.

Although the MCM is itself too large for direct use in many policy applications, traceable mechanism reduction activities carried out previously in the contract have included the development of a hierarchy of common representative intermediates (CRI) mechanisms which, for the first time, have provided a clear route for the implementation of reduced mechanisms into policy models with a demonstrably traceable link to the MCM (Jenkin et al., 2008a; Watson et al., 2008; Utembe et al., 2009). This has established a platform and methodology for future advances in the scientific understanding of atmospheric chemistry to be transferred to policy models including the OSRM and PTM.

The work carried out in **Objective 9** during this phase of the project has focused on key development areas for the Master Chemical Mechanism (MCM), and for the traceable reduced mechanism, the Common Representative Intermediates (CRI) mechanism. This has included specific focuses on solvent and biogenic emissions. The work has also considered new advances in the understanding of chemistry under NO_x limited conditions which have only very recently been identified from field, laboratory and theoretical investigations and are currently not correctly described in any atmospheric chemistry mechanism. Given the trend in the UK ozone climatology towards NO_x limitation, correct representation and implementation of such processes in policy models is likely to become increasingly important for assessment of future scenarios.

In the sections that follow, the scheme development activities carried out over the past year of the contract are described. This work has contributed to the development of the latest update of the MCM (MCM v3.2). Associated developments to the database and website are also described. The work has included the first stages of implementation of SOA codes to the OSRM as well as scheme developments for biogenic VOCs and chlorinated VOCs used in solvents.

3.2 Development and evaluation of MCM schemes for complex biogenic VOCs

The range of reactivity and structure of emitted anthropogenic VOCs (AVOCs) is very well represented by the species degraded in the MCM. In contrast, there were only four complex biogenic VOCs (BVOC) treated at the outset of the current project (i.e., in MCM v3.1), with most applications to date emitting three of these (isoprene, α–pinene and β–pinene). In practice, the emitted speciation of BVOCs includes contributions from isoprene, monoterpenes (isomeric formula $C_{10}H_{16}$), sesquiterpenes (isomeric formula, $C_{15}H_{24}$) and oxygenated VOCs (e.g., Owen et al., 2001), with typically more than 20 significant contributors identified in a given study. Owing to wide variations in reactivity, these species are oxidised on a variety of temporal and associated spatial scales in the atmosphere (lifetimes range from minutes to days), and detection of the

more reactive BVOCs (some monoterpenes and sesquiterpenes) is therefore non-trivial. The chemical structure of these compounds also has implications for degradation pathways, which can differ dramatically between BVOC, with corresponding variability in their ability to generate ozone. As a result of EU controls on AVOC emissions over the last decade, BVOCs have an increasing relative impact on regional scale photochemistry in Europe, and have potential additional significance in relation to human-influenced activities such as biofuel production.

The general aim of this task is therefore to expand the MCM by inclusion of schemes for additional monoterpenes and sesquiterpenes relevant to the UK and Europe, with the additional aim of increasing the reactivity range of the species represented. An initial survey of information on the speciation of emissions within the European region (e.g., Owen et al., 2001; Boissard et al., 2001; Jönsson et al., 2007) identified limonene and β–caryophyllene as compounds for which schemes should be developed. As shown in Table 3.1, these compounds (along with α– and β–pinene which were already treated by in MCM v3.1) would ensure that representatives of four structural classes of terpene are treated in MCM v3.2, and which can therefore be used to represent a wider variety of species (examples are also shown in the table).

Table 3.1: Selected monoterpene and sesquiterpene categories and contributing species. Category representatives to be treated in MCM v3.2 are identified, with their lifetimes with respect to reaction with OH and ozone.

Category	Compounds (representative in bold)	OH reaction lifetime of representative[a,c]	O_3 reaction lifetime of representative[b,c]
Bicyclic monoterpene - endocyclic double bond	**α–pinene**, 2-carene, 3-carene	5.2 hours	4.3 hours
Bicyclic monoterpene - exocyclic double bond	**β–pinene**, camphene, sabinene	3.5 hours	1.0 days
Monocyclic diene monoterpene	**limonene**, terpinolene, β–phellandrene, γ–terpinene	1.6 hours	1.9 hours
Reactive sesquiterpene	**β–caryophyllene**, α–humulene	1.4 hours	1.9 minutes
a: [OH] = 10^6 molec. cm^{-3}; b: [O_3] = 7.5 x 10^{11} molec. cm^{-3} (ca. 30 ppb); c: Based on data from Calvert et al. (2000)			

Limonene is substantially more reactive than α– and β–pinene, such that the represented reactivity range of monoterpenes is also increased (it is noted that limonene is also emitted from anthropogenic sources, appearing in the National Atmospheric Emissions Inventory (NAEI) speciation under the pseudonym of “dipentene”). Development of the limonene scheme was reported in the previous contract phase (Murrells et al, 2009b), and a subsequent initial evaluation of the scheme using chamber data is presented below. β–caryophyllene is the first sesquiterpene to be represented and, as a C_{15} hydrocarbon, is also the largest VOC treated. As shown in Table 3.1, it is also by far the most reactive species (in terms of atmospheric lifetime). Development and evaluation of the β–caryophyllene scheme is summarised below.

3.2.1 Development of β–caryophyllene scheme

The construction of a detailed, MCM-compatible, gas phase mechanism for the sesquiterpene, β–caryophyllene, has been completed within the current contract phase during 2010. The mechanism includes degradation initiated by reaction with OH radicals, ozone and NO3 radicals, and contains 1148 reactions of 442 new species which degrade β–caryophyllene into species which are already present in MCM v3.1. The new species include β–caryophyllene itself, about 180 peroxy and oxy radical species and about 260 new structurally complex oxygenated product species, typically containing between two and five

oxygenated functional groups. These contain subset combinations of carbonyl, nitrate, peroxy nitrate, hydroxyl, hydroperoxy, carboxylic acid and peracid groups. The construction methodology was broadly based on the prevailing MCM protocol (Saunders et al., 2003), but took account of the results of a number of studies of β–caryophyllene ozonolysis (Calogirou et al., 1997; Jaoui et al., 2003; Kanawati et al., 2008; Winterhalter et al., 2009; Nguyen et al., 2009). This information has been incorporated into the MCM v3.2 database at the University of Leeds, such that the information is fully extractable and searchable (see Section 3.6). A complete extraction of the β–caryophyllene chemistry (i.e., representing degradation through to CO2 and H2O) contains 1563 reactions of 577 species. A screenshot of part of the first page of the mechanism is shown in Figure 3.1.

Figure 3.1: Screenshot of part of the first page of the new MCM v3.2 β–caryophyllene scheme.

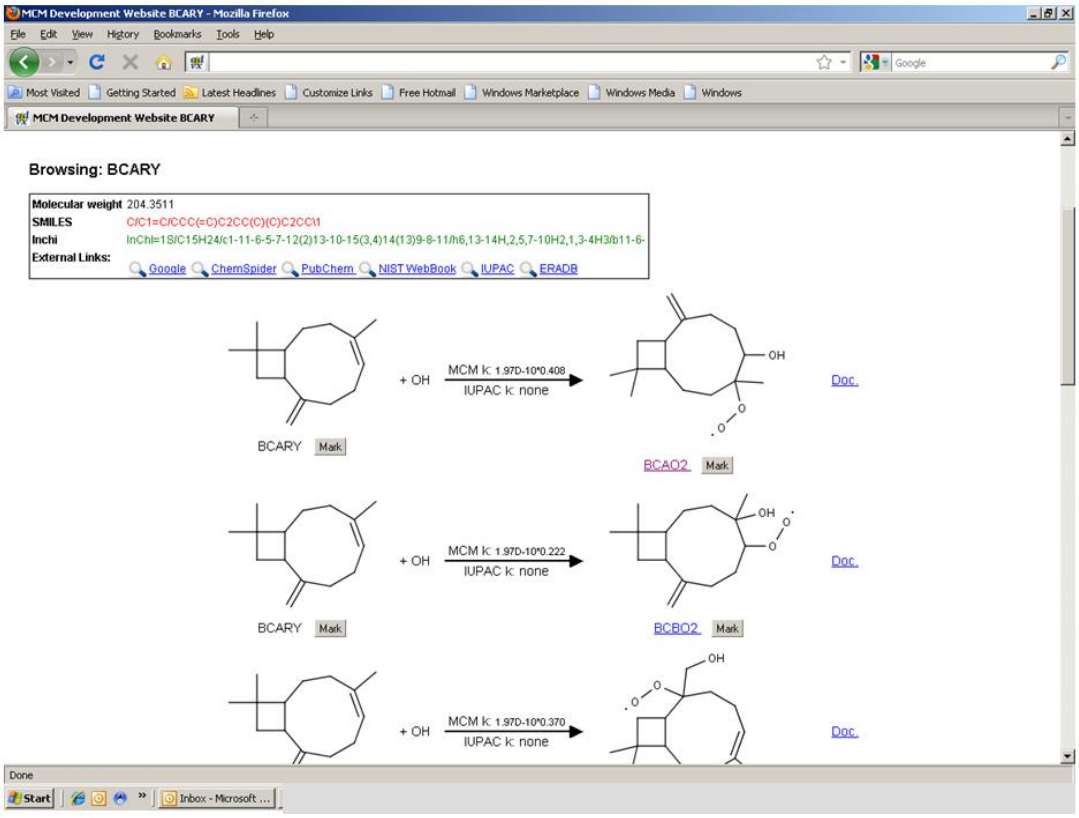

3.2.2 Initial chamber evaluation of MCM v3.2 limonene and β–caryophyllene schemes

The recently developed MCM-compatible gas phase mechanisms for the monoterpene, limonene, and the sesquiterpene, β–caryophyllene, have been evaluated using data from the University of Manchester chamber, obtained as part of the NERC APPRAISE ACES project.

Figure 3.2 shows a comparison of the performance of the limonene scheme with observations of NOx and ozone, for a photo-oxidation experiment in which initial mixing ratios of 50 ppb limonene, 22.0 ppb NO_2 and 9.8 ppb NO were irradiated with simulated sunlight. The observed behaviour follows the pattern typically observed for chamber VOC/NOx photo-oxidation, in which the radical-catalysed VOC degradation leads to progressive conversion of NO to NO_2, and resultant formation of ozone from the photolysis of NO_2. Such behaviour occurs when the VOC is oxidised significantly by reaction with OH radicals, which is a key element of the radical-catalysed NO-to-NO_2 conversion cycles.

Figure 3.2: Observed and simulated temporal profiles for ozone and NOx in a limonene-NOx photo-oxidation experiment and a β–caryophyllene-NOx photo-oxidation experiment in the Manchester Chamber (see text). Data obtained as part of the NERC APPRAISE-ACES consortium project and kindly supplied by Dr Rami Alfarra and Professor Gordon McFiggans (University of Manchester).

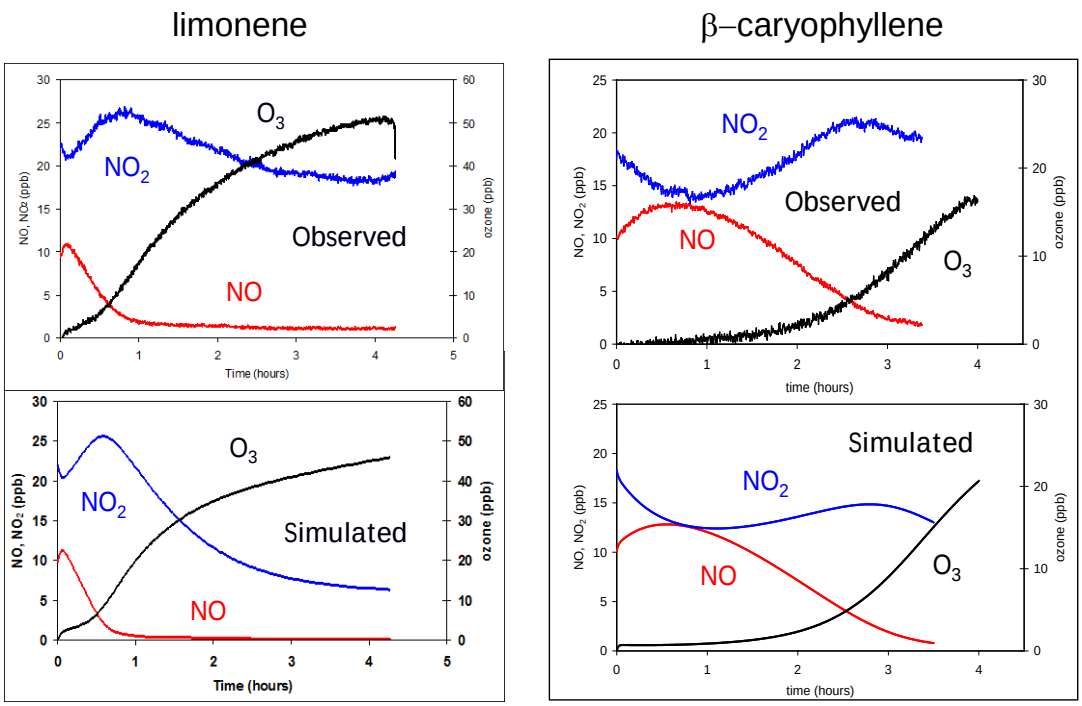

There are other important features of the chemistry apparent from the traces shown in Figure 3.2. Limonene also reacts rapidly with ozone, with this reaction being an important source of free radicals in the system (e.g., OH radicals are formed with a yield of 87%). As a result, it does not necessarily constitute a sink for ozone, because it promotes free-radical catalysed ozone formation when NO is present. Indeed, it is this reaction which initiates the chemistry at the start of the experiment. This is apparent from the initial dip in NO_2 level (which leads to formation of NO and ozone), with ozone then reacting with limonene to start the free-radical catalysed oxidation. The scheme provides a very good description of the temporal development of the system, with the formation of ozone being in good quantitative agreement with observations. It is noted that the simulated NO_2 level agrees well with that observed in the early stages of the experiment, but with a progressively increasing underestimation as experiment proceeds. This is because the NO_2 measurement relies on a conventional chemiluminescent analyser with molybdenum-catalysed thermal conversion of NO_2 to NO prior to quantification. As a result, the measurement has interferences from organic nitrogen compounds formed from limonene degradation (e.g., complex peroxyacyl nitrates) which are also converted to NO in the thermal converter.

Figure 3.2 also shows a comparison of the performance of the β–caryophyllene scheme with observations of NOx and ozone, for a photo-oxidation experiment in which initial mixing ratios of 50 ppb β–caryophyllene, 18.3 ppb NO_2 and 10.1 ppb NO were irradiated with simulated sunlight. In contrast to the limonene system, the observed behaviour does not initially follow the pattern typically observed for chamber VOC/NOx photo-oxidation. This results from two important features of the β–caryophyllene chemistry, namely its exceptionally high reactivity with ozone, and the low radical yield of that reaction. As a result, the system is initially dominated by formation of ozone and NO from NO_2 photolysis, with the ozone level suppressed by reaction with β–caryophyllene. When significant conversion of

β–caryophyllene into its ozonolysis products has occurred, the system begins to behave more conventionally, with NO-to-NO_2 conversion and ozone formation. The simulations showed that the behaviour was very sensitive to the OH radical yield assigned to the reaction of ozone with β–caryophyllene, which was optimised at about 4% for the simulation shown in Figure 2. This is comparable with, but lower than, previously reported values, which lie in the range 6-10% (Shu and Atkinson, 1994; Winterhalter et al., 2009). Further analysis is in progress to assess whether this conclusion is influenced by potential impacts of physical processes (e.g., wall removal or SOA formation) for the high molecular weight, low volatility products formed.

These evaluation activities have demonstrated that the new MCM schemes perform well in relation to their impact on ozone formation under chamber conditions, and provide a level of validation for the expanded coverage of the biogenic VOC chemistry in the MCM.

3.3 Revision of MCM degradation schemes for chlorinated VOCs

The MCM chemistry of the chlorine-substituted hydrocarbons has been reviewed and updated, with the aim of improving representation of the solvents emissions sector and providing up-to-date reference chemistry against which to develop reduced schemes for the CRI mechanism. The activity commenced with a literature review, which focused on the initiation reactions with OH, and on the reactions of the intermediate peroxy radicals (RO_2) containing chlorine (and also the other halogens, fluorine and bromine). The latter revealed some clear reactivity trends for the reactions with NO and HO_2 (e.g., see Figure 3.3), which have allowed the representation to be improved, and which also provide the basis for development of structure-reactivity relationships to help define a revised MCM protocol in the future. The impact of the updates is currently being assessed.

3.4 Implementation of CRI v2 SOA code into the Ozone Source-Receptor Model

The secondary organic aerosol (SOA) code developed previously for use with the CRI v2 mechanism in the Photochemical Trajectory Model (PTM) has been adapted for use in the Ozone Source Receptor Model (OSRM). As described in detail previously (Utembe et al., 2009), the formation of SOA is represented in terms of the equilibrium partitioning of oxidation products between the gas and condensed organic phases, according to the following relationship (Pankow, 1994):

$$C_a/C_g = K_p C_{om} \qquad (1)$$

where C_a and C_g are the concentrations of a given species in the condensed organic and gas phases, respectively, C_{om} is the total mass concentration of condensed organic material in units of µg m^{-3}, and K_p is the species-dependent partitioning coefficient (m^3 µg^{-1}). Phase partitioning is represented for the 14 CRI v2-R5 species shown in Table 3.2. These comprise ten terpene-derived biogenic species, one isoprene-derived biogenic species, and three aromatic hydrocarbon-derived species. Each species acts as a surrogate, used to represent a set of species in the MCM code (also identified in Table 3.2), which were found to make major contributions to each class of SOA in case study scenarios over the wide range of pollution conditions that were considered in the original MCM simulations (see Utembe et al., 2009). The values of K_P assigned to the surrogate species are based on those of the closest MCM v3.1 analogue species (determined as described by Johnson et al. 2006 and optimised empirically as described by Utembe et al., 2009), with those for the sets of aromatic, terpene-derived biogenic and isoprene-derived biogenic species being scaled independently, in order to optimise agreement with results from the MCM v3.1 reference simulations (see Utembe et al., 2009). The impact of implementation of these updates into the OSRM will be assessed and reported at a later date.

Figure 3.3: Rate coefficients at 298K for reactions of HO_2 with organic peroxy radicals (RO_2) containing a variety of substituent functional groups, and as a function of the mass of the organic group, R. This shows a suppression of reactivity from the presence of halogen groups adjacent to the peroxy radical centre, which increases with additional halogen substitution (black diamonds = 1 α–halogen; grey diamonds = 2 α–halogens; open diamonds = 3 α–halogens). The lines are based on an empirically-fitted function, $k = 2.2 \times 10^{-11} (1-\exp(-0.017 M_R))$ cm^3 $molecule^{-1}$ s^{-1}, for alkyl, hydroxyalkyl and hydroxyalkenyl RO_2, where M_R is the mass of the R group (in g mol^{-1}). For RO_2 containing 1, 2 and 3 α–halogen groups, k is multiplied by respective fitted factors of 0.43, 0.29 and 0.15.

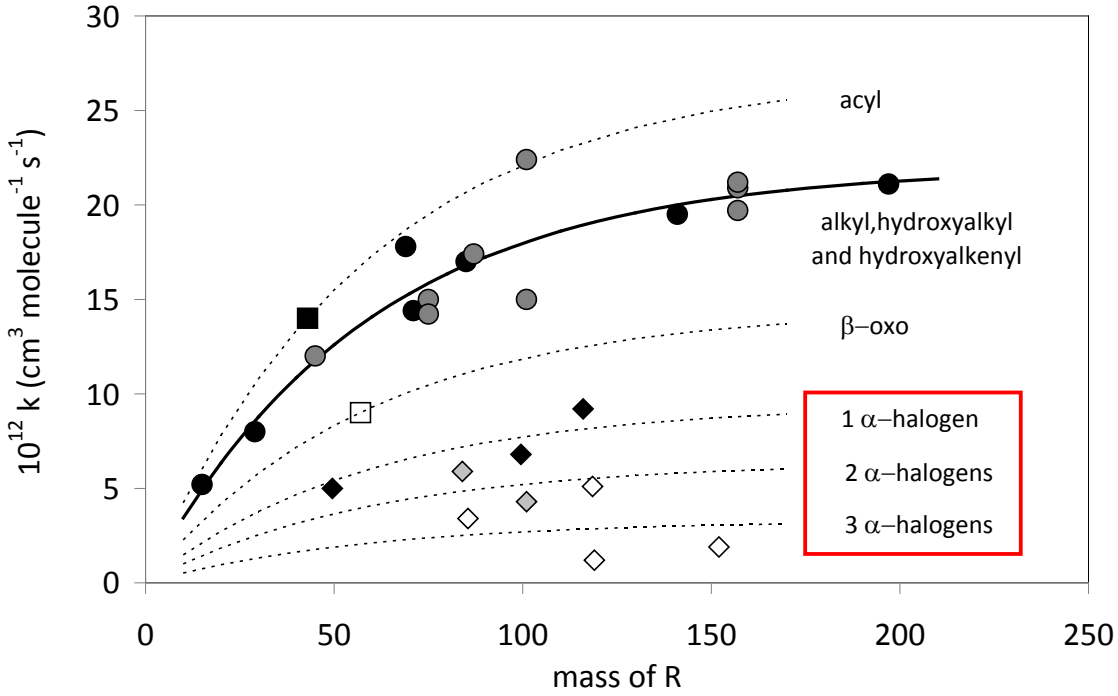

3.5 Assessment of recently reported NO_x-limited chemistry

A number of recently-published studies, reporting the results of investigations in the field, have identified potential deficiencies in the understanding of VOC oxidation chemistry under NOx limited conditions (Tan et al., 2001; Thornton et al., 2002; Martinez et al., 2003; Ren et al., 2008; Lelieveld et al., 2008; Butler et al., 2008; Hofzumahaus et al., 2009; Pugh et al., 2010). The deficiencies relate to the ability of the chemistry to recycle OH radicals when NO_x levels are low, which leads to maintenance of higher concentrations of OH and a sustained oxidation capacity. As a result, current generation models tend to underestimate VOC oxidation rates under NO_x-limited conditions, where they predict termination of the chemistry via radical-radical reactions which become increasingly important as NO_x levels are lowered. The above studies have mainly identified a pattern of underestimation in OH recycling in low NO_x locations characterized by high natural emissions of isoprene. It is probable, however, that contributions to the effect can also result from the chemistry of anthropogenic (and other biogenic) VOCs, as demonstrated most clearly by the results of Hofzumahaus et al. (2009) for the Pearl River Delta, China.

Stimulated by these observations, a number of experimental and theoretical studies have reported novel chemical processes which may influence the recycling of OH under NO_x-limited conditions. These studies have focused almost exclusively on the chemistry of

Table 3.2: Summary of species used to represent SOA formation from CRI v2-R5 in OSRM.

CRI v2 species	Description	Closest MCM analogue(s)
Biogenic species		
RTN28OOH	First-generation α–pinene product containing *-OH* and *-OOH* groups	APINAOOH, APINBOOH, APINCOOH
RTN28NO3	First-generation α–pinene product containing *-OH* and *–ONO_2* groups	APINANO3, APINBNO3, APINCNO3
RTX28OOH	First-generation β–pinene product containing *-OH* and *-OOH* groups	BPINAOOH, BPINBOOH, BPINCOOH
RTX28NO3	First-generation β–pinene product containing *-OH* and *-ONO_2* groups	BPINANO3, BPINBNO3, BPINCNO3
RTN26OOH	Second-generation α–pinene product containing *-C(=O)-* (x2) and *-OOH* groups	PINALOOH, PERPINONIC
RTN26PAN	Second-generation α–pinene product containing *-C(=O)-* and *-C(=O)OONO_2* groups	C10PAN2
RTN25OOH	Second-/third-generation α–pinene product containing *-C(=O)-* and *-OOH* groups	C96OOH
RTN24OOH	Second-/third-generation α–pinene product containing *-OH, -C(=O)-* and *-OOH* groups	C97OOH
RTN23OOH	Second-/third-generation α–pinene product containing *-OH, -C(=O)-* (x2) and *-OOH* groups	C98OOH
RCOOH25	First-/second-generation α–pinene product containing *-C(=O)-* and *-C(=O)OH* groups	PINONIC
RU12OOH	Second-generation isoprene product containing *-OH* (x2), *-C(=O)-* and *-OOH* groups	C57OOH, C58OOH, C59OOH
Anthropogenic species		
ARNOH14	Second-generation benzene product containing *-OH* and *-ONO_2* groups	HOC6H4NO2
ARNOH17	Second-generation toluene product containing *-OH* and *-ONO_2* groups	TOL1OHNO2
ANHY	Second-generation cyclic anhydride product of aromatic oxidation	MALANHY and substituted analogues

isoprene, although some aspects of the novel chemistry are relevant, or potentially transferable, to other VOC systems. In the present work, an assessment of this new chemistry has been carried out, and this has necessarily also focused on the isoprene system. The assessment work has been carried out in collaboration with the group of Prof. Dudley Shallcross at the University of Bristol, with particular contributions from Dr Alex Archibald.

The work has involved two main tasks. First, a mechanism intercomparison exercise has been carried out in which the performance of the existing isoprene chemistry in MCM v3.1 and CRI v2 has been compared with that of six other widely-applied mechanisms (MIM2, GEOS-CHEM, MOZART v4, UKCA, CBM-05 and STOCHEM) over a wide range of NO_x levels. One aim of this exercise was to confirm that suppression of OH recycling at low NOx is common to all these mechanisms. Following this, the impact of a number of reported mechanistic changes were tested within the framework of the MCM v3.1 chemistry, with a particular focus on the impact on OH recycling.

3.5.1 Isoprene mechanism intercomparison

The considered mechanisms (identified above) ranged in size and complexity from approximately 600 reactions in MCM v3.1 to approximately 25 reactions in the STOCHEM chemistry. Box model experiments were carried out over a broad range of NO emissions to assess the performances of the mechanisms over the spectrum of atmospherically relevant conditions (see Figure 3.4 for comparisons of simulated mixing ratios of key species). Although the mechanisms all showed similar trends in performance, there was some variation (up to a factor of about 1.4) in the simulated oxidation rates of isoprene and formation rates of ozone at high NO_x. The variability in performance is a consequence of the details of the underlying chemistry as represented in the mechanisms, and is generally related to different assumptions and approximations made in mechanism reduction. However, the results confirmed that all the considered isoprene mechanisms lead to substantial suppression of OH radicals at low NO_x, and that they are unable to generate/recycle OH radicals at the rates needed to match the recently reported observations at locations characterized by low levels of NOx. This indicates shortcomings in the conventional understanding of the chemistry, as represented in greater or lesser detail in all the mechanisms. The work is described in greater detail by Archibald et al. (2010a).

3.5.2 Mechanistic sensitivity test

MCM v3.1 was used as a base mechanism to test the sensitivity of the isoprene chemistry to a number of detailed mechanistic changes over a wide range of NO_x levels, using the same box model as applied in the intercomparison exercise. The sensitivity tests were carried out in three general areas (summarised in Table 3.3), and consider processes for which experimental and/or theoretical evidence has been reported in the peer-reviewed literature. The work is described in detail by Archibald et al. (2010b).

All the considered mechanistic changes were found to lead to simulated increases in the concentrations of OH, with Mechanisms 1 and 2 resulting in respective increases of up to about 7% and 16%, depending on the level of NO_x (see Figure 3.5). Mechanism 3, based on the theoretical calculations of Peeters et al. (2009), was found to have potentially much greater impacts, with enhancements in OH concentrations of up to about 230%, depending on the level of NO_x. That mechanism involves the operation of competitive isomerisation reactions of the intermediate RO_2 radicals to form hydroperoxy-substituted products, which rapidly photolyse to form OH and other radicals. As described in detail by Archibald et al. (2010b), additional tests were carried out to appraise the performance of the mechanism in relation to atmospheric observations of stable product ratios and existing laboratory data under low NO_x conditions. This suggested that Mechanism 3 cannot be fully reconciled with these data without some degree of parameter refinement and optimisation which would probably include a reduction in the RO_2 radical isomerisation rates and a consequent

Figure 3.4: Comparison of mixing ratios simulated for a series of key species in the isoprene mechanism intercomparison. Average isoprene emission rate = 1.6 × 10^{12} molecule cm^{-2} s^{-1} (6.4 mg m^{-2} h^{-1}); NO_x emission rate varied over range (5.0 – 1000) × 10^9 molecule cm^{-2} s^{-1}.

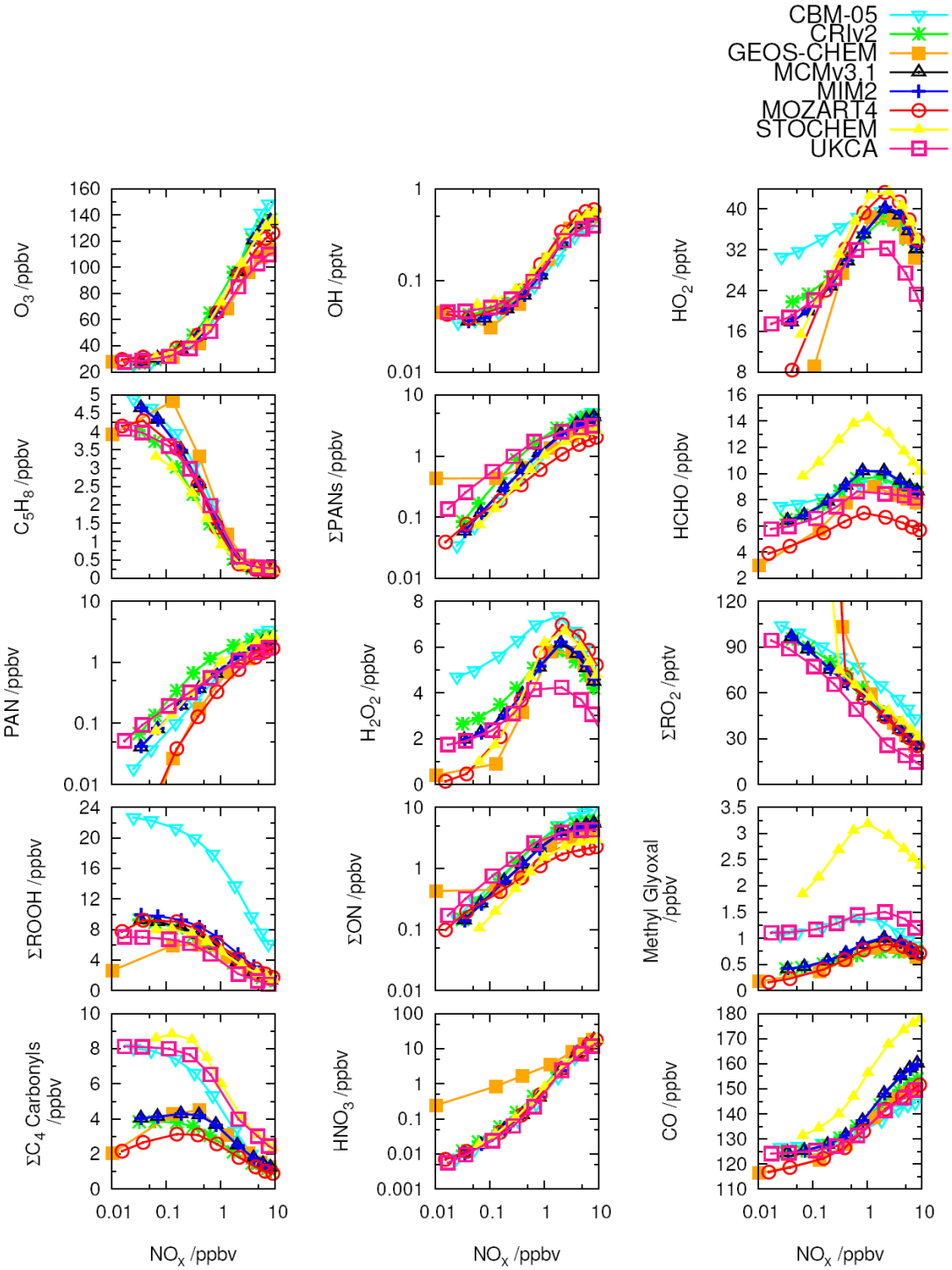

Table 3.3: Description of the main isoprene mechanistic sensitivity runs performed.

Mechanism number	Description
1	MCM v3.1 with radical propagating channels incorporated for all acyl peroxy + HO_2 and β–oxy peroxy + HO_2 reactions, based on Hasson et al. (2004), Jenkin et al., (2007, 2008) and Dillon and Crowley (2008)
2	MCM v3.1 with OH-catalysed conversion of isoprene-derived hydroxy-hydroperoxides into epoxydiols, based on Paulot et al. (2009).
3	MCM v3.1 with isomerisation reactions (and associated subsequent chemistry) included for isoprene-derived peroxy radicals, based on Peeters et al. (2009).
4	A consolidation of the changes outlined above in Mechanisms 1, 2 and 3.

Figure 3.5: Changes in mixing ratios of OH for each mechanistic variant relative to the MCM v3.1 base case as a function of the simulated NO_x level.

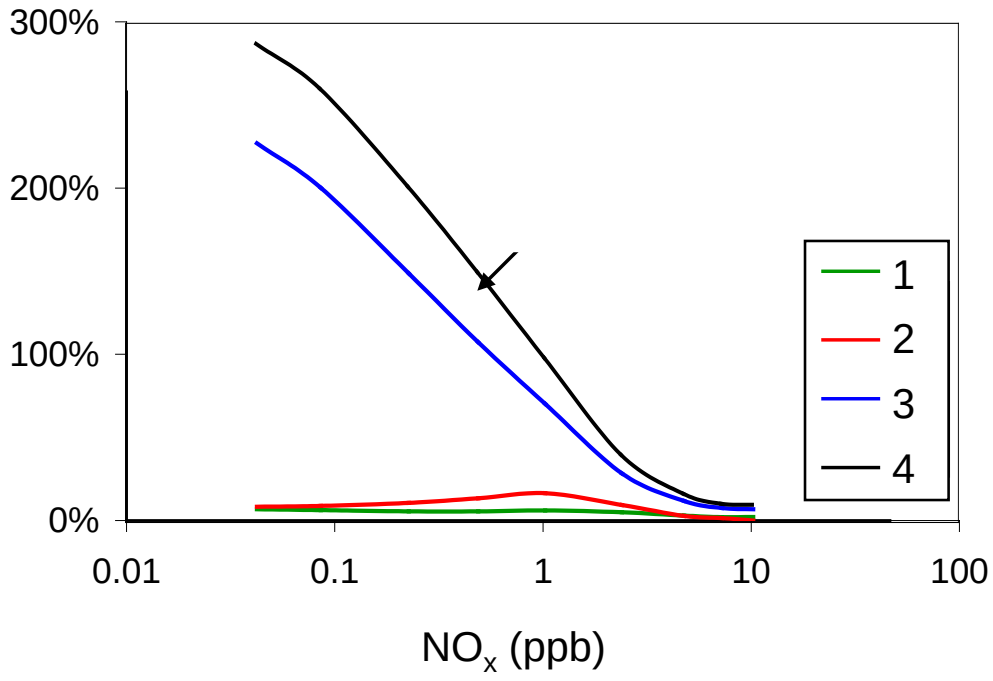

reduction in the OH enhancement propensity. However, an order of magnitude reduction in the isomerisation rates (which is probably more severe than that required for consistency with existing observations) was still found to yield notable enhancements in OH concentrations of up to a factor of about 2, with the maximum impact at the low end of the considered NO_x range. The main conclusion therefore is that the mechanism of Peeters et al. (2009) shows great potential for OH radical recycling under atmospheric conditions, but that it requires confirmation and optimization through the results of appropriately-designed laboratory experiments.

Although the specific mechanism postulated by Peeters et al. (2009) requires experimental verification, similar isomerisation reactions for RO_2 radicals formed during alkane oxidation have been reported in experimental studies (Perrin et al., 1998; Jorand et al., 2003). It is possible, therefore, that these and similar reactions for RO_2 radicals formed from a variety of precursor VOCs can contribute to the more general radical recycling under NOx-limited conditions which has been reported (Thornton et al., 2002; Hofzumahaus et al., 2009). This

area should therefore be kept under review, with a view to making recommendations for the treatment of RO_2 isomerisation reactions in atmospheric mechanisms.

3.6 The MCM website and database (http://mcm.leeds.ac.uk/MCM/)

The targeted extensions and revisions to the gas phase chemical schemes within the current project are being released as MCM v3.2, via a dedicated website facility. The main updates can be summarised as follows:

- Inclusion/integration of new schemes for limonene, β–caryophyllene and dimethyl sulphide (DMS), as developed within the present contract.
- Inclusion/integration of revised chemistry for isoprene hydroperoxides and nitrates, as carried out within the present contract.
- Inclusion/integration of new schemes for acrolein, crotonaldehyde, methacrolein, ethylene oxide and vinyl chloride, developed independently by the group of Dr Sandra Saunders at the University of Western Australia.
- Full revision of photolysis parameters.
- Formal linkage of the MCM and IUPAC gas kinetics evaluation databases, to facilitate regular updating of kinetic parameters on the basis of expert evaluated recommendations (http://www.iupac-kinetic.ch.cam.ac.uk/projects.html).
- Linkage to the "Chemical kinetics database on oxygenated VOCs gas-phase reactions" developed at CNRS-ICARE in Orléans, France (http://www.era-orleans.org/eradb/)
- Inclusion of a new description of the project, improved guidance on use of the facility and citation, and an improved log of current and historical funding sources and contributors to the project.
- Access to CRI v2 via a parallel searchable and extractable facility.

3.7 Summary and main conclusions

The main conclusions of the work of Objective 9 on the improvements to photochemical reaction schemes are summarised as follows:

Summary:

- **A new chemical reaction scheme has been developed and successfully tested for the atmospheric degradation of a highly reactive biogenic species, β-caryophyllene, the largest VOC treated to date in the Master Chemical Mechanism and the most reactive with respect to reaction with ozone. The new mechanism has expanded the coverage of biogenic VOC chemistry and extended the reactivity range of VOC species represented in the MCM. This will help to improve the prediction of ozone and other secondary air pollutants (e.g. secondary organic aerosols) from VOCs emitted from natural sources which will become increasingly important as emissions from anthropogenic sources decrease.**
- **An initial assessment of the reactivity and mechanisms for degradation of halogenated VOCs used in solvents has been made. This has shown how the reactivity decreases with additional α-halogen substitution in the VOC. The work will form the basis for development of structure-reactivity relationships to define mechanism development protocols for the MCM.**

- **The initial steps have been taken on the implementation of a reduced secondary organic aerosol (SOA) chemistry code for the OSRM. This work will continue during 2011 and the OSRM tested for modelling of SOA.**
- **A hypothesis has been developed based on independent research studies and model sensitivity tests for the OH radical-recycling under low NO_x conditions. This will help to enhance the performance of chemical mechanisms for VOC oxidation used in models which appear to be currently deficient under these conditions.**
- **The targeted extension and revisions to the MCM undertaken in this project are to be released as MCM v3.2 on the dedicated website facility maintained by the University of Leeds.**

4 Application of Chemical Transport Models for Defra Policy on Ozone and Secondary Particulate Matter

4.1 Introduction

Objective 10 involves the application of current models in support of Defra policy on ozone and secondary PM, including:

- the modelling of the UK ground-level ozone climate in 2008, 2009 and 2010 using the OSRM (Objective 10.1)
- the use of the OSRM or PTM for modelling specific emission scenarios on an ad-hoc basis to support Defra's development and implementation of ozone and secondary particulate matter (PM) policy (Objective 10.2)
- specific modelling and assessments using the PTM aimed at understanding emission uncertainty and sensitivity analyses of modelled ozone and SOA concentrations in the UK (Objective 10.3).

The work carried out in **Objective 10** during this phase of the project has focused on all three of these sub-objectives.

Details of the OSRM and PTM are given elsewhere in project reports and publications and only a brief description of the models are given here.

4.1.1 The Ozone Source Receptor Model (OSRM)

The OSRM (Hayman et al, 2010) is an established Lagrangian trajectory model that simulates the photochemical production of ozone in reactive air masses as they arrive at different receptor points in the UK. Essentially, each parcel of air picks up emissions from natural and man-made sources as it moves over land surfaces over a large spatial scale and these undergo a series of chemical reactions initiated by sunlight leading to the production of ozone. Gridded 1x1km emissions data for the UK are taken from the NAEI[1] (Bush et al, 2010) and 50x50km emissions data for the rest of Europe are taken from EMEP. Emission terms to describe natural biogenic emissions from European forests and agricultural crops are derived from the European PELCOM project. The model uses archived trajectory data from the Met Office NAME model providing boundary layer depth and other parameters. The chemical mechanism used is a modified version of the mechanisms used in the STOCHEM model, but an option is available to use the condensed CRIv2-R5 chemical scheme, linked to the MCM. Dry deposition processes are represented using a conventional resistance approach.

The OSRM calculates ozone concentrations at mid-boundary layer height at hourly intervals on a 10x10km grid covering the whole of the UK. These are corrected to account for loss of ozone due to reaction with local emissions of NO_x and deposition to land and sea surfaces in order to generate concentrations at ground-level.

The model has been used routinely for Defra to model the UK ground-level ozone climate based on meteorological conditions and emissions from 1999 to 2007 and for forecasting ozone under future UK and European-wide emission scenarios. The model has been optimised for computational efficiency and has been a vital policy tool in quantifying the response of the UK's ground-level ozone climate to measures aimed at reducing emissions of the precursor species.

[1] National Atmospheric Emissions Inventory, www.naei.org.uk/

In conjunction with GIS-based tools, the OSRM is used to derive population- and area-weighted means of different ozone concentration metrics to provide the information necessary to Defra policy makers for cost-benefit analysis of emission reduction policies.

The OSRM is also used in conjunction with a Surface Ozone Flux Model which can be used to model the uptake of ozone by different types of vegetation species under different meteorological conditions.

4.1.2 The Photochemical Trajectory Model (PTM)

The PTM has been used to describe photochemical ozone formation as well as secondary inorganic and organic aerosol formation in north-western Europe. Details are given in Derwent et al (1996, 1998, 2009), Abdalmogith et al. (2006) and Johnson et al. (2006). The model describes the chemical development within an air parcel that follows a trajectory for up to 10 days. For each mid-afternoon of each day a large number of equally probable and randomly selected 96-hour air parcel trajectories are generated using the Met Office Numerical Atmospheric dispersion Model Environment (NAME) model. The PTM uses NAEI and EMEP gridded emissions data and inventories for natural biogenic emissions. Initial and background species concentrations are taken from the EMEP site at the Valentia Observatory and the atmospheric baseline station at Mace Head, Ireland. The model has the option of using three chemical mechanisms. These are the full MCM, the condensed CRIv2 mechanism or the Carbon Bond Mechanism. Dry deposition processes are represented using a conventional resistance approach.

The PTM has been used for a variety of purposes to support Defra policy on ozone and secondary PM. These include the estimation of photochemical ozone creation potentials (POCPs) of individual VOCs (Derwent et al., 1998) and more recently in this project to estimate secondary organic aerosol formation potentials (SOAPs, Derwent et al, 2010a). It has also been used to evaluate the effectiveness of current precursor emission controls in Europe on levels of ground-level ozone in the UK (Derwent et al, 2010b) and the effectiveness of future potential emission controls.

4.2 Modelling the UK ozone climate in 2008

The previous phase of the tropospheric ozone modelling contract (2007-2009) had shown that the empirical modelling approach used in Defra's UK Ambient Air Quality Assessments (UKAAQA) model[2] traditionally gives results for ozone concentration metrics that are more representative of the measured concentrations in model verification than corresponding outputs provided by the OSRM. Hence, the UKAAQA modelling contract is used to provide the supplementary ozone modelling required for EU Air Quality Directive reporting on ozone to the European Commission each year on behalf of Defra. The OSRM, on the other hand, has a stronger role to play in scenario analysis and policy development as the OSRM can model future emission scenarios and the chemistry involved in forming and removing ozone over a large spatial scale from the emitted precursor gases, NO_x and VOCs. The OSRM is therefore maintained and evaluated each year using appropriate meteorology and emissions data and comparing calculated ozone concentrations with those from the UKAAQA empirical model and with monitoring data at specific AURN sites.

Both the UKAAQA and OSRM modelling techniques are verified against measured data to provide confidence in their performance. The two models have been compared in previous years, most recently for 2004, 2005 and 2007, which were noted as relatively "low ozone" years (Hayman et al, 2006a, Murrells et al, 2009b), and 2006 which was a relatively "high ozone" year (Murrells et al, 2008). In this phase of the project for **Objective 10.1**, during 2010, the OSRM has been used to model UK ozone in 2008. Monitoring data showed that ozone concentrations in 2008 were moderate. The maximum hourly concentration in the UK

[2] Previously referred as the Pollution Climate Mapping model (PCM)

was 194µg m^{-3} (Hull) in 2008, compared to 168 µg m^{-3} (Blackpool Marton) in 2007 and 278 µg m^{-3} (Wicken Fen) in 2006.

The performance of the OSRM for 2008 was demonstrated for the two Long-Term Objective (LTO) metrics used in the EU Air Quality Directive reporting that correspond to the specific calendar year 2008:

- Days greater than 120 µg m^{-3} as a maximum daily running mean (Long Term Objective for Human Health)
- AOT40 (Long Term Objective for Vegetation)

The multi-year Target Value metrics will not be as good an indicator of model performance during a specific year as the Long-Term Objective metrics because averaging over several years will lessen the contribution of ozone concentrations associated with a particular year. For this reason, the metrics that the evaluation concentrated on are the single year (2008) metrics for human health and vegetation.

OSRM runs for 2008 were made by implementing 6-hourly meteorological data from the Met Office NAME model and using UK emissions inventory data for 2008. The NAEI 1x1 km emissions data for 2007 were implemented and scaled to 2008 using the NAEI emission projections (UEP37) for each pollutant and source sector. The latest EMEP emissions data for other European countries were used, re-scaled to 2008. The latest initialisation adjustment data for 2008 have been obtained from Prof Derwent based on measurements at Mace Head. Ozone concentration metrics were calculated on a 10x10 km grid and at specific AURN sites.

4.2.1 Comparison of maps of OSRM and UKAAQA outputs for ozone metrics in 2008

The maps that have been generated from the outputs of the OSRM and empirical UKAAQA model for both the health and vegetation Long-Term Objective metrics are presented in Figures 4.1 to 4.4. Figure 4.1 presents the map of the number of days exceeding 120 µg m^{-3} in 2008 from the OSRM and Figure 4.2 shows the same metric output from the UKAAQA empirical model. Figure 4.3 shows the OSRM map for the AOT40 metric in 2008 and Figure 4.4 shows the corresponding map from the UKAAQA empirical model.

With 2008 being a moderate year for ozone, the NO_x titration effect is not as apparent as it had been in 2006 but more apparent than it was in 2007. Only the OSRM and UKAAQA AOT40 maps identify areas of ozone depletion due to NO_x titration in large city areas and major roads. The number of days above 120 µg m^{-3} metric maps do not show the NO_x titration effect as the values are too low. The UKAAQA model has a finer resolution (1km) than the OSRM (10km), so it identifies areas such as larger cities and major roads more readily than the OSRM. The empirical model utilises a modelled NO_x map (described in Kent and Stedman, 2008) with a coefficient to describe the decrement in ozone concentrations with increased NO_x. The OSRM uses the surface conversion post-processor in conjunction with NAEI NO_x emission maps to account for the effects of NO_x titration on local ozone concentrations.

The typical gradient seen in previous years, decreasing from higher concentrations in the south to lower concentrations in the north is not as clear as it was in 2006. In 2008 the higher ozone is a hybrid between the 2007 and 2006 maps with higher ozone in the South and East coastal areas. In both the OSRM and UKAAQA maps for the number of days above 120 µg m^{-3} most of the UK is below 5 (the lowest division on the mapped scale). The usual pattern is a natural feature of the increase frequency and magnitude of photochemical events in the more southerly and easterly areas of the UK. It has been suggested (Hayman et al, 2006b) that the relatively high concentrations in the north of Scotland may be the result of higher hemispheric background ozone concentrations here being represented in the model or intrusions of stratospheric ozone. This has less effect on the OSRM in 2008 than it did in 2007.

Figure 4.1: Number of days exceeding 120 µg m^{-3} (2008) (OSRM map)

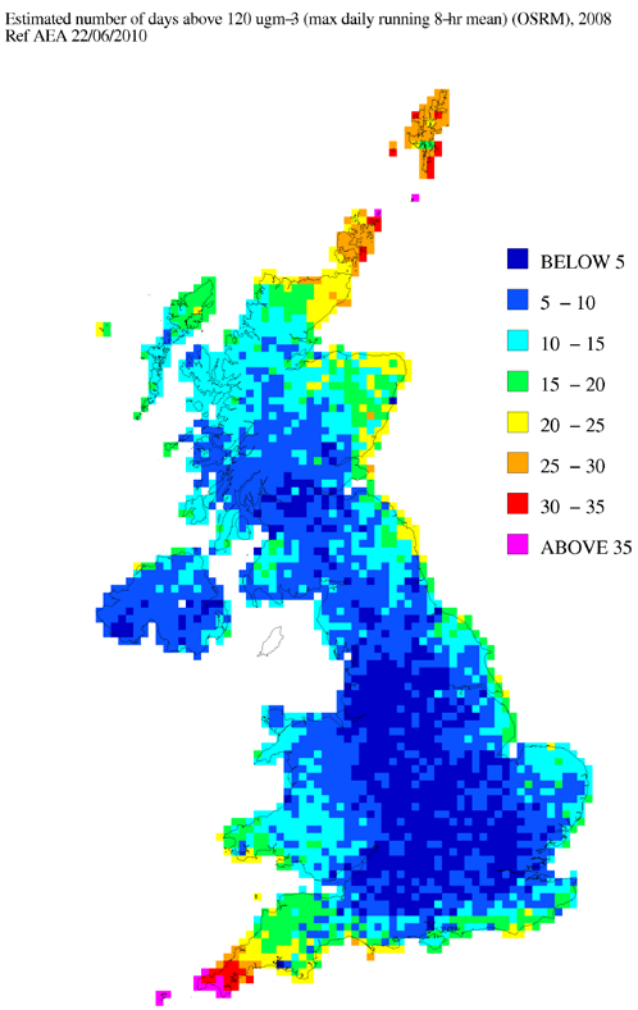

Figure 4.2: Number of days exceeding 120 µg m^{-3} (2008) (UKAAQA empirical map)

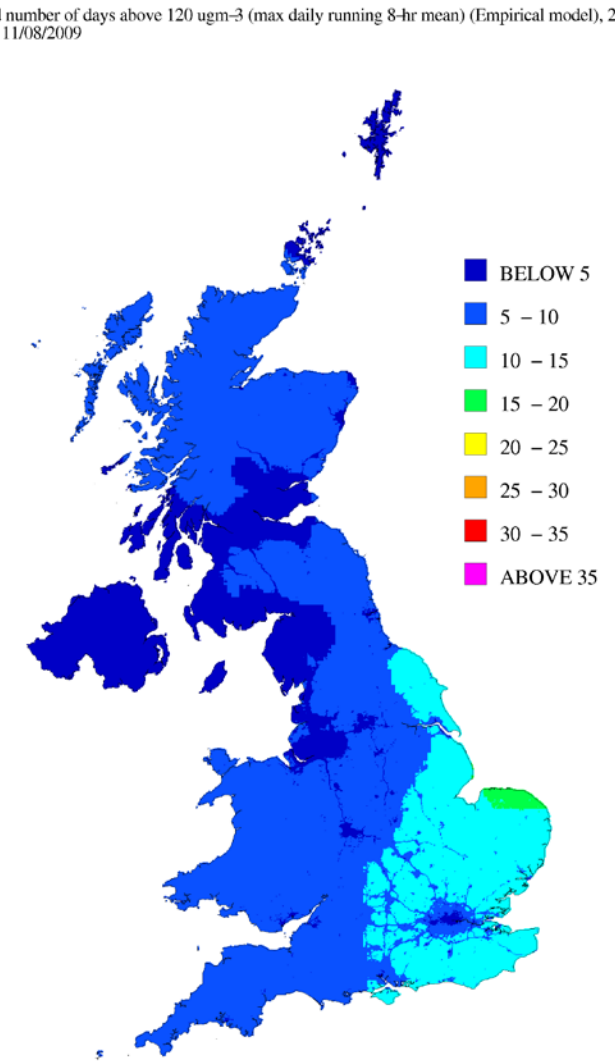

Figure 4.3: AOT40 (µg m^{-3}.hours) (2008) (OSRM map)

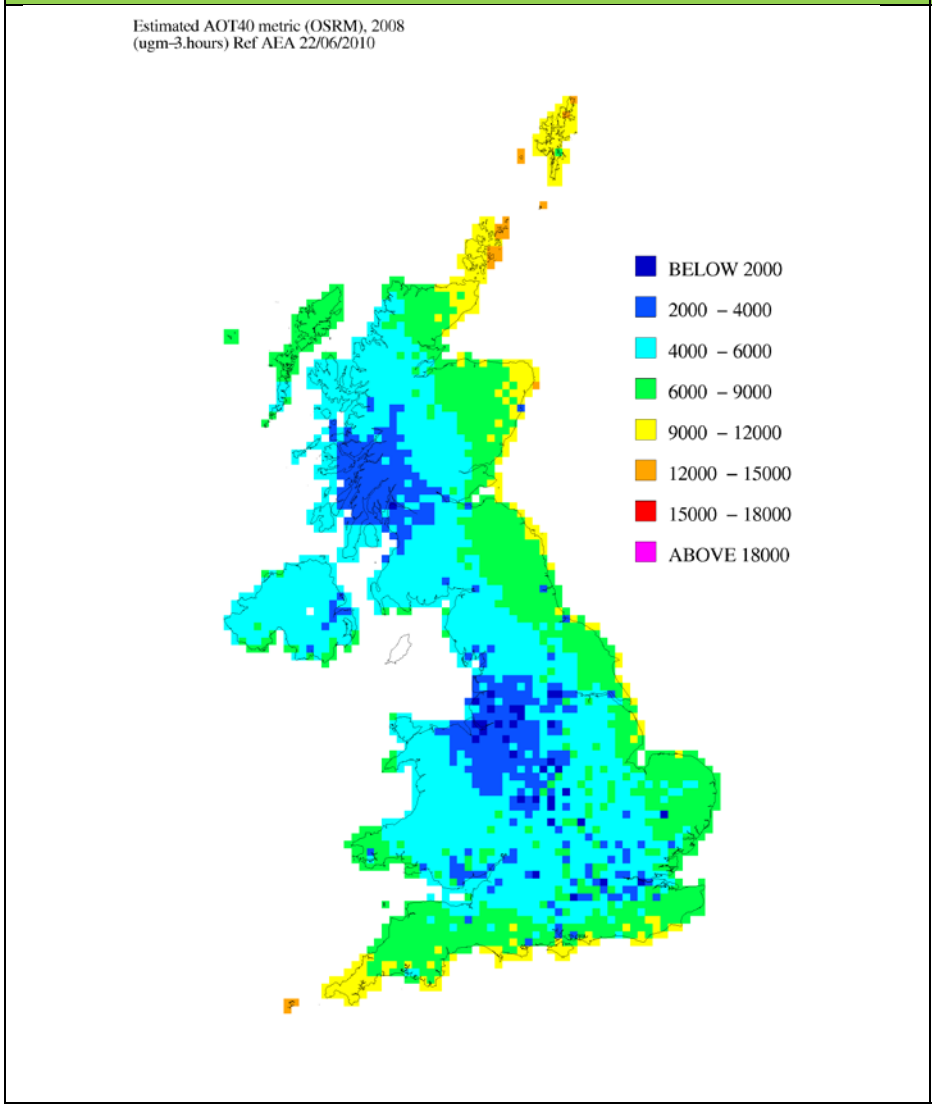

Figure 4.4: AOT40 (2008) (µg m^{-3}.hours) (UKAAQA empirical map)

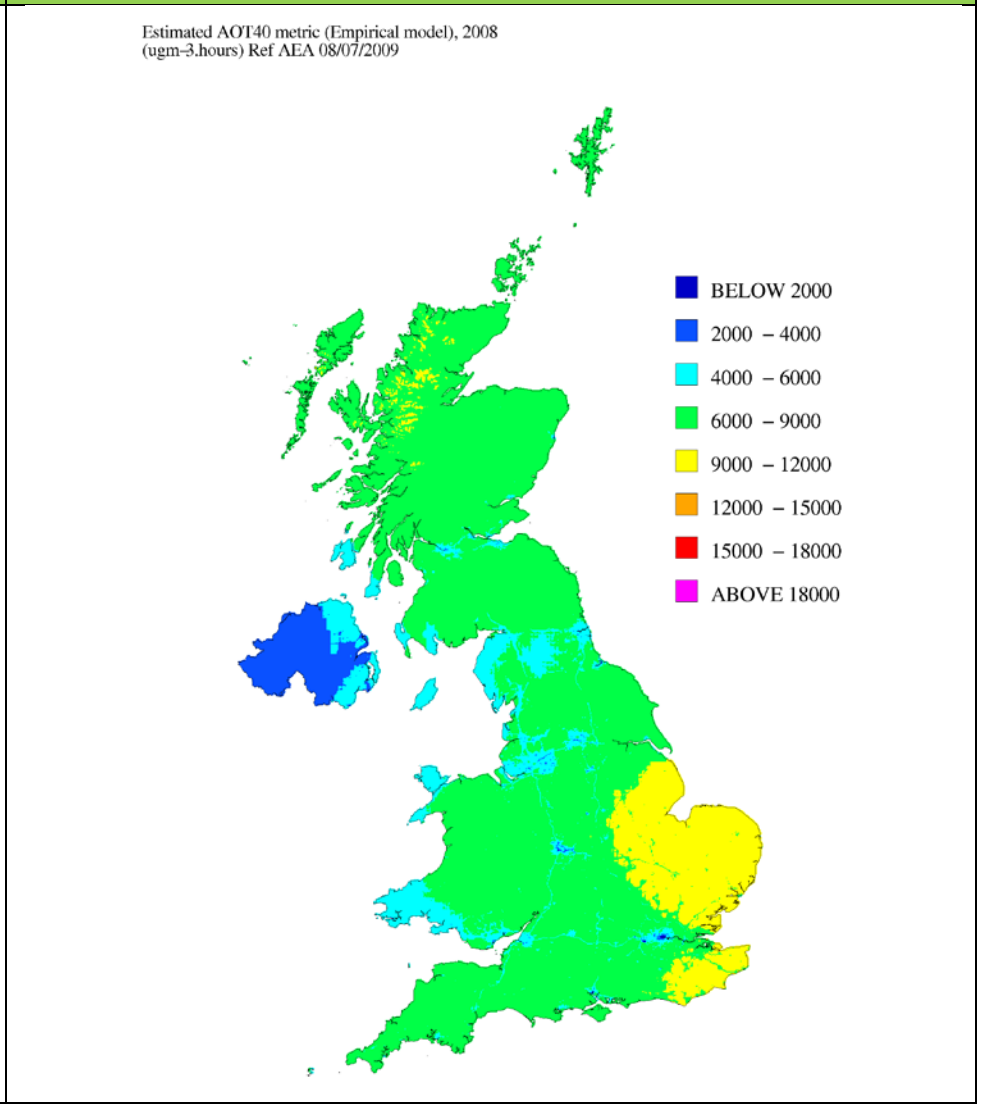

The OSRM shows broadly similar patterns to the empirical maps, however there are some specific spatial differences. The OSRM maps estimate notably higher concentrations of ozone in the south west of the country over Cornwall that have not been captured in the corresponding empirical maps. Both models show a higher number of days greater than 120 µg m^{-3} caused by higher concentrations in East Anglia than most of the rest of the UK as it did in 2007. The majority of the higher ozone concentration areas identified by OSRM in 2008 are in southern and eastern coastal fringe areas. This is consistent with OSRM outputs from previous years. This effect had been seen in previous OSRM modelled years and it has been suggested by Hayman et al (2006b) that this coastal 'edge effect' might be the result of the lack of ozone deposition over the sea surface or limitations of meteorological datasets. 2008 was a moderate ozone year and this effect is even more visible than in the higher ozone year (2006).

The highest modelled value of both the AOT40 and the days greater than 120 µg m^{-3} metrics in the empirical map were located in East Anglia and resulted from the high measured concentrations from the Wicken Fen monitoring site. The highest AOT40 and days greater than 120 µg m^{-3} values on the OSRM map are in north-east Scotland (Orkneys and Shetlands) and Cornwall. The OSRM map for the AOT40 metric is quite different to the UKAAQA map. The highest concentrations are in coastal north-east Scotland and south-west England. The high levels of ozone modelled in Cornwall for both AOT40 and days greater than 120 µg m^{-3} do not seem to be shown in the AURN sites in the south-west.

4.2.2 Verification of OSRM and UKAAQA outputs for ozone metrics in 2008

An evaluation of OSRM and UKAAQA model performance has been undertaken, comparing model results for 2008 with measured concentrations from monitoring campaigns around the UK and against each other.

The model verification is represented in scatter plots comparing the model outputs with the corresponding measured metrics at ozone monitoring sites around the UK (Figures 4.5 to 4.8) for OSRM and the UKAAQA empirical model (for the same health- and vegetation-based Long-Term Objective metrics as compared in the maps). Two groups of sites are presented in the verification charts and summary tables:

- national network (AURN) monitoring sites
- verification sites

The AURN sites were used as a direct input to the UKAAQA empirical model and therefore provide a useful check during the verification process, but are not able to provide a completely independent representation of model performance. For this reason there is a separate group of sites labelled 'verification sites' that are completely independent from the UKAAQA model. These typically come from local authorities, research institutions and *ad-hoc* monitoring campaigns for which AEA holds and ratifies the data. These monitoring data are ratified to the same standard as the AURN. Both groups of sites provide an independent verification of the OSRM because this is a process model which does not use monitoring data as an input or a calibration method. A data capture threshold of 75% has been applied to the monitoring data prior to analysis.

The verification charts also present a 1:1 line and lines representing the data quality objectives (DQO) defined in the EU Air Quality Directive (+/- 50%).

Corresponding summary tables (Tables 4.1 to 4.4) are also provided which display the average of the measured concentrations, the average of the modelled estimates, the R^2 of the fit line, the number of monitoring sites used and the percentage of these monitoring sites that fall outside the DQO.

Figure 4.5: OSRM verification

(Days greater than 120 µg m^{-3})

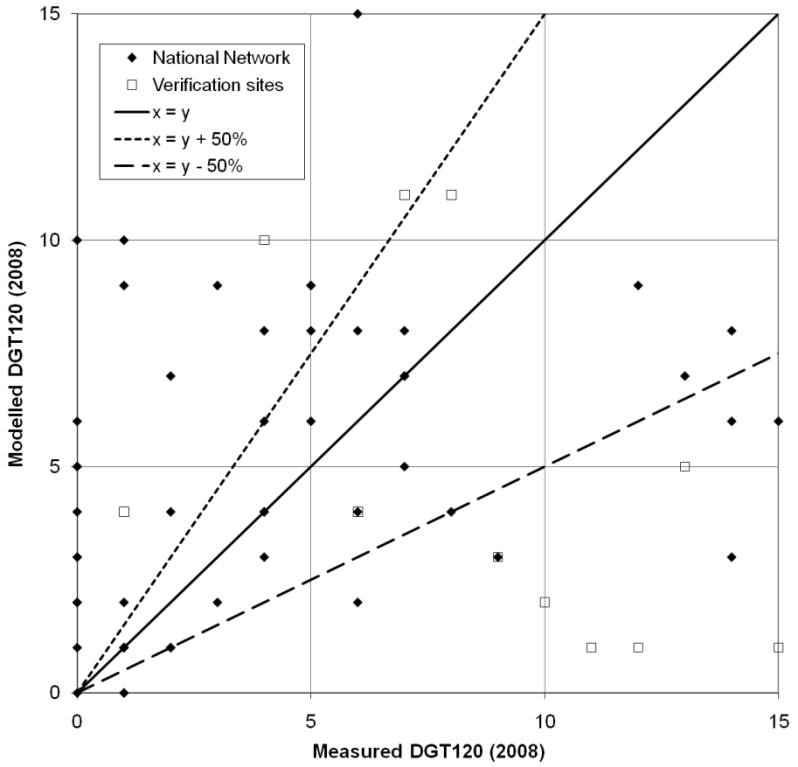

Figure 4.6: UKAAQA empirical model verification

(Days greater than 120 µg m^{-3})

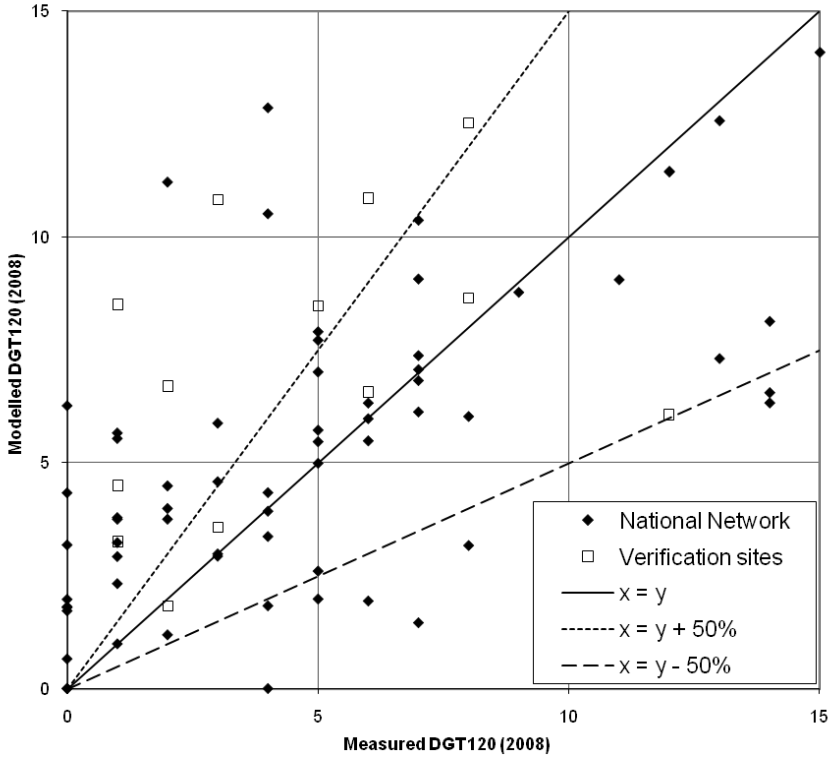

Figure 4.7: OSRM verification

(AOT40, µg m^{-3}.hours)

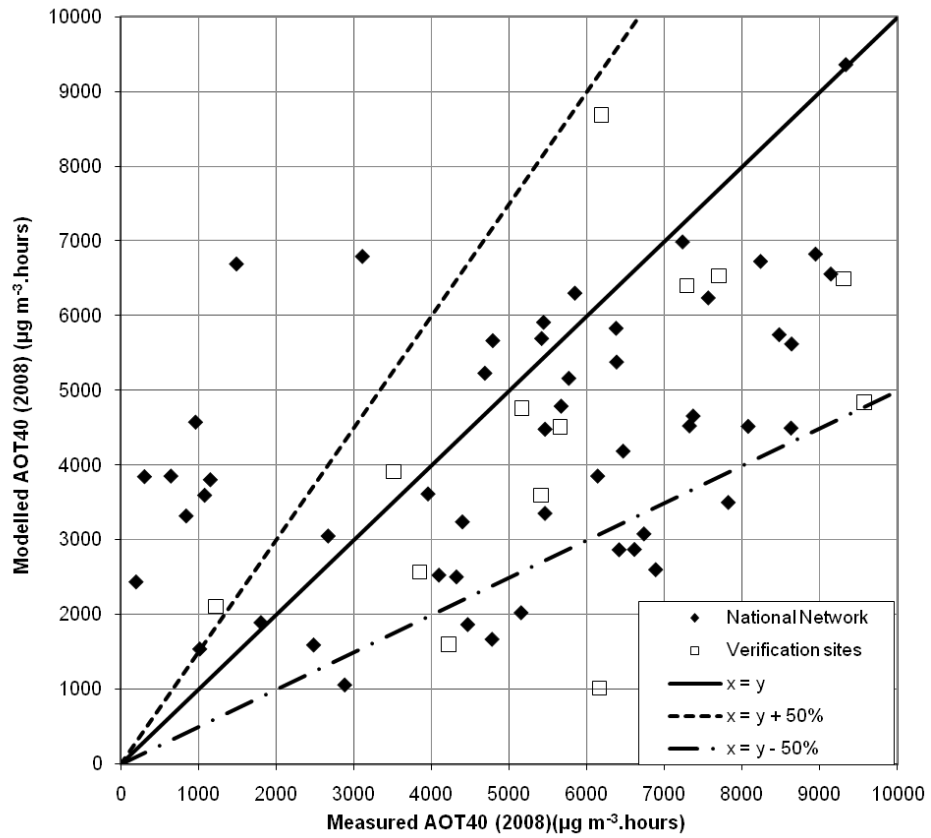

Figure 4.8: UKAAQA empirical model verification

(AOT40, µg m^{-3}.hours)

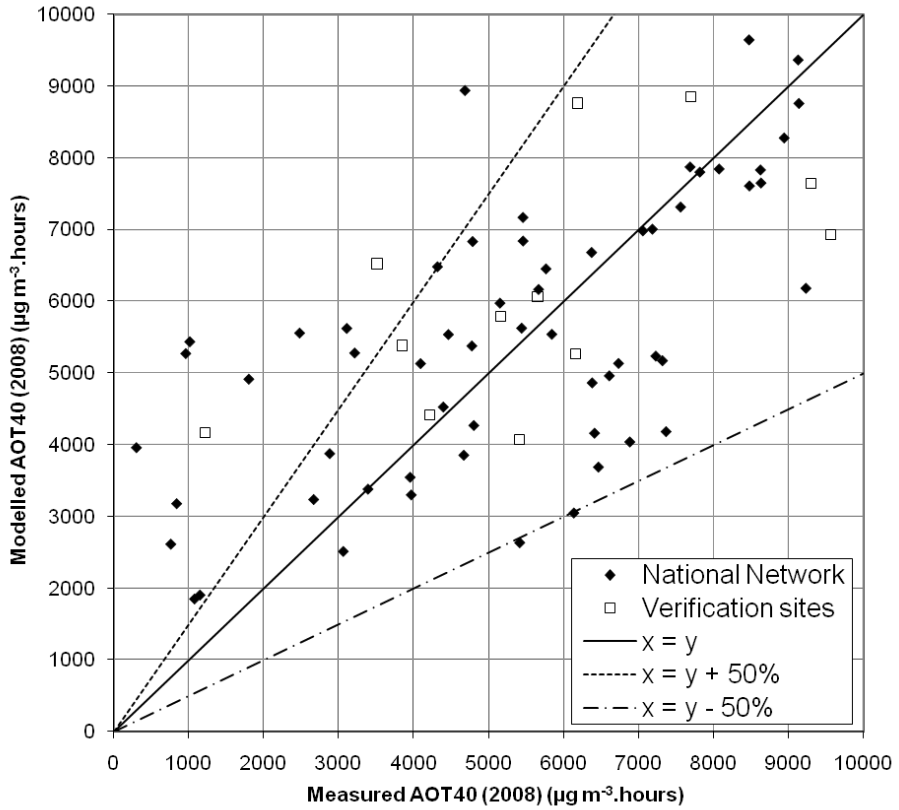

Table 4.1: OSRM verification summary, days greater than 120 µg m^{-3} (2008)

DGT 120 metric	Year	Mean of measurements (days)	Mean of model estimates (days)	R^2	% outside DQO	No. sites used in assessment
National network	2008	5.3	6.5	0.19	44.8	58
Verification sites	2008	4.5	6.5	0.16	38.5	13

Table 4.2: UKAAQA empirical model verification summary, days greater than 120 µg m^{-3} (2008)

DGT 120 metric	Year	Mean of measurements (days)	Mean of model estimates (days)	R^2	% outside DQO	No. sites used in assessment
National network	2008	4.9	5.4	0.47	49.3	67
Verification sites	2008	4.5	7.1	0.16	58.3	13

Table 4.3: OSRM verification summary – AOT40 metric (2008)

AOT40 metric	Year	Mean of measurements (µg m^{-3}.hours)	Mean of model estimates (µg m^{-3}.hours)	R^2	% outside DQO	No. sites used in assessment
National network	2008	6025	4444	0.23	16.4	61
Verification sites	2008	5787	4559	0.33	23.1	13

Table 4.4: UKAAQA empirical model verification summary – AOT40 metric (2008)

AOT40 metric	Year	Mean of measurements (µg m^{-3}.hours)	Mean of model estimates (µg m^{-3}.hours)	R^2	% outside DQO	No. sites used in assessment
National network	2008	6160	5985	0.36	25.3	75
Verification sites	2008	5787	6475	0.38	15.4	13

The OSRM days greater than 120 µg m^{-3} verification presented in Figure 4.5 and Table 4.1, show that there is a high degree of scatter across all sites in 2008. **In general the OSRM over predicted the measured metric** as it did in 2007, though the overall bias in the 2008 simulations is smaller than it was for 2007 (Murrells et al, 2009b). Table 4.1 suggests that the model performance was similar for the national network and verification sites. The overall performance may be slightly better than it was for 2007 and this might partly reflect the improvements made in the initialisation parameters for the OSRM since the 2007 simulations were done. The percentage of sites outside the DQO range was 38.5% for the verification sites and 44.8% for national network sites.

Figure 4.6 shows that the UKAAQA empirical map of the days greater than 120 µg m^{-3} metric has no obvious bias. However, the percentage of sites outside the data quality objective for both the national network (49.3%) and verification sites (58.3%) is similar to or higher than the OSRM map. Table 4.2 shows that the average UKAAQA modelled and measured results

are similar for both the national network sites and fairly similar for the independent verification sites that provide a more meaningful indicator of model performance.

For the AOT40 metric, **the OSRM** (Figure 4.7 and Table 4.3) **generally under predicted concentrations** and the UKAAQA empirical map (Figure 4.8 and Table 4.4) performed better. Again, the overall bias in the 2008 OSRM simulations is smaller than it was for 2007.

In addition to the verification plots, the model outputs from the OSRM and the UKAAQA empirical model at each monitoring station have been plotted against one another for both metrics as shown in Figures 4.9 and 4.10. Figure 4.9 (the days greater than 120 µg m^{-3} metric) and Figure 4.10 (AOT40 metric) show that OSRM estimates higher concentrations than the UKAAQA empirical model in the national network sites for the days greater than 120 µg m^{-3}, but underestimates the AOT40.

Past analysis (Hayman et al, 2006b) has shown that the OSRM has slightly under predicted measured concentrations in some cases and slightly over predicted measured concentrations in others. In general, it has underpredicted ozone metrics in high ozone years (e.g. 2003 and 2006) and slightly overpredicted ozone metrics in low ozone years (2004, 2005 and 2007, Murrells et al, 2009b).

Tables 4.5 and 4.6 below present the average measured and averaged modelled results from OSRM for the years 2004, 2005, 2006, 2007 and 2008. These illustrate the model performance during high (2006) and low (2004, 2005, 2007) years for both metrics. The difference between the concentrations predicted by the OSRM and the measured concentrations is larger for 2006 than for 2004, 2005, 2007 and 2008. However, the 2008 OSRM results are not directly comparable with earlier years because the initialisation parameters have been improved and this may have led to slightly better agreement with measurements in 2008 than is apparent for 2007.

4.2.3 Summary and main conclusions

The main conclusions of the work of Objective 10.1 on modelling the UK ozone climate for 2008 using the OSRM are summarised as follows:

Summary:

- **When comparing the OSRM results with measured data for the two EU Air Quality Directive ozone metrics for 2008 the OSRM has generally overestimated the days greater than 120 µg m^{-3} metric and underestimated the AOT40 metric.**
- **Previously the OSRM overestimated these ozone metrics in low ozone years (2004, 2005 and 2007) and underestimated them in high ozone years (2003 and 2006) compared with measured data. In 2008, a moderate ozone year, a mixed effect was observed, but overall there is less of a systematic bias in the model results in the 2008 simulations than there was in the 2007 simulations.**
- **The UKAAQA empirical model continues to produce results that are closer to the measured concentrations than the OSRM and should continue to be used in its current capacity (contributing modelled data in fulfilment of UK reporting obligations to the European Commission).**

Work is in progress modelling the UK ground-level ozone climate for 2009. This will be based on meteorology data and emission estimates for the 2009 calendar year. The meteorology data have been acquired and processed and the emissions data developed by forecasting one year on from the 2008 inventory (2008 NAEI).

Figure 4.9: Comparison of OSRM against UKAAQA empirical model (Days greater than 120 µg m^{-3})

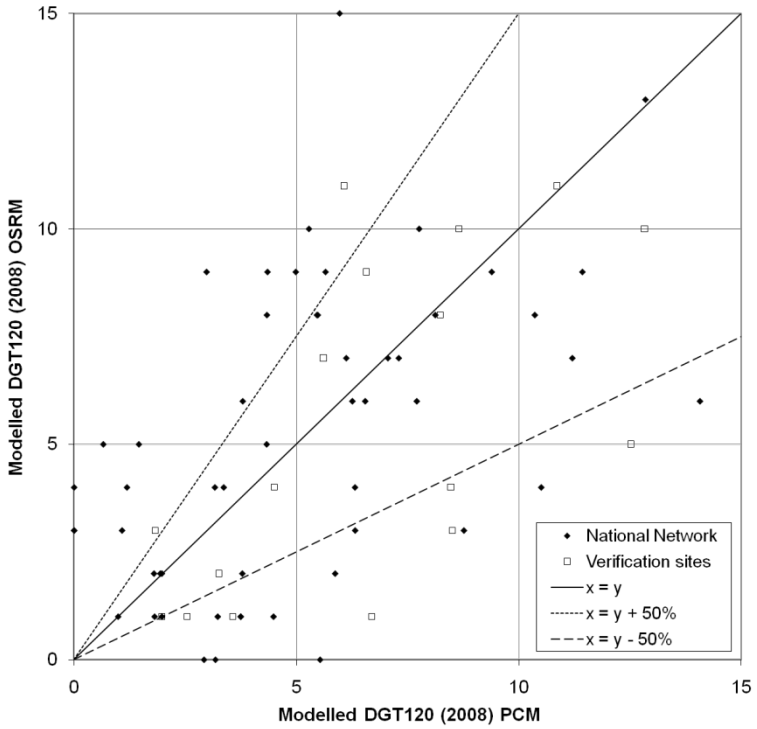

Figure 4.10: Comparison of OSRM against UKAAQA empirical model (AOT40, µg m^{-3}.hours)

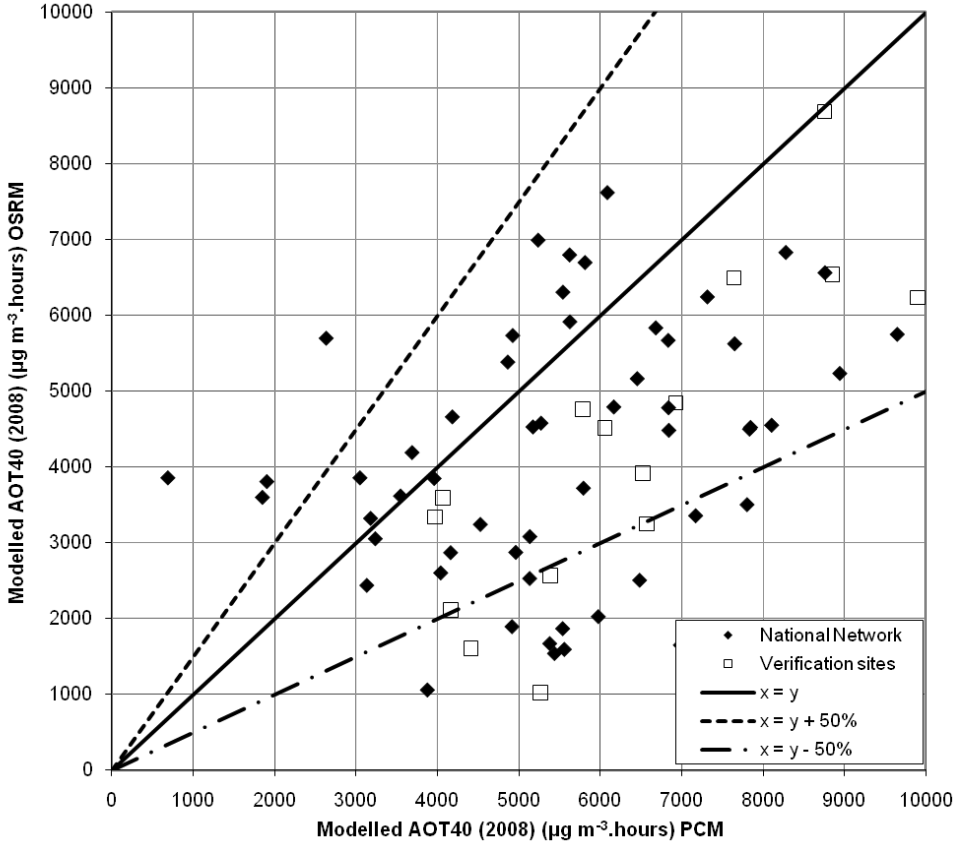

Table 4.5: Days greater than 120 µg m^{-3}. OSRM results from 2004-2008

		National network		Verification sites	
Year modelled	**NAEI Year**	**Mean of measured**	**Mean of modelled**	**Mean of measured**	**Mean of modelled**
2004	2004	13	12	7	6
2005	2004	3	6	4	5
2005	2005	3	6	4	5
2006	2005	13	8	8	8
2007	2006	2	4	2	6
2008	2007	5	6	5	7

Table 4.6: AOT40 (µg m^{-3}.hours). OSRM results from 2004-2008

		National network		Verification sites	
Year modelled	**NAEI Year**	**Mean of measured**	**Mean of modelled**	**Mean of measured**	**Mean of modelled**
2004	2004	2888	2056	3681	2256
2005	2004	3650	4165	3810	3088
2005	2005	3650	4099	3810	3372
2006	2005	10497	5043	5061	6574
2007	2006	2281	4503	3061	5211
2008	2007	6025	4444	4913	4559

4.3 Modelling support for policy development and implementation

Objective 10.2 is largely to support Defra's development and implementation of policy relating to ozone and secondary PM on an *ad-hoc* basis, either through running simulations with the OSRM or PTM for different scenarios or by providing general advice and analysis on specific topics.

During the 2010 reporting year, there have been two main areas of activity.

The OSRM has been used to forecast UK ozone concentrations in 2020 for two different meteorology conditions using the latest emission projections in the NAEI and EMEP. The projections have been updated twice during 2010 and further simulations are being performed for various alternative emission reduction scenarios to inform Defra on specific policies.

The PTM has been used to perform probabilistic uncertainty analysis to assess uncertainties in modelled ozone concentrations due to different chemical reaction schemes and other model parameters.

4.3.1 UK ozone concentrations in 2020 modelled using the OSRM

One of the principal aims of the modelling support for Defra policy development and implementation has been to develop UK ozone projections for 2020 to use as a base case against which alternative future emission scenarios can be assessed. An example is for assessing the impact of alternative national emission ceilings proposed or considered under revisions to various international protocols and directives.

As ground-level ozone concentrations are strongly influenced by meteorology conditions, the OSRM has been used to model UK ozone in 2020 characterised by two different meteorology situations: that characterised by conditions in 2006, a year when there were hot, dry periods in the summer leading to high episodes of ozone concentrations and that characterised by conditions in 2007 which was a relatively low ozone year.

4.3.1.1 Modelling approach and assumptions

During the course of the reporting year, two groups of simulations were performed using different UK and European baseline emissions data.

Initially, UK-scale simulations were performed for base year emissions in 2007 and 2020 using 2006 and 2007 meteorology (Phase 1). This enabled us to see how changing emissions (from 2007 to 2020) affects UK ozone using the same meteorology (either 2006 or 2007) and how UK ozone calculated for the same emissions (2020) depends on different meteorology conditions (2006 and 2007).

The UK emissions for 2007 were based on the 2007 version of the NAEI 1x1km gridded inventory (Bush et al, 2010). NAEI emission projections for 2020 at the SNAP 1 sector level derived from the UEP37 energy projections were applied to the 2007 NAEI gridded inventory. For other European countries in the EMEP domain, a combination of the 2007 EMEP 50x50km gridded emissions ('expert emissions') and country totals were used and these were scaled forward to 2020 using EMEP 2020 country totals. For shipping emissions, the gridded inventory recently developed by Entec for 2007 was used in place of the EMEP inventory for shipping and 2020 emissions for SO_2 were scaled down by 80% for all sea areas in accordance with the MARPOL agreement (Entec, 2010).

In the next phase (Phase 2), the 2020 ozone simulations were updated with more recent gridded inventory data and emission projections for the UK and rest of Europe and runs repeated using 2006 and 2007 meteorology. These simulations used 2008 NAEI 1x1km gridded inventory for the UK combined with 2020 emission projections from the UEP38 energy projections. For other European countries in the EMEP domain, a combination of the 2008 EMEP 50x50km gridded emissions and country totals were used and were scaled forward to 2020 using country totals from the 2020 PRIMES baseline projections in the IIASA CIAM report "Scope for further environmental improvements in 2020 beyond baseline projections" (IIASA, 2010). For countries/pollutants with no value given in that report, the 2020 EMEP values (projected from 2008) were used. As these projections are more consistent with other air quality modelling and assessments currently being undertaken for Defra policy, the ozone results from this phase will be used as the 2020 base for alternative emission scenarios to be assessed.

The initialisation conditions used for each year were monthly 1998 STOCHEM values with the addition of the O_3 trend derived from the STOCHEM business-as-usual plus climate change scenario for ozone concentrations and linear interpolation between 1998 and 2030 STOCHEM values for the concentrations of other species initialised in the model. This differs from the approaches used for the recent annual simulations which used a Mace Head adjustment to account for annual variability in hemispheric baseline ozone concentrations (see Section 4.2). With no adjustment available for 2020, it was decided to use the same, unadjusted initialisation parameters based on STOCHEM to make the 2007 and 2020 simulations comparable.

The hourly ozone concentrations results for each of the four scenarios were processed to produce averages or population-weighted means of four different ozone concentration metrics for England, Scotland, Wales, Northern Ireland, Inner and Outer London and the whole of the UK. The metrics were:

- AOT40
- Number of days where the maximum 8-hour mean exceeds 120µgm^{-3}
- Annual mean
- Daily maximum 8-hour mean

The focus will be on the first two metrics as these relate to the target values and long-term objectives for ozone in the Air Quality Directive as shown in Tables 4.7 and 4.8. They are included here to put the predicted ozone concentrations for 2020 in context.

10x10 km maps of each of these metrics were also produced for each scenario.

Table 4.7: Target values for O_3

Objective	Averaging period	TV	Date by which TV is to be met[3]
Protection of human health	Maximum daily eight-hour mean[4]	120 µg m^{-3} not to be exceeded on more than 25 days per calendar year averaged over three years	1 January 2010
Protection of vegetation	May to July	AOT40 (calculated from 1 h values) 18 000 µg m^{-3}. h averaged over five years[5]	1 January 2010

Table 4.8: Long term objectives for O_3

Objective	Averaging period	LTO	Date by which LTO is to be met
Protection of human health	Maximum daily eight-hour mean within a calendar year	120 µg m^{-3}	Not defined
Protection of vegetation	May to July	AOT40 (calculated from 1 h values) 6000 µg m^{-3}. h	Not defined

4.3.1.2 Comparing UK ozone projections in 2020 with ozone in 2007

Table 4.9 shows the results for the **AOT40 metric** for 2007 and 2020 modelled assuming 2006 meteorology. Table 4.10 shows the corresponding results assuming 2007 meteorology.

Apart from Scotland, the AOT40 values are higher under 2006 meteorology conditions than under 2007 conditions and in both cases, the change in emissions for 2020 leaves to higher AOT40 values in 2020 than in 2007.

[3] Compliance with target values will be assessed as of this date. That is, 2010 will be the first year the data for which is used in calculating compliance over the following three or five years, as appropriate.
[4] The maximum daily eight-hour mean concentration shall be selected by examining eight-hour running averages, calculated from hourly data and updated each hour. Each eight -hour average so calculated shall be assigned to the day on which it ends. i.e. the first calculation period for any one day will be the period from 17:00 on the previous day to 01:00 on that day; the last calculation period for any one day will be the period from 16:00 to 24:00 on the day.
[5] If the three or five year averages cannot be determined on the basis of a full and consecutive set of annual data, the minimum annual data required for checking compliance with the target values will be as follows:
— for the target value for the protection of human health: valid data for one year,
— for the target value for the protection of vegetation: valid data for three years.

Table 4.9: UK ozone concentrations expressed as the AOT40 metric based on 2006 meteorology.

	2006 Met Year	
AOT40 (µgm^{-3}.hr)	**Base 2007**	**Base 2020**
Scotland	5414	9066
Wales	6410	10628
Northern Ireland	5518	8874
Inner London	3911	8012
Outer London	3963	7962
Rest of England	5635	10488
All UK	5609	9916

Table 4.10: UK ozone concentrations expressed as the AOT40 metric based on 2007 meteorology.

	2007 Met Year	
AOT40 (µgm^{-3}.hr)	**Base 2007**	**Base 2020**
Scotland	6016	10381
Wales	5457	9150
Northern Ireland	4637	7906
Inner London	2549	6152
Outer London	2743	6519
Rest of England	4873	9329
All UK	5276	9564

Figures 4.11-4.14 show maps of AOT40 for 2007 and 2020 emissions under each set of meteorological conditions.

The maps generally show higher AOT40 values in 2020 than 2007, but there are different spatial patterns for the two different meteorology years. The highest concentrations are found in the far south-west of the country when using the 2006 meteorological data, with high concentrations along the south coast and the far north-west of Scotland. With the 2007 meteorology there are still high concentrations in the south-west (though lower than for the 2006 meteorology), but the highest concentrations are in the north-east of Scotland.

The reason for the higher concentrations predicted using the 2007 meteorology in Scotland (as also seen in the regional averages in Tables 4.9 and 4.10) seems to be due to the "coastal effect". This was described in previous project annual reports (Murrells et al 2009b) and appears to be more pronounced when using the 2007 meteorological data than the 2006.

Figure 4.11. UK ozone concentrations in 2007 for the basecase expressed as the AOT40 metric for the protection of vegetation based on 2006 meteorology.

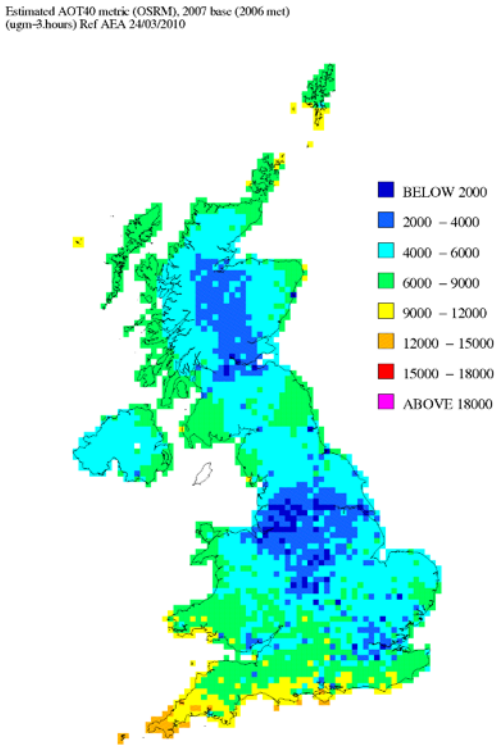

Figure 4.12. UK ozone concentrations in 2020 for the basecase expressed as the AOT40 metric for the protection of vegetation based on 2006 meteorology.

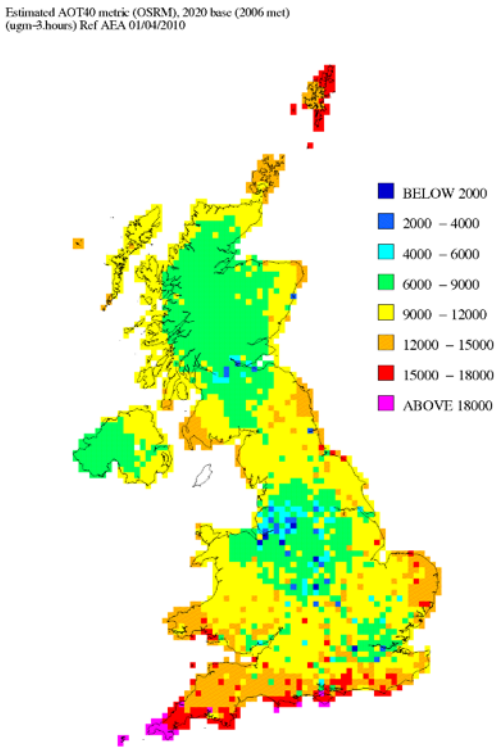

Figure 4.13: UK ozone concentrations in 2007 for the basecase expressed as the AOT40 metric for the protection of vegetation based on 2007 meteorology.

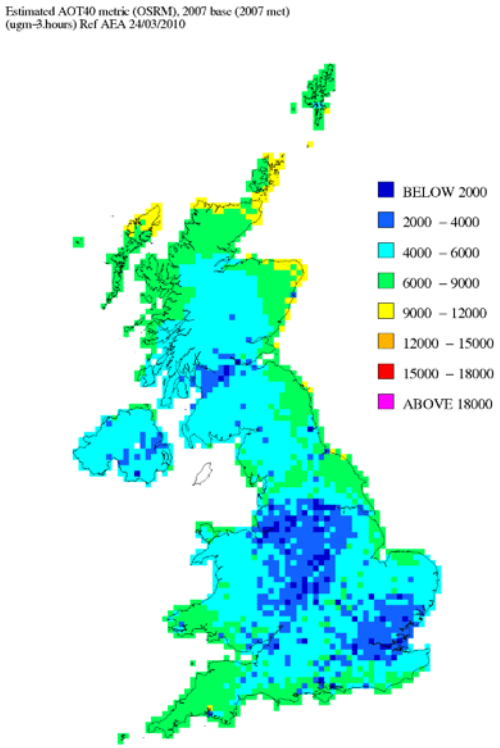

Figure 4.14: UK ozone concentrations in 2020 for the basecase expressed as the AOT40 metric for the protection of vegetation based on 2007 meteorology.

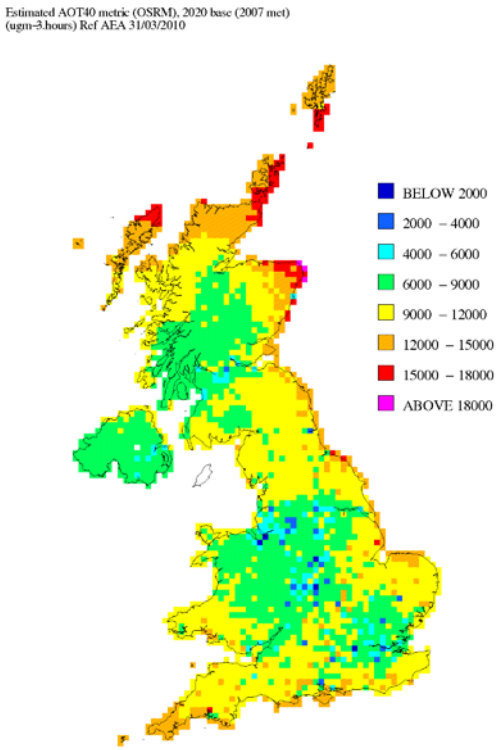

Table 4.11 shows the population-weighted mean results for **the Days Greater than 120 µgm^{-3} metric** for 2007 and 2020 modelled assuming 2006 meteorology. Table 4.12 shows the corresponding results assuming 2007 meteorology.

Table 4.11: UK ozone concentrations expressed as the population-weighted number of days when the maximum 8-hour mean exceeds 120 µgm^{-3} based on 2006 meteorology.

	2006 Met Year	
Population-weighted no. days exceeding 120µgm^{-3}	**Base 2007**	**Base 2020**
Scotland	3.53	7.18
Wales	9.88	15.39
Northern Ireland	6.24	10.83
Inner London	5.86	9.20
Outer London	5.56	7.79
Rest of England	6.15	10.81
All UK	6.05	10.41

Table 4.12: UK ozone concentrations expressed as the population-weighted number of days when the maximum 8-hour mean exceeds 120 µgm^{-3} based on 2007 meteorology.

	2007 Met Year	
Population-weighted no. days exceeding 120µgm^{-3}	**Base 2007**	**Base 2020**
Scotland	4.48	9.62
Wales	2.74	7.27
Northern Ireland	0.90	2.32
Inner London	0.09	5.11
Outer London	1.44	6.05
Rest of England	2.82	7.10
All UK	2.68	7.02

The results show a similar pattern to the AOT40 metric, with the model predicting more days exceeding in 2020 than in 2007 under the same meteorology conditions. There are also predicted to be more days exceeding in the runs using the 2006 meteorology than the 2007 meteorology in all regions except Scotland. The difference between the results from the different meteorology years is more striking than that seen with the AOT40 metric. This indicates that the 2006 meteorological conditions produced far more very high peak ozone days than the 2007 conditions.

Figures 4.15-4.18 show maps of Days Greater than 120µgm^{-3} metric for 2007 and 2020 emissions under each set of meteorological conditions.

Figure 4.15: UK ozone concentrations in 2007 expressed as the number of days when the maximum 8-hour mean exceeds 120 μgm^{-3} based on 2006 meteorology.

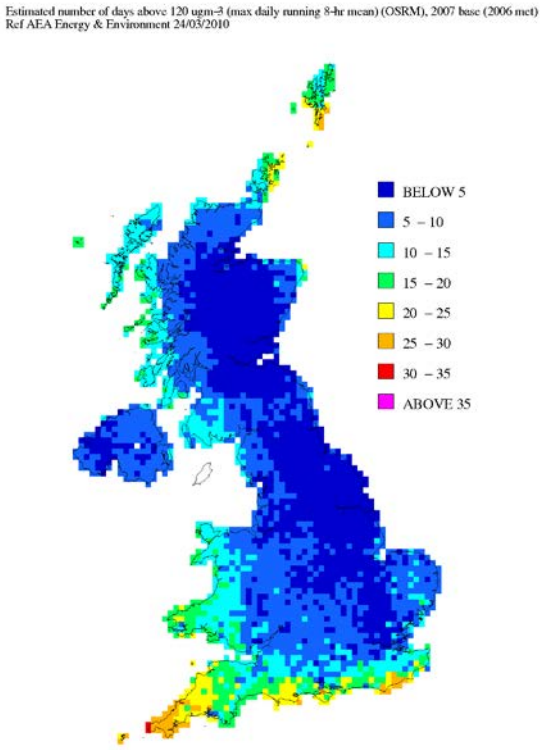

Figure 4.16: UK ozone concentrations in 2020 expressed as the number of days where the maximum 8-hour mean exceeds 120 μgm^{-3} based on 2006 meteorology.

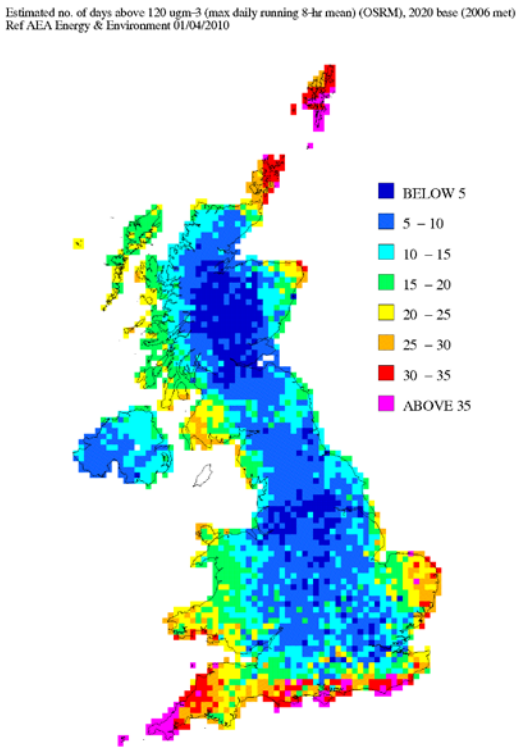

Figure 4.17: UK ozone concentrations in 2007 expressed as the number of days when the maximum 8-hour mean exceeds 120 µgm^{-3} based on 2007 meteorology.

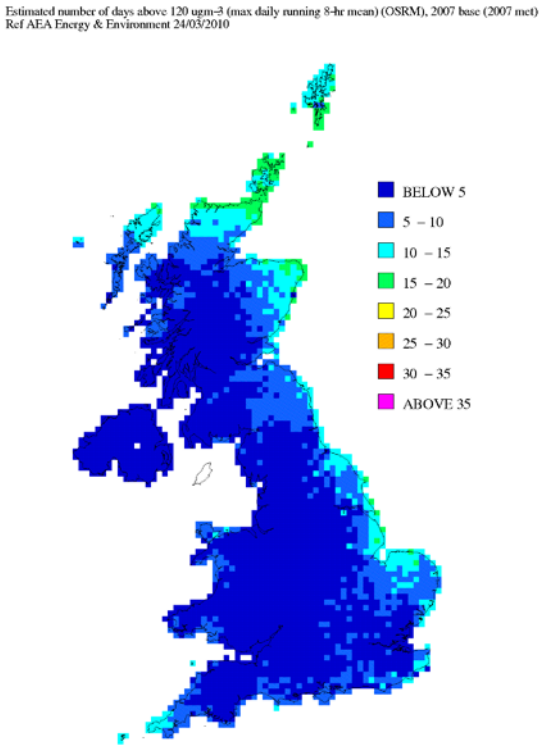

Figure 4.18: UK ozone concentrations in 2020 expressed as the number of days when the maximum 8-hour mean exceeds 120 µgm^{-3} based on 2007 meteorology.

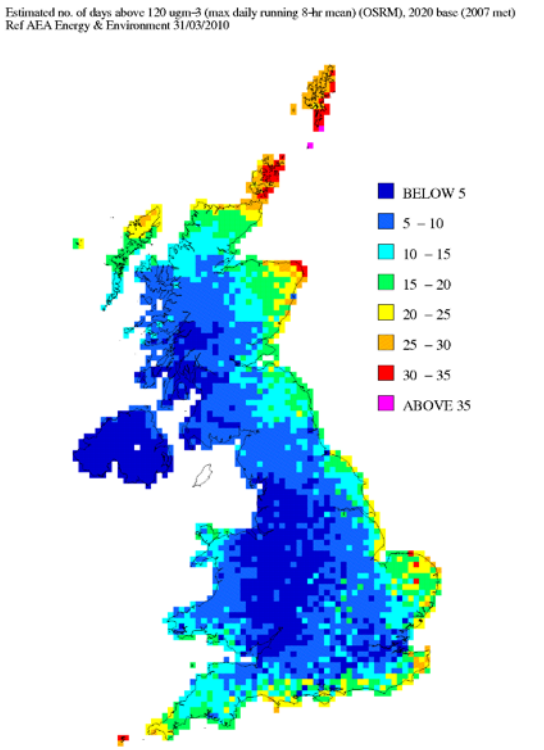

As seen for the AOT40 metric, the maps generally show higher number of days greater than 120 μm^{-3} occurring in 2020 than in 2007, but there are different spatial patterns for the two different meteorology years. Using the 2006 meteorological data, the highest number of exceedence days are in the south-west of the UK. There is a more distinct decrease in the metric value as you move north and east, but with higher values again occurring in the far north-east of Scotland. When using the 2007 meteorology the highest concentrations are in the north-east of Scotland, with a much smaller increase apparent in the south-west relative to the rest of the UK. The values found when using the 2006 meteorological data are generally larger than those from the 2007 meteorological data.

The main conclusion to emerge for this work is that ozone concentrations expressed in different metrics are predicted to be higher in 2020 than in 2007 as a results of changes in emissions when the same meteorological conditions are assumed. The spatial pattern in concentrations and the effect of meteorological conditions are different for different metrics.

4.3.1.3 Updated UK ozone projections for 2020

As described earlier, the base UK ozone projections for 2020 were updated with more recent gridded inventory data and emission projections.

Table 4.13 shows the population-weighted metric for the number of days when the daily maximum running 8-hour mean concentration exceeds 120 μgm^{-3} for different areas of the UK and UK as a whole assuming 2006 and 2007 meteorology.

Table 4.13: Population-Weighted Number of Days when the Daily Maximum Running 8 Hourly Ozone Concentration exceeds 120 ugm^{-3} for Areas of the UK and the UK as a Whole

Population-Weighted Number of Days when the Daily Maximum Running 8 Hourly Ozone Concentration exceeds 120 ugm^{-3}	Scotland	Wales	Northern Ireland	Inner London	Outer London	Rest of England	All UK
2020 Base (Met 2006)	7.5	16.3	11.1	16.3	15.6	14.2	**13.8**
2020 Base (Met 2007)	10.2	7.5	2.4	10.3	10.1	8.2	**8.4**

The results indicate higher ozone concentrations in 2020 than had previously been forecast (Tables 4.11 and 4.12), but still show lower ozone levels for 2007 meteorology compared with 2006 meteorology in most areas of the UK except Scotland.

Table 4.14 shows the area-weighted AOT40 metric for different areas of the UK and UK as a whole assuming 2006 and 2007 meteorology.

Table 4.14: Area-Weighted AOT40 Crops (ugm^{-3}.hours) for Areas of the UK and the UK as a Whole

Area-Weighted AOT40 Crops (ugm^{-3}.hours)	Scotland	Wales	Northern Ireland	Inner London	Outer London	Rest of England	All UK
2020 Base (Met 2006)	9117	11082	9147	12514	12155	12317	**10962**
2020 Base (Met 2007)	10147	9706	7884	9346	9250	10227	**10015**

Again, the results indicate higher ozone concentrations in 2020 than had previously been forecast (Tables 4.9 and 4.10), but still show lower ozone levels for 2007 meteorology compared with 2006 meteorology in most areas of the UK except Scotland.

Table 4.15 shows annual mean concentrations of ozone for different areas of the UK and UK as a whole assuming 2006 and 2007 meteorology.

Table 4.15: Area-Weighted Annual Mean (ugm^{-3}) for Areas of the UK and the UK as a Whole

Area-Weighted Annual Mean (ugm^{-3})	Scotland	Wales	Northern Ireland	Inner London	Outer London	Rest of England	All UK
2020 Base (Met 2006)	68.7	71.2	69.1	61.1	60.5	65.5	**67.2**
2020 Base (Met 2007)	71.9	71.9	71.5	60.1	59.9	66.0	**68.7**

For this metric, concentrations are generally higher when using 2007 meteorology than 2006 meteorology.

Updated maps of the days greater than 120 μgm^{-3} and AOT40 metrics for 2020 using 2006 and 2007 meteorology are shown in Figures 4.19 to 4.22.

The results from this work will form the baseline ozone concentrations against which the effects of alternative emission reduction scenarios in the UK and the rest of Europe will be modelled.

Figure 4.19: 2006 Meteorology Runs: Days greater than 120ugm^{-3} Map

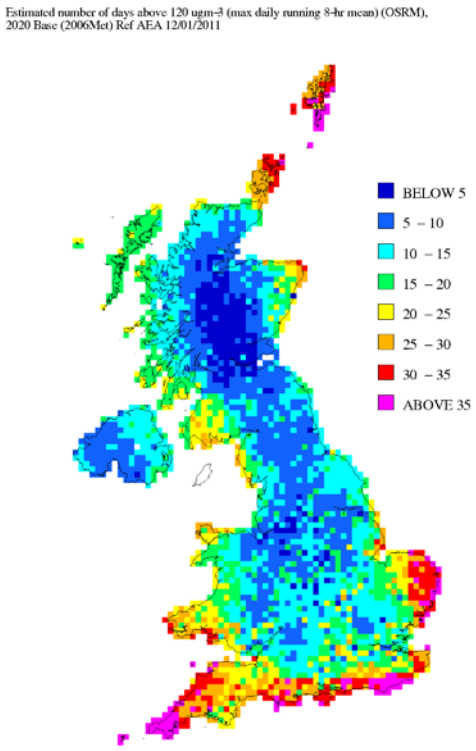

Figure 4.20: 2007 Meteorology Runs: Days greater than 120 ugm^{-3} Map

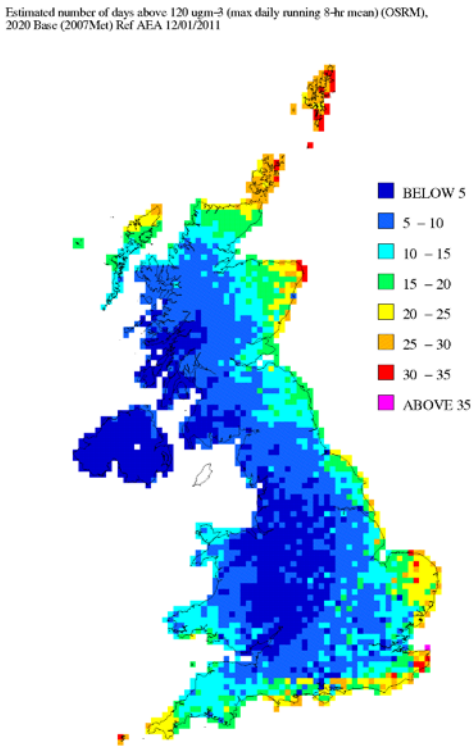

Figure 4.21: 2006 Meteorology Runs: AOT40 (ugm^{-3}.hours) Map

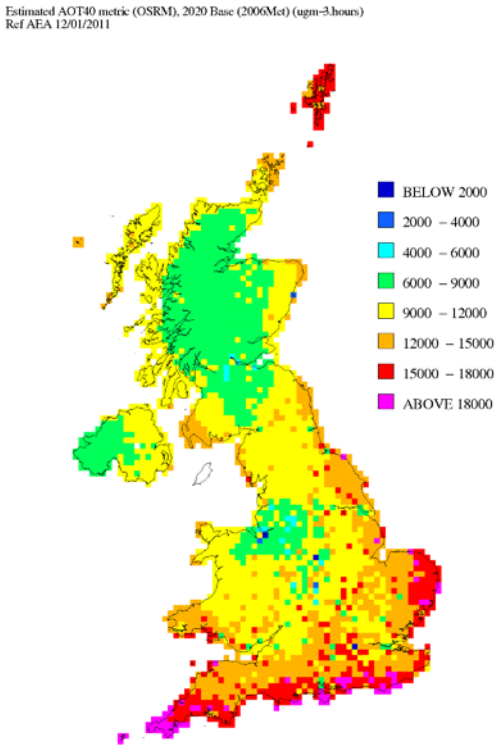

Figure 4.22: 2007 Meteorology Runs: AOT40 (ugm^{-3}.hours) Map

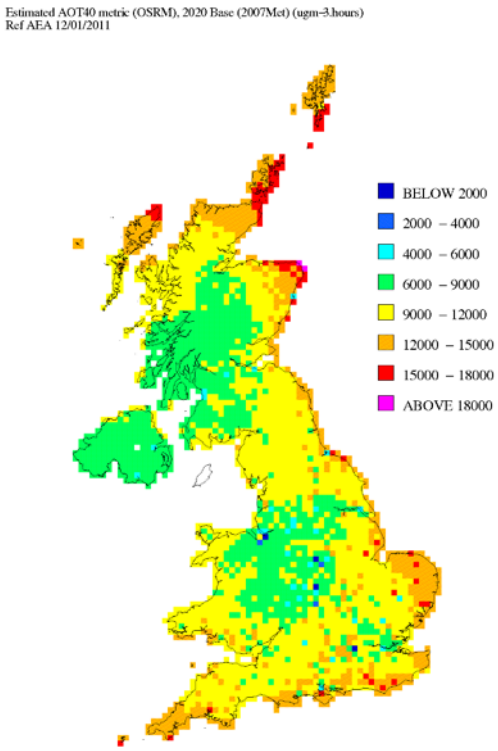

4.3.2 Probabilistic uncertainty analysis of sample emission scenarios using the PTM

Probabilistic model evaluation addresses the issues surrounding how to handle uncertainty within policy models used for analyses and assessment. It is recognised that tropospheric ozone models contain a large number of process descriptions and parameterisations and that each of these contain a number of input parameters to be fixed beforehand for the model to run successfully. Some of these parameters are well constrained by theory or by observation. However, many may be uncertain or may only be well constrained by observations in some regions of the model domain. Many different parameter sets within a model may be acceptable for reproducing observations. Equally well, it may not be possible to find a single optimal set of parameters which are able to reproduce all available observations. This is the equifinality issue.

Probabilistic uncertainty analysis techniques are being developed to address how best to handle uncertainty within the framework of the policy analyses and assessments being carried out by Defra.

4.3.2.1 Monte Carlo analysis of chemical mechanism uncertainties

An essential element of any tropospheric ozone model is some form of chemical mechanism. We cannot say that the atmospheric chemistry required to describe ozone formation is fully understood and so the choice and the detail represented in any chemical mechanism introduces uncertainties into the model results. By selecting different chemical mechanisms we can show how sensitive the model results are to the choice of chemical mechanism but this does not address the issue of uncertainty. Are highly explicit chemical mechanisms such as the Master Chemical Mechanism intrinsically more uncertain than compact and highly simplified mechanisms such as the Carbon Bond Mechanism? Where does the bulk of the uncertainty lie in a given chemical mechanism?

Following the Walker et al. (2009) PTM study of the PUMA Campaign in Birmingham during the summer of 1999, we have investigated in some detail the observed ozone episode on 26th June. The NAME model was used to provide 1000 equal probability 96-hour back-track air mass trajectories that arrived between 14:00 and 14:15 hrs at the surface at the Pritchatts Road, Birmingham monitoring site. Of these, one particular trajectory was selected such that, when employed in the PTM model, gave ozone predictions within the range of the observations for a range of AURN sites across the West Midlands conurbation. PTM model runs were employed using both the Carbon Bond Mechanism and the Master Chemical Mechanism.

Each of the 1193 rate coefficients in the MCM CRI v2 chemical mechanism or the 100 rate coefficients in the Carbon Bond Mechanism were allocated a 2-σ (or 95% confidence) uncertainty range of ± 30%. Then 10,000 PTM runs were performed in which each rate coefficient was randomly sampled within its uncertainty range. The ozone predictions for the 10,000 model runs were then ranked by ozone mixing ratio and the percentiles of the ozone distribution were evaluated. The 50%-ile ozone predictions were found to be 79.0 ppb with the Carbon Bond Mechanism and 79.2 ppb with the MCM CRI v2. This level of agreement indicates that the PTM shows little sensitivity to chemical mechanism for this ozone episode during the PUMA Campaign.

The 16%-ile to 84%-ile or 1-σ ranges were 22.0 and 22.3 ppb for the Carbon Bond Mechanism and CRI v2 mechanism, respectively, showing that the uncertainty ranges differed little despite there being a factor of 12 difference in the relative sizes of the chemical mechanisms. This is a surprising result that would tend to suggest that the bulk of the uncertainty in chemical mechanisms does not reside in the VOC chemistry since this chemistry is markedly different between the Carbon Bond and CRI v2 mechanisms. These results are being studied further to see whether they reflect the specific chosen conditions of the PUMA Campaign or whether they have more general validity.

A further Monte Carlo Analysis was performed in which the uncertainties in the VOC chemistry were set to zero and the only uncertainties sampled were in the 50 chemical reactions common to both mechanisms that set up the fast photochemical balance between the OH and HO_2 radicals. These are the so-called inorganic reactions. The 50%-ile ozone predictions were found to be 80.2 and 80.3 ppb, respectively, for the Carbon Bond and CRI v2 mechanisms, with the 16%-ile to 84%-ile ranges 21.0 and 21.3 ppb, respectively. By comparing the 16%-ile to 84%-ile ranges between the two Monte Carlo experiments, we see that the bulk of the uncertainty lies in the inorganic chemistry. There is little increase in the uncertainty of ozone model predictions in going from the compact and condensed Carbon Bond Mechanism to the CRI v2 mechanism which is based on the Master Chemical Mechanism, at least under the conditions studied here.

4.3.2.2 Monte Carlo analysis of all PTM model uncertainties

The above Monte Carlo study of the uncertainty arising in the PTM model predictions from the uncertainties in the rate coefficients in the chemical mechanism was then extended to address the uncertainties due to all model input parameters. To this end, subjective estimates have been made of the uncertainties in each of the input parameters to the PTM model. The estimated uncertainty ranges are illustrated in Table 4.16.

Then 10,000 PTM runs were performed in which each model input parameter was randomly sampled within its uncertainty range. The ozone predictions for the 10,000 model runs were then compared with the observed range of the AURN observations across the West Midlands conurbation for the afternoon of 26th June 1999. Where the PTM prediction was within the range of the observations, the combination of model input parameters was considered acceptable. If the model prediction was outside of the observed range, the run was rejected. Of the 10,000 model runs, 2602 were found to be acceptable. These acceptable model runs were subsequently used for policy analyses.

Table 4.16: Subjective estimates of uncertainty in each of the PTM model input parameters.

Parameter	Nature of uncertainty	Uncertainty range
Dry deposition velocity	multiplicative scaling	x 0 – 1
Longitude of position	additive	± 0.45^{o}
Latitude of position	additive	± 0.28^{o}
Emissions of NH_3, NO_x, SO_2, CO and CH_4	multiplicative scaling	x 0.7 – 1.3
VOC speciation	multiplicative scaling	x 0.7 – 1.3
isoprene emissions	multiplicative scaling	x 0.25 – 4.0
initial concentrations of O_3, CO, CH_4, H_2, NO_x, SO_2	multiplicative scaling	x 0.8 – 1.2
boundary layer depth	multiplicative scaling	x 0.7 – 1.3
relative humidity	multiplicative scaling	x 0.7 – 1.3
air temperature	additive	± 3^{o}
rate coefficients	multiplicative scaling	x 0.7 – 1.3
choice of trajectory	random selection out of 1000 equal probability 96-hour back track trajectories	

Two further sets of 10,000 PTM runs were then performed in which VOC and NO_x emissions were reduced by 30% across-the-board. For each of the 2602 acceptable model runs, the VOC and NO_x control responses were determined by difference from the base case. These VOC and NO_x control responses were then ranked in ascending order and the distribution percentiles were estimated. These distributions are illustrated in Figure 4.23.

The 95% confidence or 2-σ ranges of the VOC and NO_x control responses were found to be 2.7 – 38.1 ppb and -0.4 – 25.6 ppb, respectively. Hence there was a 10% chance that the emission reduction would bring the predicted ozone mixing ratio below 60 ppb with VOC control and a 5% chance with NO_x control. VOC controls would appear to be more likely to bring ozone below 60 ppb than NO_x controls for the specific episode conditions found during the PUMA Campaign of 26th June 1999.

Figure 4.23: Probabilistic assessment of responses to 30% reductions in NO_x or VOC emissions

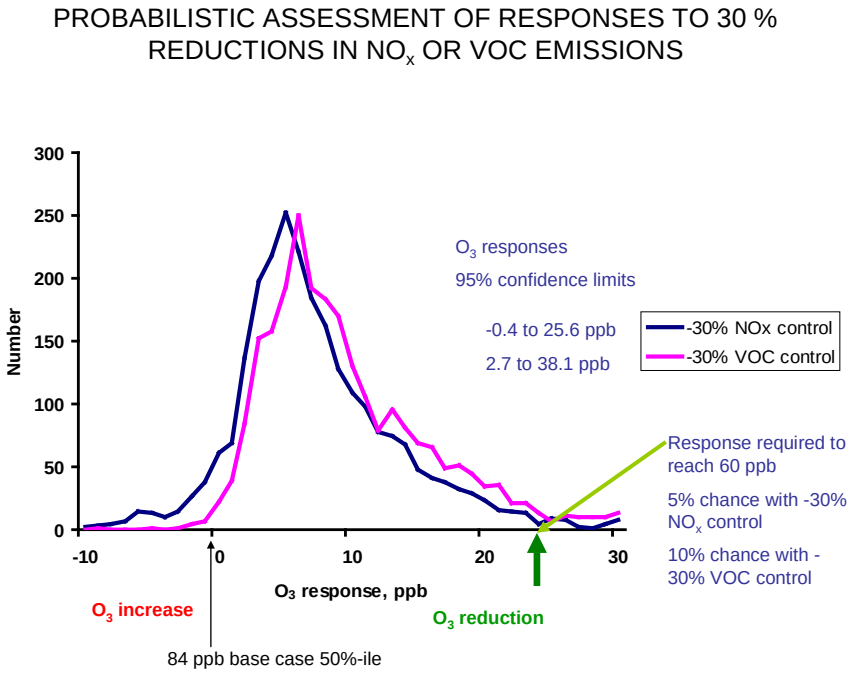

4.3.3 Summary and main conclusions

The main conclusions of the work of Objective 10.2 in terms of modelling support for Defra policy are summarised as follows:

Summary:

- **The OSRM has been used in conjunction with current UK and European emission projections to forecast the UK's ground-level ozone climate in 2020 assuming meteorology conditions representative of 2006 and 2007.**
- **Ozone concentrations expressed in different metrics are predicted to be higher in 2020 than in 2007 as a results of changes in emissions when the same meteorological conditions are assumed**
- **Concentrations are generally lower for 2020 when 2007 meteorology is assumed compared with concentrations modelled for 2020 assuming 2006**

meteorology. However, the spatial pattern in concentrations and the effect of meteorological conditions are different for different metrics.

- **The results from this work will form the baseline ozone concentrations for the UK against which the effects of alternative emission reduction scenarios in the UK and the rest of Europe will be modelled.**
- **Probabilistic uncertainty analysis using the PTM for simulating an ozone episode observed in Birmingham during the summer of 1999 showed that there was little sensitivity in the ozone model predictions to the choice of chemical mechanism used: the Carbon Bond Mechanism or CRIv2 condensed mechanism. However, this conclusion would need to be verified for other conditions to ascertain whether this conclusion had general validity.**
- **Probabilistic assessments of the PTM responses to 30% reductions in NO_x or VOC emissions indicated that for simulations leading to peak ozone concentrations in the West Midlands during 1999 there was only a 10% chance that VOC emission reductions would bring predicted ozone concentrations below 60ppb. However, there was only a 5% chance with NO_x emission control indicating that VOC controls would more likely bring ozone below 60ppb than NO_x control for these specific conditions.**

4.4 Specific modelling and assessments for policy development on secondary organic aerosols

Objective 10.3 involves specific modelling and assessments aimed at understanding sources of secondary air pollutants in the UK and the sensitivities to emission sources and model parameters.

During the 2010 reporting year, the focus has been on modelling secondary organic aerosols (SOA) using the PTM and in particular the spatial distribution of SOA and temporal variability in the context of man-made and natural precursor emissions.

4.4.1 Setting up a SOA scheme within the PTM model

This work began with the secondary organic aerosol (SOA) code coupled to the CRI mechanism as described in Utembe et al. (2009). The CRIv2 mechanism with the SOA code was implemented in the Photochemical Trajectory Model (PTM) and found to provide an efficient tool for the prediction of ozone and SOA concentrations.

The PTM was set up to provide mid-afternoon O_3 and SOA concentrations for each day of 2005/2006 for the Churchill Pumping Station site (CPSS), 20 km west of Birmingham using 96-hour back-track trajectories provided by the Met Office NAME model. The CPSS location was chosen because of the availability of daily organic carbon PM observations as reported by Yin et al. (2010).

The CRIv2 mechanism treated the degradation of methane and 115 non-methane VOCs and contained 1183 reactions involving 434 species. To describe SOA formation, 14 species were identified as appropriate surrogates for the species contributing to SOA formation in the MCMv3.1 simulations previously performed. Of these 14 species, 11 were formed from the oxidation of α- and β-pinene and so represented biogenic SOA formation and 3 were formed from the oxidation of aromatic compounds and so represented man-made SOA formation. Because the CRIv2 mechanism only addresses 115 non-methane VOCs, the VOC emissions were scaled up by a factor of 0.9079 to represent the same VOC emission mass as the PTM model runs using the MCMv3.1.

To represent the formation of intermediate or ISOA from the oxidation of the higher alkanes, 5 additional partitioning species were identified in the CRIv2 code as reasonable representations of the 1,4 hydroxycarbonyls formed from the oxidation of n-octane through to n-dodecane in the MCMv3.1 mechanism. The NAEI speciated VOC inventory provides for 18 additional C_8 – C_{14} alkanes that are not explicitly treated in the CRIv2 mechanism. They were then added to the model and their OH oxidation allocated to the peroxy radical product of the OH oxidation of n-dodecane. Diesel engine exhaust emissions contain higher C_{10} – C_{33} alkanes that are not carried in the NAEI and these were inferred relative to the diesel emissions of acetaldehyde as described in Liu et al. (2010).

To represent the formation of SOA from the oxidation of the higher aromatics, attention was first given to 4 aromatic compounds that are identified in the NAEI but are not explicitly treated in CRIv2. Their OH oxidation was allocated to peroxy radical products of a suitable aromatic that was in the CRIv2. Diesel engine exhaust emissions, in addition, contain C_{11} and higher aromatic compounds that are not in the NAEI. These were expressed relative to acetaldehyde using Liu et al., (2010) and added to the model.

4.4.2 Comparison of the PTM model results with observations for the Birmingham area

Figure 4.24 presents the time series of observations of PM_{10} organic carbon provided by the University of Birmingham for the Churchill Pumping Station site together with the daily 95%-ile, 84%-ile, 50%-ile, 16%-ile and 5%-ile points from the PTM model for the first half of 2006. The PTM model is able to account for all of the observed organic carbon episodes, particularly those during early January, early February, the middle of March and throughout May.

Figure 4.24: Time series of observed organic carbon concentrations shown as plus signs at the Churchill Pumping Station site near Birmingham for the first half of 2006, together with the PTM model 95%-ile, 84%-ile, 50%-ile, 16%-ile and 5%-ile points.

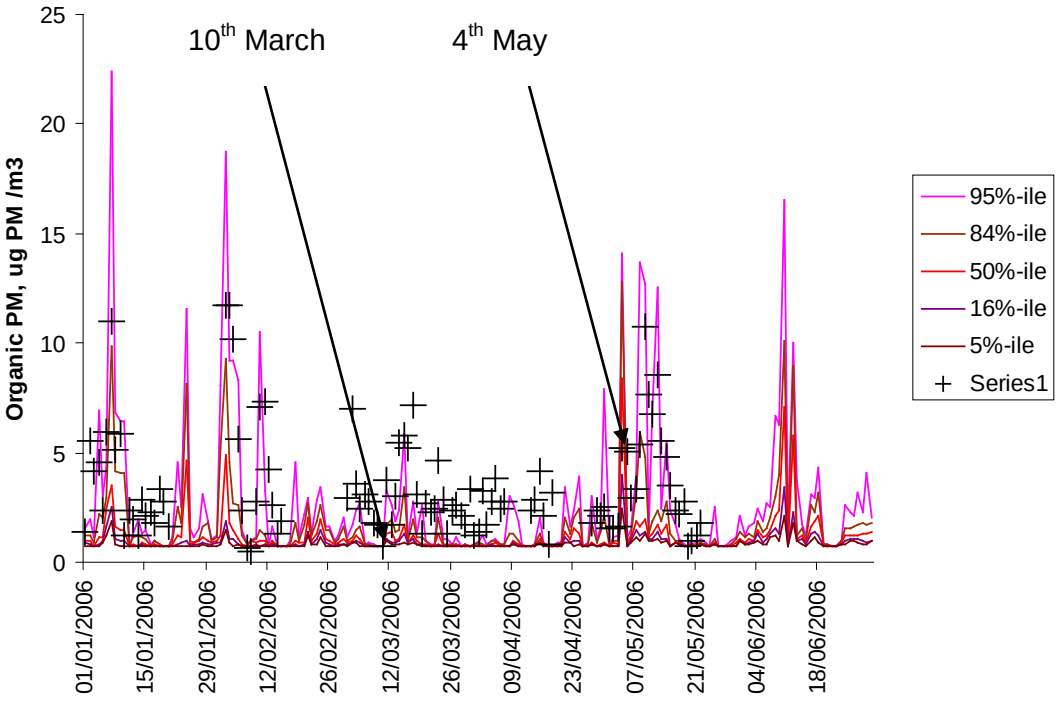

Of particular note were the model and observed features for 10th March and 4th May, see Figure 4.24. The observed OM episode on 4th May reached 5.2 µg C m^{-3} and was well predicted by the model with a 50%-ile of 8.4 µg OM m^{-3}. Inspection of the back-track trajectories indicated long range transport from France, Spain and Portugal as the likely

source of the SOA. The model SOA speciation pointed to biogenic emissions as the source of the model SOA.

Also of note was the observed feature on 10th March which showed exceptionally low observed OM levels of 0.7 µg C m^{-3} which compared well with the model predictions of 0.7 µg OM m^{-3}. The back-track trajectories indicated north westerly winds advecting clean air to the CPSS site. These results show that the background OM levels set in the SOA code are representative of the observations under clean air conditions.

However, the model shows a significant negative bias with the mean observed concentration 3.5 µg C m^{-3} and the model 50%-ile 1.11 µg OM m^{-3}. The mean normalised bias of the 50%-ile daily points was -0.59 and the fraction of points within a factor of 2 was 0.17. Both these evaluation metrics became acceptable if the 95%-ile points were selected. However, because the observations are reported in µg C m^{-3} instead of µg OM m^{-3}, model performance is in reality even poorer than these statistics would suggest.

The PTM model provided for each mid-afternoon time point a description of the speciation of the PM organic matter. The PTM model time series for the total organic PM mass, anthropogenic SOA, biogenic SOA, intermediate SOA (anthropogenic SOA from the oxidation of long chain alkanes and aromatics) and primary organic matter were then compared against the observed time series using scatter plots and linear regression. Of all the model PM organic components, the best correlations were found between the observed organic carbon concentrations and the model anthropogenic SOA concentrations (R^2 = 0.49). Whilst this level of correlation is considered acceptable, the slope of the linear regression shows that the model is significantly underestimating the observed organic carbon concentrations, see Figure 4.25. The level of correlation between the observed organic carbon concentrations and the model biogenic SOA, in comparison, was R^2 = 0.03 and this pointed to there being no significant association. Indeed, there was little elevation in model biogenic SOA levels during the periods when high organic carbon PM levels were observed. This pointed to anthropogenic SOA (or primary organic aerosol mass) as the cause of the observed organic PM episodes and not biogenic SOA.

The scatter plot between the observed organic carbon concentrations and the model calculated concentrations of primary organic aerosol mass also showed some evidence of an association, with R^2 = 0.47. However, the slope of the regression pointed to a considerable model underestimation of the model primary organic aerosol mass.

To investigate a number of possible explanations of the model underestimation of the observed organic PM mass concentrations reported by Yin et al., (2010), a series of model sensitivity experiments were performed. These sensitivity experiments were characterised as follows:

- base case,
- VOC*5: man-made VOC emissions scaled by a factor of 5,
- POAM*5: emissions of primary organic aerosol mass scaled by a factor of 5,
- the addition of oligomerisation to the SOA processes,
- terpene*5: biogenic terpene emissions scaled by a factor of 5,
- new terpene: addition of a detailed natural biogenic terpene emission inventory for the UK.

Inspection of the observed and model time series for the sensitivity cases showed that the model is able to account for most of the observed OC episodes with few exceptions. Most days in January are predicted reasonably well by the VOC*5 and POAM*5 cases. However, the 14th – 20th January period showed significant model underestimation, independent of sensitivity case. Most days in February were predicted reasonably well by the VOC*5 and POAM*5 cases. The pattern of model performance for March was mixed: the periods 6th – 9th and 26th – 30th were characterised by model underestimation. The episodes on 15th March, 15th April, 12th May were best predicted by the VOC*5 case, whereas those on 11th March

Figure 4.25: Scatter plot of the model 50%-ile anthropogenic SOA concentrations against the observed organic carbon PM concentrations for the first half of 2006 at the Churchill Pumping Station site near Birmingham

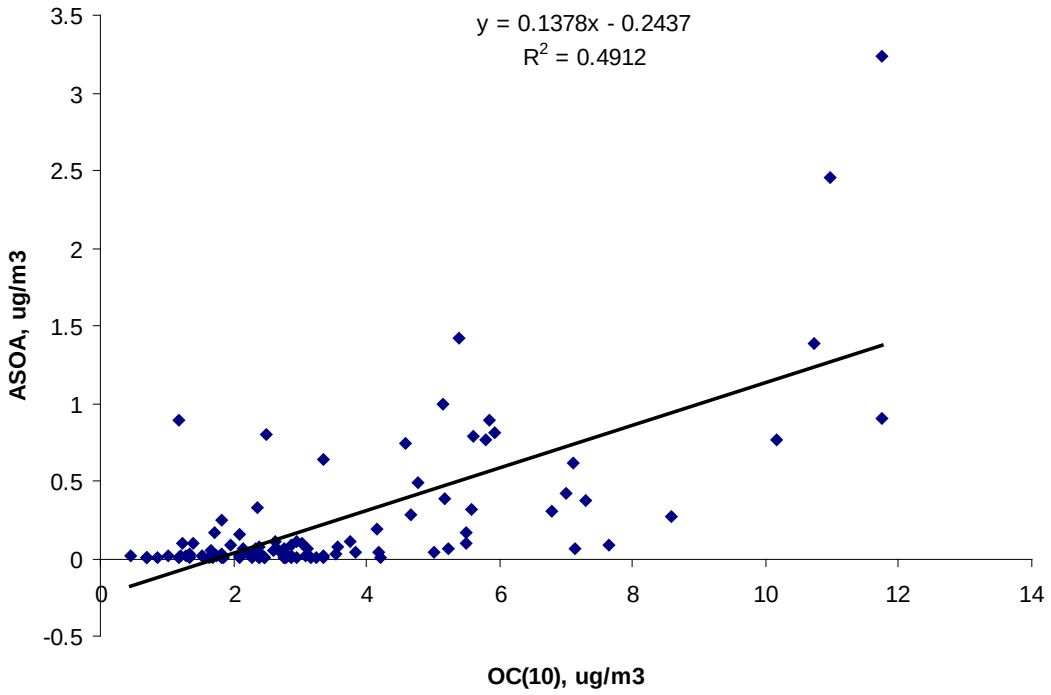

and 12th May were best predicted by the terpene*5 case. Interestingly, the long range transport episode described above on 4th May was best predicted by the base case model experiment and grossly overestimated by the terpene*5 case.

Model performance against observations is summarised in Table 4.17. On the basis of Table 4.17, a final SOA code was put together containing man-made VOC emissions scaled by a factor of 5, oligomerisation using the parameterisation described by Sakulyanontvittaya et al., (2008) and the natural biogenic terpene emission inventory for the UK from Stewart et al. (2003).

Table 4.17: Summary of model performance against observations for the five sensitivity cases covering the first half of 2006 for the CPSS site.

Statistics	Base case	VOC*5	POAM*5	Oligo	Terpene*5	New terp
model mean, µg OM m^{-3}	1.37	3.56	2.18	1.62	2.70	1.75
mean bias, µg OM m^{-3}	-2.13	+0.06	-1.32	-1.88	-0.80	-1.75
mean fractional bias	-0.53	-0.045	-0.32	-0.47	-0.21	-0.43
days within ± x2	27	53	51	35	48	42
RMS error, µg OM m^{-3}	2.86	3.86	2.25	2.71	5.56	2.59
slope of scatter plot	0.32	1.51	0.70	0.41	0.72	0.42
intercept of scatter plot	0.26	-1.73	-0.27	0.20	0.20	0.20
R^2 for scatter plot	0.42	0.51	0.51	0.37	0.09	0.40

4.4.3 Estimating the distribution of SOA across the UK for 2008

The final SOA code as described above was implemented in the PTM model. The emission inventory totals for SO_2, NO_x, VOC, NH_3 and CO were adjusted to the 2008 totals as given by the EMEP webdab. The Met Office NAME model was then used to provide 30 96-hour back-track inventories for 15:00z on each day of 2008 for 6 locations: Aston Hill, Auchencorth Moss, Glazebury, Harwell, High Muffles and Rochester. These meterological data were then interpolated for a further 6 locations: Eskdalemuir, Lullington Heath, Narberth, Sibton, Strath Vaich Dam and Yarner Wood.

Table 4.18 presents the main components of the organic aerosol from the PTM model for 2008 for the 12 sites. ASOA refers to the secondary organic aerosol formed from the oxidation of the man-made VOCs that are currently in the NAEI speciation. This component peaks at the Rochester site with a mass concentration of 0.84 µg PM m^{-3} because of its situation in the extreme south-east of the UK, receiving long range transport from continental Europe. ISOA refers to the man-made secondary organic aerosol that is formed from the additional man-made alkane and aromatic VOC precursors that are currently missing from the NAEI VOC speciation. ISOA levels peak at about 0.3 µg PM m^{-3} at the Glazebury and Rochester sites because of the proximity of these sites to sources of VOCs in the north of England and in the continent of Europe, respectively. Adding together the man-made contributions from ASOA and ISOA, total man-made SOA peaks at just under 1.2 µg PM m^{-3} at the Rochester site. Levels of total man-made SOA show a minimum at the Auchencorth Moss site in the lowlands of Scotland reaching a level that is about one half of the level predicted for Rochester.

Table 4.18: Mass concentrations of the organic aerosol components predicted for 12 UK sites in 2008 using the PTM model.

Site	ASOA, µg PM m^{-3}	ISOA, µg PM m^{-3}	Total man-made SOA, µg PM m^{-3}	BSOA, µg PM m^{-3}
Aston Hill	0.535	0.196	0.730	1.115
Auchencorth	0.444	0.159	0.603	2.195
Eskdalemuir	0.411	0.142	0.553	2.197
Glazebury	0.765	0.312	1.077	0.930
Harwell	0.729	0.282	1.012	1.528
High Muffles	0.680	0.251	0.936	1.135
Lullington	0.607	0.228	0.835	1.013
Narberth	0.406	0.141	0.547	1.241
Rochester	0.844	0.311	1.154	1.218
Sibton	0.750	0.262	1.012	0.957
Strath Vaich	0.676	0.239	0.915	1.212
Yarner Wood	0.429	0.140	0.569	0.910
12-site mean	**0.607**	**0.222**	**0.829**	**1.304**

Secondary organic aerosol formed from natural biogenic aerosol precursors, BSOA, see Table 4.18, peaks at the Auchencorth Moss and Eskdalemuir sites at just under 2.2 µg PM m^{-3} because of its proximity to the high terpene emission areas in the lowlands of Scotland in the natural biogenic emission inventory of Stewart et al. (2003). Here, biogenic SOA is over 3 times that from man-made SOA. At all the other sites, biogenic SOA levels are more comparable to those of man-made SOA but biogenic SOA appears to predominate over man-made SOA at the majority of sites.

The 12-site network average levels of ASOA was found to be 0.61 µg PM m^{-3} and that of ISOA, 0.22 µgPM m^{-3}, see Table 4.18. The corresponding level of BSOA was 1.30 µgPM m^{-3}. Over the UK as a whole then, the secondary organic PM averaged 2.1 µg PM m^{-3}, of which 39% was of man-made origins and 61% was biogenic. This compares well with the observed non-fossil contribution to the secondary organic aerosol of 52% reported by Gelencser et al., (2007) for a range of remote sites across Europe for both summer and winter conditions.

4.4.4 Seasonal cycles in SOA concentrations

The seasonal cycles in ASOA concentrations are shown in Figure 4.26. The sites show a high degree of correlation which is driven by the meteorological conditions and exhibit maxima in February, May and September. There is a clear gradient in levels with sites in the remote north and west showing lowest levels during the seasonal maxima and those adjacent to sources of pollution showing the highest levels.

The seasonal cycles in BSOA are characteristically different from those in ASOA, see Figure 4.27. BSOA levels exhibit a single maxima during May with relatively low levels during the winter and spring months. During May, BSOA levels are highest at Eskdalemuir and Auchencorth Moss in Scotland and lowest at Glazebury.

Figure 4.26: Seasonal cycles in anthropogenic SOA at the 12 sites for 2008.

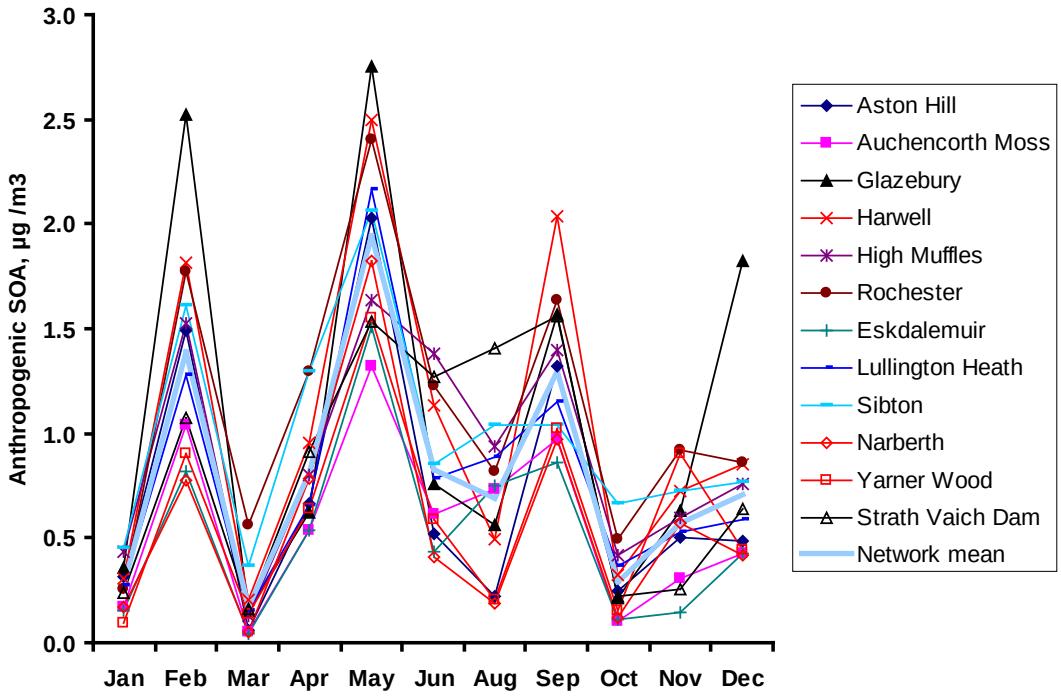

Figure 4.27: Seasonal cycles in biogenic SOA at the 12 sites for 2008.

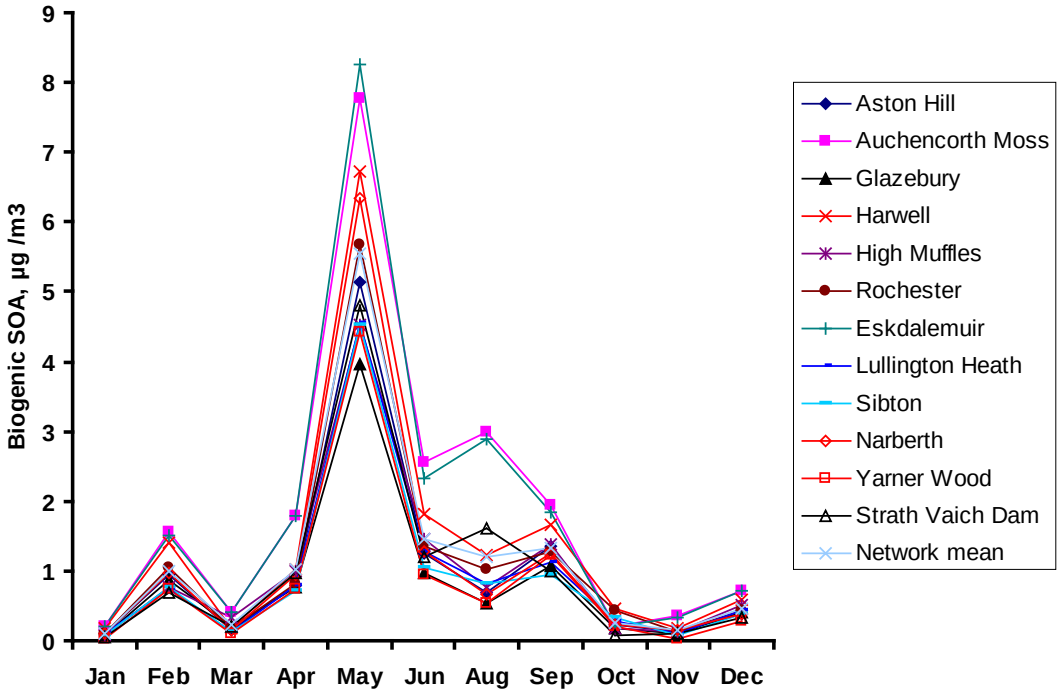

Taking together all of the sites and the anthropogenic and biogenic components to make the network mean total SOA, then the seasonal cycles of the biogenic components dominate, giving a seasonal cycle that peaks during May, see Figure 4.28. During May, biogenic sources account for three-quarters of the SOA with anthropogenic sources one-quarter.

Figure 4.28: Seasonal cycle in total (= anthropogenic + biogenic) SOA across the UK.

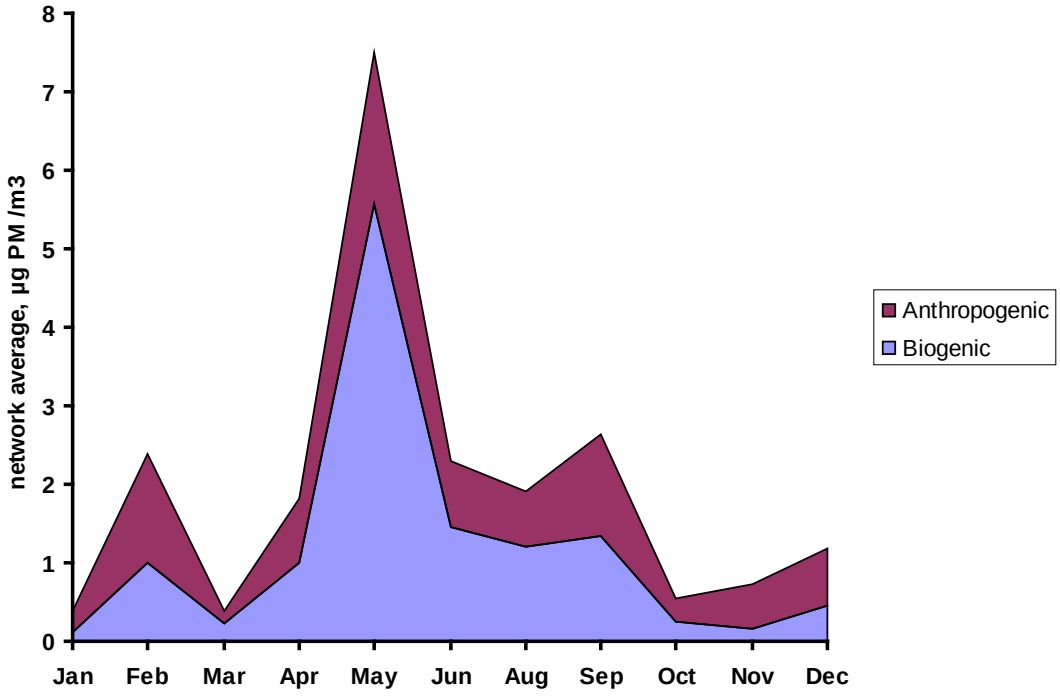

4.4.5 Episodic levels of SOA

The model levels of secondary organic aerosol show significant day-by-day variability and the presence of episodes of high concentrations. Table 4.19 lists the days when the highest levels of anthropogenic and biogenic SOA were modelled at each site during 2008, together with the level recorded. Such levels have resulted not only from photochemical production within the UK but also from long-range transport of SOA formed from SOA precursors emitted in the rest of Europe. The contribution from local UK production and long range transboundary transport varied between each episode and each site.

The highest biogenic SOA mass concentrations were generally modelled during the period from 9th to 12th May, except for 24th September at the High Muffles site. The meteorological situation during the period in May was characterised by trajectories travelling up from France and Spain. Much of the biogenic SOA modelled in southern Britain was therefore of transboundary transport origins. However, levels of biogenic SOA were even higher in northern Britain showing that there must also have been a significant contribution from SOA precursor emissions within the UK. In contrast, the meteorological situation was quite different on 24th September when the highest levels of biogenic SOA were modelled at High Muffles. On this occasion, the trajectories were from the north-easterly direction and brought high levels of biogenic SOA from precursor emissions sources in Norway and Sweden. Under these conditions, there was apparently no contribution from UK emission sources.

Table 4.19: The highest daily anthropogenic and biogenic SOA mass concentrations and the days on which they were modelled during 2008.

Site	Highest ASOA µg m^{-3}	Date	Highest BSOA µg m^{-3}	Date
Aston Hill	10.1	28th July	17.4	11th May
Auchencorth	8.3	13th February	19.6	10th May
Eskdalemuir	6.2	29th July	20.9	10th May
Glazebury	16.7	24th December	12.6	11th May
Harwell	16.6	20th September	16.7	10th May
High Muffles	15.8	3rd June	20.4	24th September
Lullington	12.4	31st August	14.6	10th May
Narberth	6.2	20th April	23.8	11th May
Rochester	12.7	28th July	19.9	10th May
Sibton	10.0	5th May	15.8	10th May
Strath Vaich	11.4	4th July	17.5	9th May
Yarner Wood	6.3	14th February	12.8	12th May

The highest anthropogenic SOA mass concentrations were recorded on a varied range of days across the UK with no clear-cut pattern as there was for biogenic SOA. Three sites, Aston Hill, Eskdalemuir and Rochester recorded highest concentrations on 28th – 29th July, whilst Auchencorth Moss and Yarner Wood recorded theirs on 13th – 14th February. Otherwise the sites recorded maxima on different days. Eskdalemuir recorded its maximum on 29th July when the trajectories passed over Germany, the Low Countries and then the whole length of England. Under these meteorological conditions, there would be significant contributions from local UK sources and from transboundary sources in Europe. Harwell recorded its maximum on 20th September when trajectories brought anthropogenic SOA from

both sources in the south-east of England and from the Low Countries and Germany. The Lullington Heath maximum modelled on 31st August was explained by transboundary transport of SOA formed from anthropogenic emissions in France, Belgium and Germany. Easterly transport from the Low Countries, Germany and northern Europe brought elevated SOA levels to Narberth on 20th April, supplementing a contribution from local UK sources. The event recorded at Strath Vaich Dam on 4th July was apparently caused solely by anthropogenic SOA precursors of UK origins. The easterly long range transboundary transport event that was modelled at Yarner Wood brought SOA from precursor emissions from France, Germany, Czech Republic and Poland.

4.4.6 Sensitivity of model SOA concentrations at Aston Hill to changes in emissions

The annual emission inventory scaling factors were changed from 2008 in the base case to 2020 in a sensitivity case based on the future emission scenarios available from the EMEP webdab. The influence of the future emission scenario case was tested for the Aston Hill site. In response to the shift from 2008 to 2020 emissions, the total man-made SOA declined from 0.73 to 0.61 µg PM m^{-3}, that is a decrease of about 16%. In contrast, biogenic SOA increased from 1.11 to 1.15 µg PM m^{-3}, that is, an increase of 3%. The different SOA components are thus responding differently to the NO_x and VOC controls that make up the 2020 scenario case.

The separate responses to 30% NO_x and 30% VOC emission reductions were studied, relative to the 2008 base case. The response to the 30% NO_x control case at Aston Hill was to bring about a decrease in total man-made SOA from 0.73 to 0.68 µg PM m^{-3}, representing a decrease of 6.2%. In contrast, biogenic SOA increased from 1.115 to 1.148 µg PM m^{-3}, an increase of 3.0%. Overall, SOA decreased by a fraction of a percent.

The response to the 30% VOC reduction case was to decrease total man-made SOA from 0.73 to 0.49 µg PM m^{-3}, a reduction of about 32%. This reduction is slightly more than linear because the reduction in formation of SOA leads to a reduction in the uptake of all SOA precursors into the SOA. The biogenic SOA decreased from 1.11 to 1.08 µg PM m^{-3}, a decline of 2.8% due to the same non-linearity argument as for the man-made SOA response.

Biogenic and anthropogenic SOA mass concentrations therefore display significant non-linear responses to NOx and VOC emission reductions. It will be important to include these non-linearities in assessing the responses of $PM_{2.5}$ mass concentrations to future emission scenarios.

4.4.7 Summary and main conclusions

The main conclusions of the work of Objective 10.3 in terms of the modelling of SOA are summarised as follows:

Summary:

- **Using the newly developed chemistry mechanism for SOA formation in the CRI, the PTM was able to account for organic carbon episodes observed at a site in Birmingham during 2006. However, the model showed an overall negative bias, tending to underpredict SOA concentrations**
- **Correlations between model predictions and observations pointed towards SOA components from anthropogenic sources as the main cause of organic PM episodes at this site.**
- **Model sensitivity runs showed how the performance of the PTM could be optimised by increasing precursor emissions and changing certain model parameterisations**
- **The optimised model was used to estimate the distribution of SOA across the**

UK in 2008. The results showed that the contribution of anthropogenic (ASOA) and biogenic (BSOA) sources varies across the country with the highest biogenic contributions occurring at sites in Scotland where they are 3 times higher than anthropogenic sources. At other sites, the contributions of ASOA and BSOA are comparable, but biogenic sources tend to dominate. Across the whole of the UK, about 61% of SOA was from biogenic sources, 39% from man-made sources.

- Seasonal cycles in SOA from anthropogenic sources are highly variable and driven by meteorology conditions. Seasonal cycles in BSOA at all sites showed a strong maximum in May. During May 2008, 75% of all SOA are from biogenic sources.
- Analysis of trajectories showed the varying influence of long-range transport and local emission sources to BSOA at different sites. ASOA also peaks at different times at different sites due to different contributions from precursors transported from continental Europe and UK sources.
- Based on future emissions, ASOA modelled at Aston Hill is predicted to decline by 16% between 2008 and 2020, whereas BSOA is expected to show a small increase, illustrating how SOA components respond differently to NO_x and VOC controls.
- Sensitivity studies showed that BSOA and ASOA display non-linear responses to NO_x and VOC emission reductions. It will be necessary to account for this when assessing responses of overall $PM_{2.5}$ concentrations to future emissions. Overall, SOA decreased to a greater extent in response to changes in VOC emissions than NO_x.

5 Assessments of Background and Urban-Scale Oxidant

5.1 Introduction

It is well-established that the behaviour of ozone (O_3), NO and NO_2 in the atmosphere is coupled by the following reactions,

$$NO + O_3 \rightarrow NO_2 + O_2 \quad (1)$$

$$NO_2 + \text{sunlight} (+ O_2) \rightarrow NO + O_3 \quad (2)$$

and it is because of this strong chemical coupling that the term “oxidant” is sometimes used as a collective term for NO_2 and O_3. This reaction cycle partitions NO_x between its component forms of NO and NO_2, and oxidant between its component forms of O_3 and NO_2, but conserves both NO_X and oxidant. As a result, oxidant derived from background O_3 is partitioned between the forms of NO_2 and O_3, with a progressively greater proportion in the form of NO_2 as NO_x increases as a result of received emissions. In urban areas, oxidant can also be derived significantly from directly emitted NO_2, and this is also partitioned between the forms of NO_2 and O_3, with a progressively greater proportion in the form of O_3 as NO_x decreases with dilution.

Consistent with this, previous analyses of ambient data have shown that the level of oxidant, [OX], at a given location in the UK is made up of a combination of a background (NO_x-independent) source and a local, (NO_x-dependent) source (e.g., Clapp and Jenkin, 2001; Jenkin 2004), denoted here as $[OX]_B$ and $[OX]_L$, respectively:

$$[OX] = [OX]_B + [OX]_L \quad (i)$$

$[OX]_L$ is derived from primary emissions of NO_2, and is usually represented by the term $f_{NO2}[NO_x]$, where f_{NO2} is the fraction of NO_x emitted as NO_2 (AQEG 2007). $[OX]_B$ provides a quantification of the ozone concentration which would exist at the given location in the notional absence of NO_x, i.e. when the local-scale chemical coupling described above cannot occur.

The work carried out in **Objective 11** during this phase of the project has focused on characterising the geographical variation of annual mean $[OX]_B$ over the UK, and developing an improved mapping methodology at 1km x 1km resolution. This has been used to produce maps for each of the years in the period 2001-2009. In view of a previously reported strong altitude dependence of ozone concentrations at UK rural sites (PORG, 1997), attention has also be given to investigating the strength of any site altitude dependence of $[OX]_B$, to allow the relative contributions of ozone deposition and oxidant partitioning to the previously reported dependence for ozone to be considered. All these activities provide input data to help improve and inform NO_2 and ozone modelling activities in the UK Ambient Air Quality Assessments programme (UKAAQA).

5.2 Geographical variation of $[OX]_B$ over the UK

It is well established that $[OX]_B$ must be greatly influenced by baseline surface ozone concentrations entering the British Isles from the north Atlantic under prevailing meteorological conditions (e.g., Derwent et al., 2007). However, it may also be modified by processes occurring regionally over the UK and north-west Europe, which may be both positive (i.e., production from regional-scale chemistry) or negative (i.e., removal by deposition). In the present analysis, data from UK sites have been examined to estimate the

contribution to $[OX]_B$ which derives from the hemispheric baseline, and the impact of regional-scale processes in modifying this baseline.

The spatial analysis has made use of background oxidant, $[OX]_B$, data for 16 UK sites using measurements over the period 2001-2006, which were reported previously (Jenkin and Clapp, 2008). In that study, $[OX]_B$ was further separated into an estimate of the hemispheric baseline, $[OX]_H$, and a regional modification to this baseline, $[OX]_R$, on the basis of site specific air mass histories described by four-day back trajectories (from the British Atmospheric Data Centre, ECMWF, 2007), such that:

$$[OX]_B = [OX]_H + [OX]_R \quad \text{(i)}$$

The values determined for annual mean $[OX]_H$, based on the average of data over the period 2001-2006, were found to vary over the range 30.4 – 35.9 ppb , depending on location within the UK. This indicates that the true hemispheric baseline is modified during passage of air across the UK, most likely due to removal of ozone through deposition to the ground. The screened air mass trajectories used to determine $[OX]_H$ were dominated by the prevailing westerlies and south-westerlies, and the distance across land from the Atlantic to each site from a south-westerly direction was previously used to represent the extent of oxidant loss through deposition. On the basis of a broader appraisal of sector contributions (e.g., Jones, 2002) the present work has alternatively made use of the distance across land on a bearing of 63˚ (i.e., from an approximately west-southwesterly direction; denoted "d_1"), allowing a slightly better description of the spatial variability of the observed $[OX]_H$, and its parameterisation (see Figure 5.1). On this basis, the following optimized expression for $[OX]_H$, in ppb, was determined:

$$[OX]_H = [OX]_H^\circ \exp(-3.30 \times 10^{-4}\, d_{1\circ}) \quad \text{(ii)}$$

where $[OX]_H^\circ = 35.8$ ppb and $d_{1\circ} = d_1 \exp(-1.57 \times 10^{-3}\, d_2)$. Here, $d_{1\circ}$ is a adjusted value of d_1, which takes account of the progressively greater average wind speeds towards the north and west of the British Isles (i.e., shorter contact time with land per unit distance). This was done on the basis of a north-westerly co-ordinate defined relative to the most south-easterly site, Lullington Heath (denoted "d_2").

Figure 5.1: Correlation of $[OX]_H$ at 16 UK sites with adjusted distance across land from the west-southwest ($d_{1\circ}$).

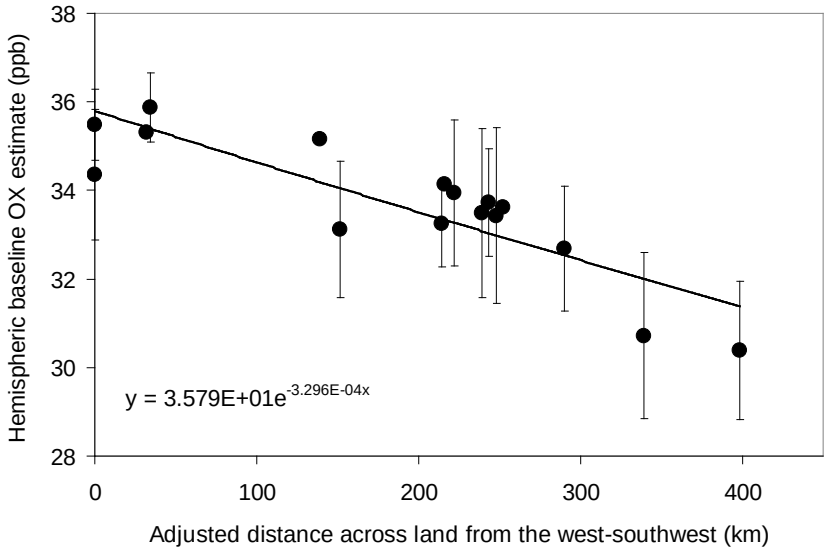

The values determined for the annual mean regional modification ($[OX]_R$), based on the average of data over the period 2001-2006, were found to vary over the range -0.5 – 2.0 ppb , depending on location within the UK. As previously, two contributory factors were identified and parameterised: (i) a photochemical contribution, showing a south-easterly to north-westerly gradient within the UK, and (ii) oxidant loss via deposition during east-northeast to west-southwest transit across the UK (this being a minor modification to the northeast to southwest transit considered previously). A multiple regression of the data indicated that $[OX]_R$, in ppb, can be reasonably well described by the expression,

$$[OX]_R = F.[OX]_{R\ chem} + [OX]_{R\ dep} \qquad \text{(iii)}$$

Where the photochemical contribution, $[OX]_{R\ chem} = (1.563 – (1.68 \times 10^{-3}\ d_2))$, and the deposition contribution, $[OX]_{R\ dep} = (–3.02 \times 10^{-3}\ d_3)$, with d_3 being the distance across land during east-northeast to west-southwest transit across the UK. The parameter "F" in equation (iii) is a scaling factor to account for variations in the level of photochemical pollution, which has a value of unity in the present reference case.

The above analyses have allowed parameterisation of background oxidant levels within the UK. Example maps of average $[OX]_H$ and $[OX]_B$ for the UK over the period 2001-2006 are illustrated in Figure 5.2, with values calculated for each 1km x 1 km Ordnance Survey grid square, based on the co-ordinates of the grid square centres.

Figure 5.2: Illustration of the spatial variation of the average hemispheric oxidant component, $[OX]_H$, and the summed background oxidant, $[OX]_B$ (= $[OX]_H$ + $[OX]_R$) over the UK (in ppb) for the period 2001-2006. Values are assigned to each 1 km x 1km Ordnance Survey grid square, based on the co-ordinates of the grid square centres.

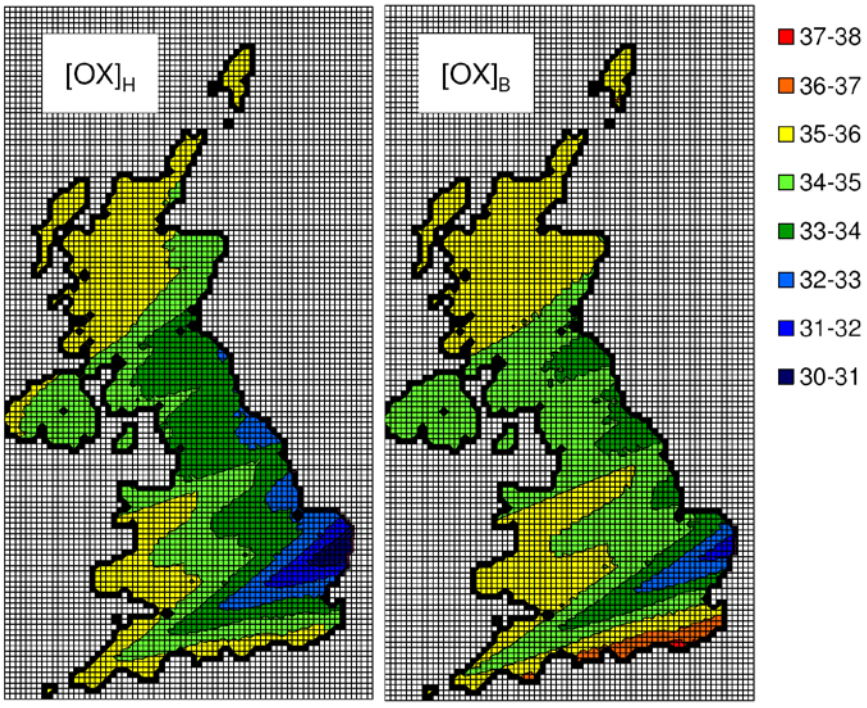

5.3 Generation of optimised annual mean $[OX]_B$ maps for 2001-2009

The oxidant components described above show year-to-year variability, by virtue of variations in the magnitude of regional and global scale influences on emissions and chemical processing (e.g., Derwent et al., 2007; AQEG, 2009). Modelling of annual mean data for individual years therefore requires year-specific values of the oxidant components. As described in detail previously (Jenkin and Clapp, 2008), this is achieved by scaling the $[OX]_H$ and $[OX]_R$ 2001-2006 reference maps, by applying optimised values of $[OX]_H°$ and F (the photochemical pollution scaling factor) for a given year.

This was done for each year in the period 2001-2009 through comparison of $[OX]_B$ data from up to 40 sites throughout the UK with the values calculated for the 1 km x 1 km grid squares containing those sites. The sites were selected to be comparatively unpolluted (annual mean $[NO_x] < 25$ ppb) so that the initial correction for $[OX]_L$ (derived from primary NO_2) was small. For the years 2001-2006, the $[OX]_R$ data from the subset of 16 sites used in the above analysis was used to set values of F for each of the individual years, as described by Jenkin and Clapp (2008) (see Table 5.1). For the years 2007-2009, $[OX]_R$ data are not readily available, as this requires an extension to analysis of screened air mass data. Instead, estimates of F were based on consideration of the variation of a number of elevated ozone and related metrics (e.g. maximum hourly-mean ozone at long-running rural sites; hours $\geq$ 90 ppb ozone at long running sites; average summer temperature). A comparison of such metrics with the values of F rigorously determined for the 2001-2006 period confirmed that they could reasonably be used as a surrogate, and were found to be particularly good in identifying high photochemistry years like 2003 and 2006. These analyses suggested that the values of F in all the years 2007-2009 should lie between zero and 0.5 (i.e., lower than all the years 2001-2006), as shown in Table 5.1, consistent with the generally poor summertime weather in the recent years. The wider $[OX]_B$ dataset from up to 40 sites was then used to optimize values of $[OX]_H°$ for each year in the time series, by minimising the square deviation. Values of $[OX]_H°$ and F are shown in Table 5.1.

Table 5.1: Year-specific annual mean values of $[OX]_H°$ and F for use in empirical modelling.

Year	2001	2002	2003	2004	2005	2006	2007	2008	2009
$[OX]_H°$ (ppb)	34.82	34.53	36.27	34.97	33.97	34.67	33.73	34.81	33.10
F	0.859	0.816	1.334	0.988	0.581	1.422	0.25	0.5	0.5

A comparison of the observed and parameterised $[OX]_B$ values is shown in Figure 5.3 for 2009, for the averages of the zones throughout the UK. This shows a reasonably good correlation, with the exceptions of the West Midlands, where the observed $[OX]_B$ is notably lower than that calculated, and North Wales, where the observed $[OX]_B$ is notably higher. It should be noted that for 4 zones (North Wales, North East, Northern Ireland and Scottish Borders) the comparison is based on data from a single site.

The associated parameterisation of $[OX]_B$ over the UK for all the considered years is shown in Figure 5.4, with values calculated for each 1km x 1km OS grid square, based on the co-ordinates of the grid square centre. Time series for selected sites are compared with those calculated for the grid squares containing those sites in Figure 5.5, demonstrating that the method generally captures the geographical and temporal variation.

Figure 5.3: Comparison of observed and parameterised $[OX]_B$ for UK zones in 2009.

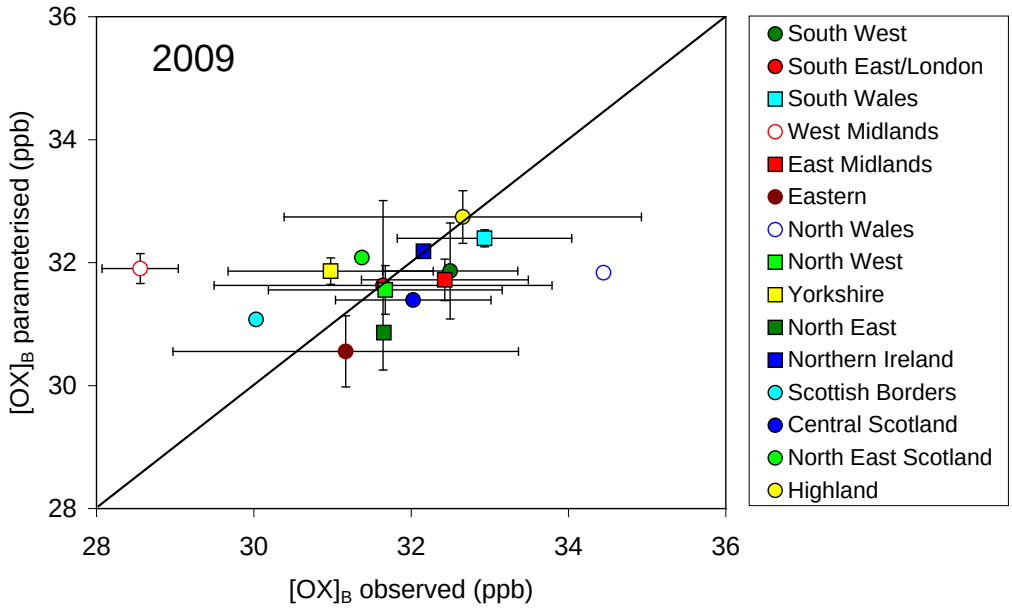

Figure 5.4: Parameterised spatial variation of $[OX]_B$ (= $[OX]_H$ + $[OX]_R$) over the UK (in ppb) for each year in the time period 2001-2009.

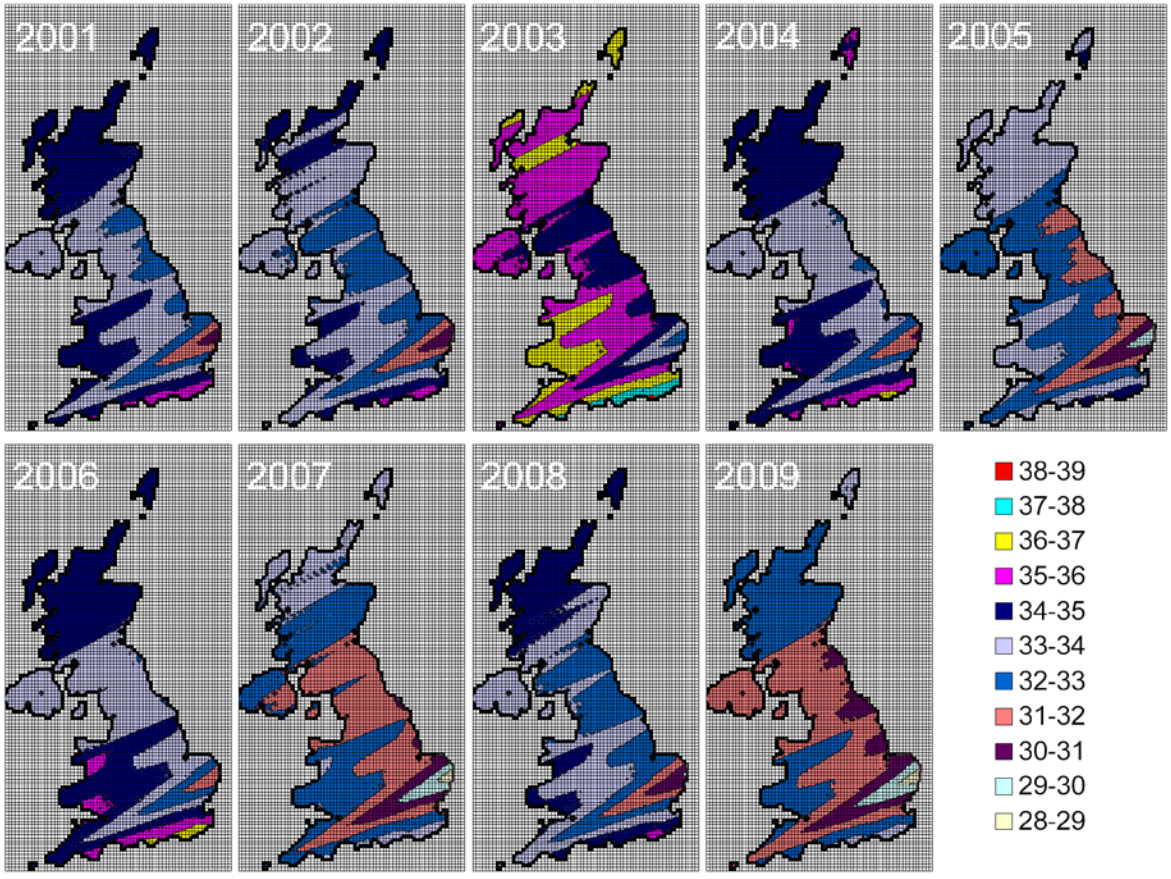

Figure 5.5: Time series of $[OX]_B$ (= $[OX]_H$ + $[OX]_R$) at selected UK sites compared with those calculated for the OS 1km x 1km grid squares containing those sites over the period 2001-2009.

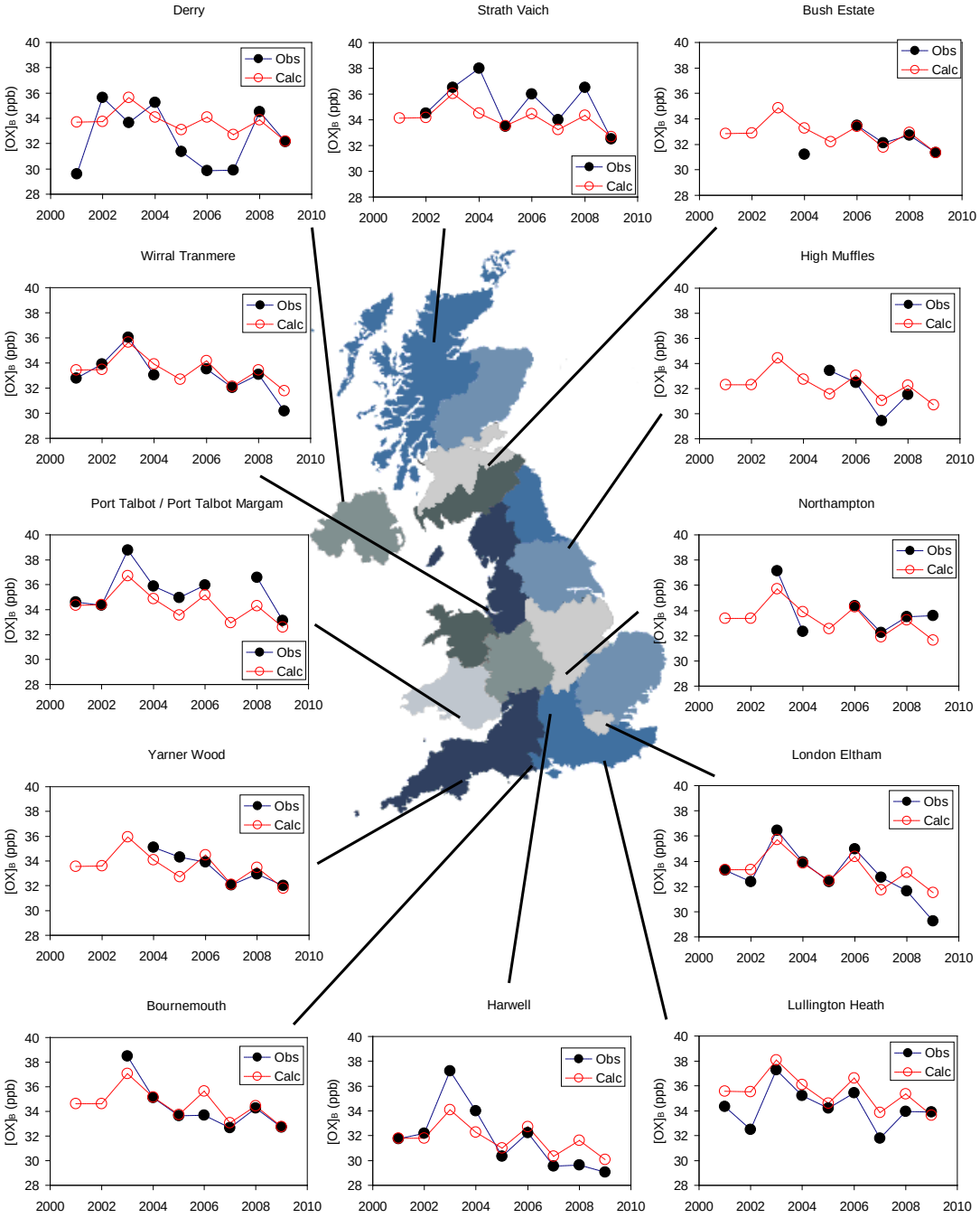

5.4 Investigation of site altitude dependence of annual mean $[OX]_B$

A strong site altitude dependence of ozone concentrations, $[O_3]$, at UK rural sites was previously reported by PORG (1997), which was interpreted in terms of the lower altitude sites being more likely to become decoupled from the air aloft when a shallow night-time inversion layer forms, and therefore being more influenced by ozone removal via deposition. However, a contribution to the reported dependence for $[O_3]$ may be due to the lower altitude sites being characterised by systematically higher levels of NO_x, so that a greater proportion of the available oxidant is present in the form of NO_2. Investigation of the altitude dependence of both $[OX]_B$ and $[O_3]$ therefore allows the relative roles of ozone deposition and oxidant partitioning to be examined, therefore informing empirical modelling activities in the UK Ambient Air Quality Assessments programme (UKAAQA).

The optimisation of the 2009 $[OX]_B$ map reported in Section 5.3 considered data from 39 rural and urban background sites throughout the UK. The sites were selected because they are comparatively unpolluted (annual mean $[NO_x] < 25$ ppb) so that the initial correction for $[OX]_L$ (derived from primary NO_2) is small. Figure 5.6 confirms that, although there is some scatter, the annual mean $[NO_x]$ at these sites shows a general inverse correlation with altitude. Because the majority of sites with 12.5 ppb < $[NO_x]$ < 25 ppb are at low altitude (< 50 m), the altitude variation is most pronounced for the 17 sites with $[NO_x] < 12.5$ ppb, and these were considered further in an analysis of $[OX]_B$ and $[O_3]$.

Figure 5.6: Variation of annual mean $[NO_x]$ in 2009 with site altitude for 39 relatively unpolluted rural and urban background sites in the UK. Sites with $[NO_x] < 12.5$ ppb (indicated by the broken line) were considered further in the $[OX]_B$ and $[O_3]$ analysis.

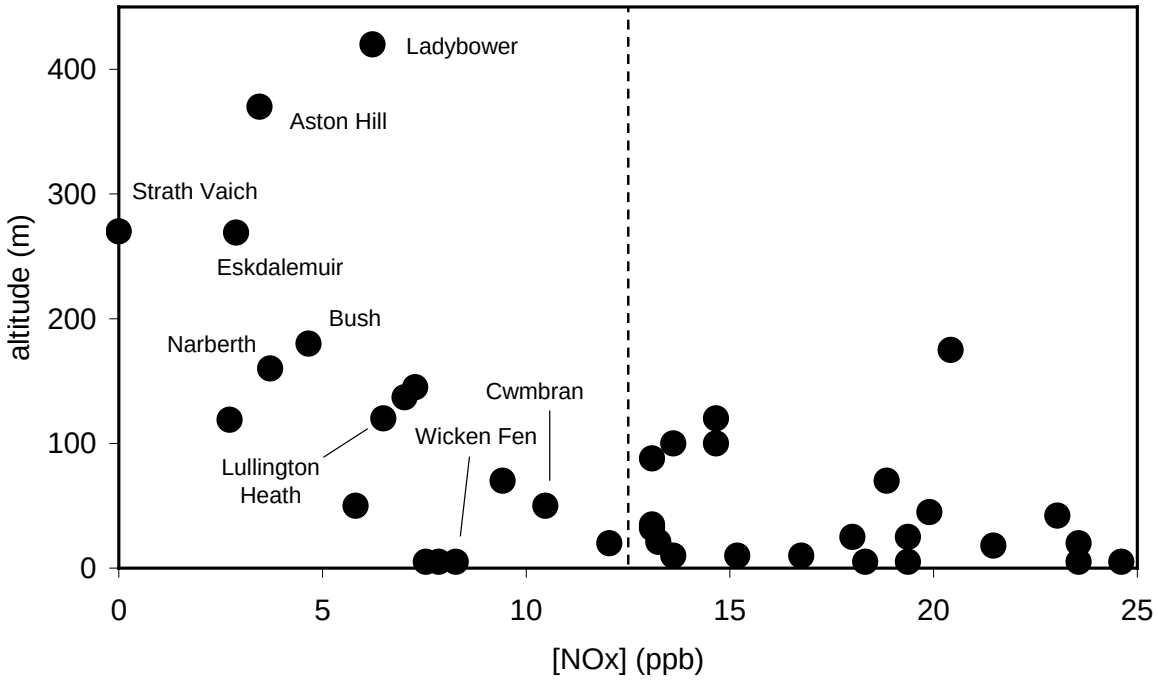

Figure 5.7 shows the variation of both $[OX]_B$ and $[O_3]$ with site altitude for these 17 sites. Despite some scatter, the annual mean $[O_3]$ data show a pronounced site altitude dependence, which is also consistent with that reported by PORG (1997). The annual mean $[OX]_B$ data logically show a much reduced altitude dependence, and also some reduction in the level of scatter, suggesting that both these observations in the $[O_3]$ data have contributions from the influence of oxidant partitioning.

Figure 5.7: Variation of annual mean $[O_3]$, $[OX]_B$ and $[OX]_H°$ in 2009 with site altitude for 17 sites with $[NO_x] < 12.5$ ppb. $[OX]_H°$ are values of $[OX]_B$ corrected for geographical deposition and chemistry on the basis of the geographical parameters reported in Section 5.3. Continuous curve is a representation of the altitude ozone dependence reported by PORG (1997). Other lines are linear regressions of data, as follows: (dotted line) $[O_3] = 0.0123 \times$ altitude + 25.6; (broken line) $[OX]_B = 0.0044 \times$ altitude + 30.8; (continuous line) $[OX]_H° = 0.0032 \times$ altitude + 32.4.

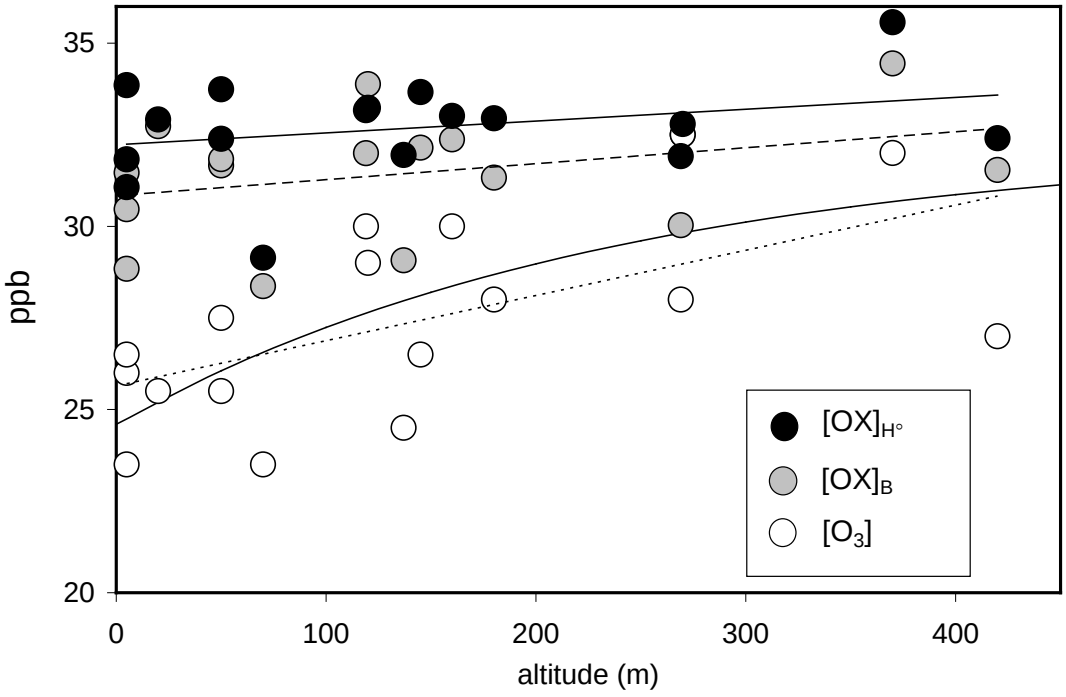

The analysis of the spatial dependence of $[OX]_B$ reported above predicts that a contribution to remaining scatter results from the variability of site location within the UK, and particularly the associated variability in the magnitude of depositional losses during transit over land prior to arrival at the site. The $[OX]_H°$ data in Figure 5.7 aim to account for this by correcting the observed $[OX]_B$ values for the idealised deposition and chemistry modifications calculated above during optimisation of the 2009 $[OX]_B$ map. As shown in Figure 5.7, these corrections further reduce the amount of scatter, and also lead to a further slight reduction in the altitude dependence derived from linear regression of the data, which is about a factor of four lower than that obtained from the $[O_3]$ data. It is noted that if the geographical correction worked perfectly (and there is no altitude effect), all the $[OX]_H°$ data should lie on a horizontal line at 33.1 ppb (see Table 5.1). This appears consistent with the majority of the data, with the exception of two outlying points which mainly account for the residual slope.

On the basis of the analysis presented here, it appears that the site altitude dependence in $[O_3]$ reported previously (PORG 1997) is probably largely a result of an approximate inverse dependence of the proximity of NO_x sources on site altitude and the impact this has on temporary sequestration of O_3 in the form of NO_2 (i.e., oxidant partitioning). Consequently,

the effect should be already accounted for in empirical models using an oxidant partitioning approach, without the necessity to impose an additional site altitude correction.

The only elevated site which shows consistent clear evidence for an oxidant enhancement is Aston Hill (370 m) in the Welsh Borders. This was confirmed through inspection of annual mean data from several additional years (2005-2008) in comparison with data from Ladybower (420 m) in the Peak Distict and High Muffles (267 m) in the North Yokshire moors. Although the analysis presented here does not support a general site altitude dependence, it does not rule out factors related to local topography or altitude differential which are site specific and which may lead to enhanced surface decoupling. However, it is suggested that, over the typical UK range, the altitude of a ground-based location relative to sea level alone is not a reliable marker of propensity for surface decoupling.

5.5 Summary and main conclusions

The main conclusions of the work of Objective 11 on the assessment of background and urban-scale oxidant are summarised as follows:

Summary:

- **A method based on the analysis of ambient data on O_3, NO_2 and NO_x has been developed to characterise the geographical variation in annual mean background oxidant concentrations over the UK at 1x1km resolution.**
- **The method has been used to generate optimised maps of annual mean background oxidant concentrations for each year between 2001 and 2009. The time-series has been tested by comparison with concentrations measured at 12 UK monitoring sites.**
- **The previously reported altitude dependence of ozone concentrations in the UK has been investigated and found to be largely due to the roughly inverse dependence of the proximity of NO_x emission sources on site altitude and the impact this has on sequestering ozone in the form of NO_2 leading to a much weaker altitude dependence of total oxidant.**
- **The background oxidant maps and parameterisations developed in this work are being used to inform and improve NO_2 and O_3 empirical modelling activities in the UK Ambient Air Quality Assessments programme (UKAAQA) for air quality directive reporting and further Defra policy analysis.**

6 Development of the Surface Ozone Flux Model

6.1 Introduction

Elevated ozone concentrations have the potential to effect crop yield and the growth of vegetation. The RoTAP report concluded that the AOT40 metric reported under the EU Air Quality Directive for ozone is no longer fit for purpose and that ozone risk assessments for vegetation should in the future be based on ozone flux metrics (i.e. Accumulated stomatal ozone Flux above a threshold Y (AFstY)). As yet, no policy tools exist that are capable of estimating ozone fluxes to different ecosystem types at a fine enough spatial resolution to capture the influence of both local UK ozone precursor emissions and longer-range transport of ozone and ozone precursor emissions from Europe.

The International Cooperative Programme (ICP) on Modelling and Mapping of Critical Loads & Levels and Air Pollution Effects, Risks and Trends works under the Convention on Long-range Transboundary Air Pollution (CLRTAP) of the United Nations Economic Commission for Europe (UNECE). The ICP Modelling and Mapping Manual is the basic guideline for modelling and mapping critical levels for ozone and helps Parties to CLRTAP to fulfil their obligations to use harmonized methods to derive data for effects and risk assessments.

The Manual defines critical levels for assessing the effects of ozone on vegetation as “the concentration, cumulative exposure or cumulative stomatal flux of atmospheric pollutants above which direct adverse effects on sensitive vegetation may occur according to present knowledge”. It provides a detailed description of how to calculate critical levels for ozone both in terms of cumulative exposure and cumulative stomatal flux. It specifies methods to calculate cumulative stomatal flux for:

- Wheat
- Potatoes
- Beech

AEA developed the Surface Ozone Flux Model (SOFM) in 2004 to enable stomatal fluxes to be calculated from ozone concentrations predicted using the in-house Ozone Source Receptor Model (OSRM) or from measured ozone concentrations. SOFM2004 used a canopy-scale stomatal flux algorithm based on work by Emberson et al (2000) to calculate ozone concentrations at the canopy height from the modelled or measured concentrations. It also used a simple isothermal box model to estimate soil moisture content.

The Manual has been revised since 2004 and Dr Emberson and colleagues at Stockholm Environment Institute (University of York) have carried out further work to develop the canopy-scale stomatal flux algorithms. The developments have been included in the DO_3SE model developed by Dr Emberson’s team. The work carried out in **Objective 12** during this phase of the project has focused on collaborating with Dr Emberson in order to implement parallel developments within SOFM. This has included:

- A latitude model to take account of the effect of latitude on the start and end of the growing season
- Penman-Montieth models of the rate of transpiration from vegetation and evaporation from soils for the calculation of soil moisture content
- Changes in recommended parameters

- Parameters consistent with the published version of the Manual available in June 2010

The OSRM includes a simple model to take account of the changes in ozone deposition velocity throughout the year. The midday surface resistance decreases from 500 s/m in the winter to 143 s/m in May and June. A small modification to OSRM was made to increase the surface resistance when the SOFM soil moisture content model predicts reduced stomatal conductivity in the UK because of dry soil conditions.

This section provides a summary of the SOFM model and describes the new latitude model and the soil moisture content model in more detail. It also describes the modifications made to the OSRM to take account of dry soil conditions. Outputs from the models are presented for the year 2006, the model year agreed as part of a wider study assessing the impacts of the changes made to the DO_3SE formulations used in conjunction with other ozone models. The report focuses on the results from the OSRM and SOFM, with results and conclusions from the wider assessments involving other modelling groups to be presented in a peer-reviewed paper for publication.

The SOFM model and post-processor are described in more detail in the appendices to a separate report covering the work for this Objective recently submitted to Defra (Abbott and Cooke, 2010) and are not repeated here.

6.2 Ozone Flux Model

Figure 6.1 shows the basic model framework and the route of the transfer of data between the model components.

Figure 6.1: Framework of program modules

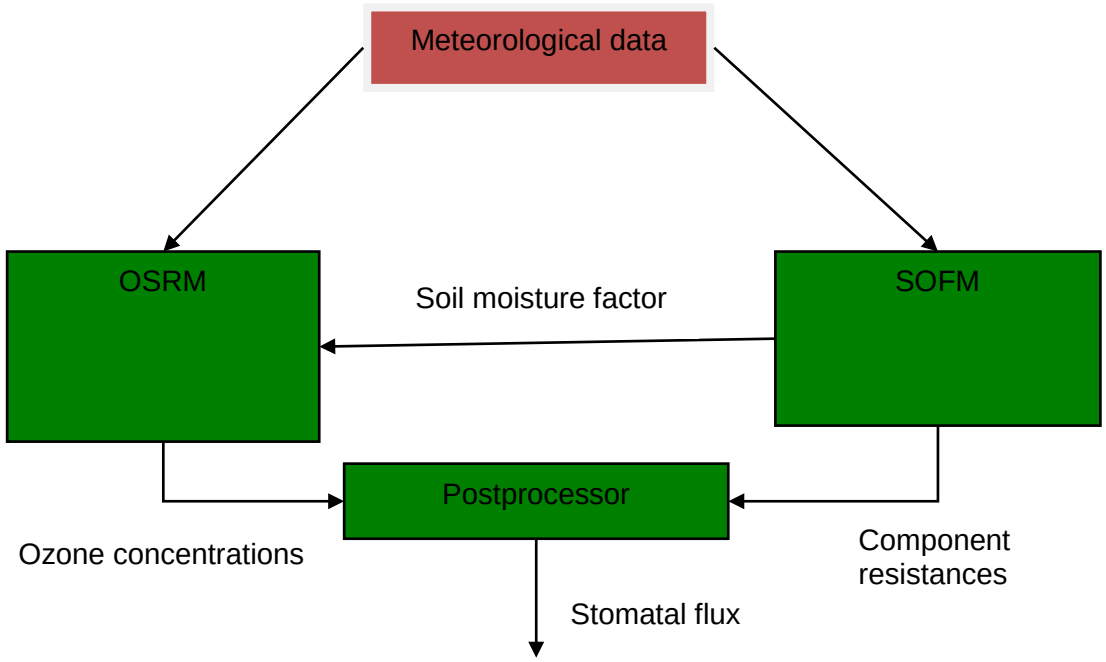

The OSRM and SOFM are the main components of the model and use the same meteorological data. A post-processor linked to these components is used for the flux calculations.

The Surface Ozone Flux Model may be represented by the resistance analogue model shown in Figure 6.2.

Figure 6.2: Resistance analogue of ozone transfer between the atmospheric surface layer and terrestrial ecosystems.

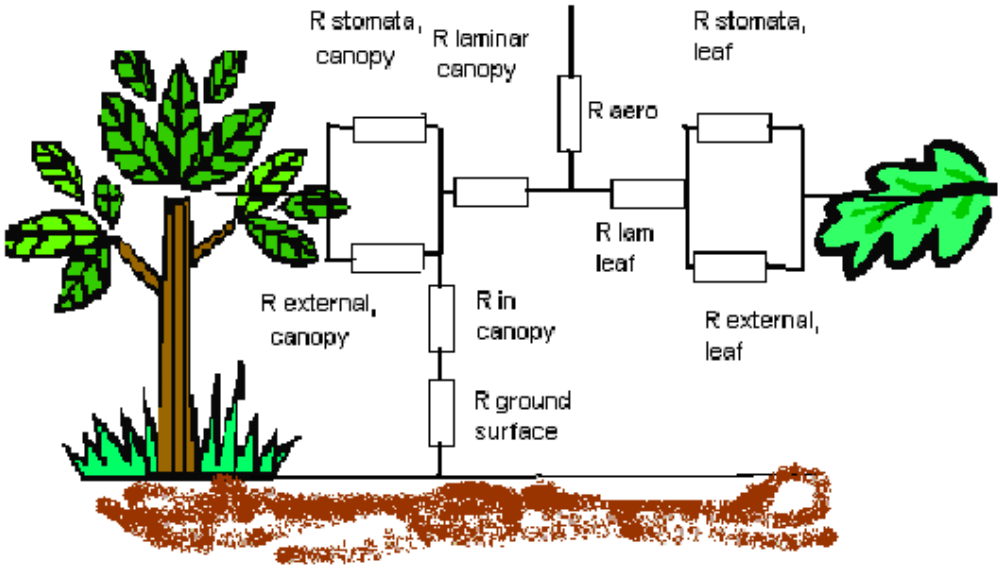

The purpose of the Surface Ozone Flux Model is to calculate the values of component resistances to ozone flux between a reference height and the bulk canopy, the upper canopy leaves or flag leaves and the ground. The individual leaf on the right hand side of Figure 6.2 represents the uppermost canopy leaf for beech and potatoes and the flag leaf for wheat. The whole plant on the left hand side represents the vegetative canopy as a whole. The surface area of the individual upper canopy leaf or flag leaf is very small so that it has little effect on the ozone concentrations and so the ozone concentrations in the canopy are dominated by the fluxes to the canopy and to the ground. However, the yield loss in crops or loss of biomass in woodland is related to the ozone flux to the upper canopy leaf or the flag leaf. It is therefore necessary to calculate the ozone flux to the whole canopy in order to determine the flux to the most sensitive leaves.

The component resistances are:

- Aerodynamic resistance from a specified reference height to the canopy displacement height;
- Stomatal resistance of the bulk canopy
- The external resistance to external plant tissue in the canopy
- The quasi-laminar resistance to the canopy
- The in-canopy air resistance below the displacement height
- The ground surface resistance
- Stomatal resistance to the upper canopy/ flag leaf

- The external resistance to external plant tissue of the leaf
- The quasi-laminar resistance to the leaf

The ICP Modelling and Mapping Manual describes the methods to calculate the stomatal resistance, external resistance and quasi-laminar resistance to the upper canopy leaf: these methods have been implemented within the surface ozone flux model for winter wheat, potatoes and beech trees.

Methods to calculate the bulk canopy resistances are not specified in the Mapping Manual. The methods currently used in the Surface Ozone Flux Model have been developed from those reported by Emberson et al (2000) and presented in the EMEP Unified Model description (Simpson et al., 2003). The developments have involved extensive detailed discussions with Dr Emberson at SEI.

The stomatal conductances are calculated using a multiplicative algorithm with the following formulation:

$$g_{sto} = g_{\max} \times \left\lfloor \min(f_{phen}, f_{O_3}) \right\rfloor \times f_{light} \times \left\lfloor \max\left(f_{\min}, (f_{temp} \times f_{VPD} \times f_{SWP})\right) \right\rfloor$$

where g_{sto} is the stomatal conductance at specified conditions;

g_{max} is the species specific maximum stomatal conductance.

The factors f_{phen}, f_{O3}, f_{light}, f_{temp}, f_{VPD} and f_{SWP} are in the range 0-1. They take account of the effect of plant phenology, ozone-induced senescence, light levels, temperature, water vapour pressure deficit and soil water pressure.

Appendix 1 of the project report by Abbott and Cooke (2010) describes how SOFM calculates the components of resistance and the factors f_{phen}, f_{light}, f_{temp}, f_{VPD} and f_{SWP}. SOFM calculates these values for each hour at gridded locations at 1 degree latitude and longitude resolution throughout the UK. The factor f_{O3} is not calculated in SOFM: it is applied in the postprocessor.

The model calculates bulk canopy resistances for up to ten vegetation types:

- Coniferous forest
- Deciduous forest (e.g. beech)
- Needleleaf forest
- Mediterranean broadleaf forest
- Temperate crops (e.g. wheat)
- Mediterranean crops
- Root crops (e.g. potatoes)
- Semi-natural vegetation
- Grassland
- Mediterranean scrub

It calculates leaf-level resistances for three types:

- Beech
- Wheat
- Potatoes

The purpose of the flux post-processor is to calculate the flux of ozone to the stomata of the upper canopy leaf for beech and potatoes and the flag leaf for winter wheat from the outputs of the OSRM and SOFM models. This is described in detail in Appendix 2 of the project report by Abbott and Cooke (2010).

The postprocessor calculates the ozone concentration at the interface node I (Figure 6.2) from the average boundary layer height concentration calculated by OSRM and the bulk canopy resistances.

The postprocessor calculates the factor ozone senescence factor, f_{O3} for wheat and potatoes and adjusts the stomatal resistance to the upper canopy/flag leaves where f_{O3} is less than f_{phen}. It then calculates the ozone flux through the leaf stomata using the concentration at the interface node at the top of the canopy and the components of resistance.

Finally, it calculates the accumulated stomatal flux for beech, wheat and potatoes as specified in the ICP Mapping Manual (June 2010). The program calculates the accumulated sum of the stomatal flux over specified thresholds for beech, wheat and potatoes for periods specified in the ICP Mapping Manual:

$$AF_{st}X = \frac{3600}{10^6}\sum_i (F_{sti} - X) \qquad \text{mmoles m}^{-2}\text{ projected leaf area}$$

where X is the threshold flux, nmol m^{-2} s^{-1}.

The sum is calculated as the sum of hourly fluxes over daylight hours in the accumulation period. Table 6.1 shows the values of the threshold flux and accumulation period specified in the ICP Mapping Manual.

Table 6.1: Threshold fluxes and accumulation periods specified in the ICP Mapping Manual (at June 2010)

	Threshold flux	Accumulation period
Wheat	6 nmol m^{-2} s^{-1} on a projected leaf area basis	55 days starting 15 days before mid-antithesis. Mid-antithesis occurs at year day 2.57×latitude^{o} +40.
Potatoes	6 nmol m^{-2} s^{-1} on a projected leaf area basis	70 days starting at plant emergence. Emergence occurs on day 146.
Beech	1.6 nmol m^{-2} s^{-1} on a projected leaf area basis	180 days between day 90 and day 270

6.3 Further development of the Surface Ozone Flux Model

For this project Objective, further developments of SOFM were made based on the recent developments made to the DO_3SE model at SEI York.

6.3.1 The latitude model

The DO_3SE model uses a simple approach to estimate the start and end of the growing season for many vegetative types based on the latitude. The latitude model was incorporated within the Surface Ozone Flux Model.

The user specifies as input the start and end of the growing season for the vegetation type at 50^{o} N.

For temperate forest and coniferous forest types, the start of the growing season (SGS) is delayed by 1.5 days for every degree latitude north of 50 degrees. The end of the growing season (EGS) is brought forward by 2 days for every degree latitude north of 50 degrees. The start of the growing season is also delayed and the end of the season brought forward by 1 day for every 100 m above sea level.

For temperate crops (other than wheat) and Mediterranean crops, the SGS is delayed by 3 days for every degree latitude north of 50 degrees. The end of the growing season is also delayed by 3 days for every degree latitude north of 50 degrees.

For wheat, the SGS is delayed by 2.57 days for every degree latitude north of 50 degrees. The end of the growing season is also delayed by 2.57 days for every degree latitude north of 50 degrees.

The user of the model has the option of disabling the latitude model. This is a useful feature for coniferous forests at latitudes less than 55 degrees north for which the growing season is determined by the ambient temperature.

6.3.2 Evaporation and transpiration rates from the leaf surface and the soil

The vapour pressure deficit and soil water pressure factors, f_{VPD} and f_{SWP} depend on the water vapour pressure above the canopy and the water content of the soil. These in turn depend on the rates of evaporation and transpiration from the leaves and the soil.

The model considers three different conditions:

- Evaporation from wet leaves following rain;
- Transpiration from dry leaves with a dry soil surface;
- Transpiration from dry leaves combined with evaporation from a wet soil surface.

In each case, the total rate of evaporation/ transpiration is calculated using the Penman-Monteith approach. Further details on this approach are given in the report by Abbott and Cooke (2010)

The calculation of the rate of evaporation depends on the stomatal resistance, r_{stom}, which is an output from the model. The model uses the value of r_{stom} calculated for the previous hour in the calculation of the rate of evaporation.

6.4 Modifications to the Ozone Source Receptor Model

The OSRM includes a simple approach to take account of the changes in ozone deposition velocity throughout the year. The midday surface resistance decreases from 500 s/m in the winter to 143 s/m in May and June. For this study, the approach was modified in a simple way to take account of dry periods that increase the surface resistance in dry summers.

SOFM calculates soil water pressure factors, f_{SWP}, in the range 0-1 that are used to calculate the reduction in ozone stomatal conductance resulting from dry soils. The modified OSRM reads in these factors for each day of the year for a representative location, vegetation type and soil type.

The midday surface resistance used in the OSRM is then adjusted:

$$\frac{1}{r_{m,dry}} = f_{SWP}\frac{1}{r_m} + (1 - f_{SWP})\frac{1}{r_n}$$

where $r_{m,dry}$ is the midday surface resistance for dry conditions;

r_m is the midday surface resistance for normal conditions;

r_n is the night-time surface resistance.

The values of f_{SWP} used were for grass growing on loam in East Anglia (52.5N 1.5 E).

6.5 Model outputs

A number of model outputs are presented for OSRM/SOFM simulations done for 2006. Upper leaf surface conductance was predicted for beech, wheat and potatoes for selected sites calculated using the new version of SOFM. Predictions of accumulated flux to these vegetation types at UK rural monitoring sites calculated using the new SOFM post-processor based on ozone concentrations predicted by the OSRM are compared with fluxes based on measured ozone concentrations. Maps of accumulated ozone flux over threshold and crop yields based on OSRM model runs at 10 km resolution and calculated using the new SOFM post-processor are presented. Following on from this the ozone metrics calculated for UK rural monitoring sites using the updated version of the OSRM and new SOFM are compared with those calculated from the old OSRM and SOFM2004. Finally, UK maps of two ozone concentration metrics calculated using the updated OSRM and new SOFM are given.

6.5.1 Upper leaf surface conductance

The upper leaf surface conductance is calculated as the ratio of the ozone flux to the upper leaf (or flag leaf per unit projected leaf area) to the ozone concentration at the displacement height, F_{st}/c.

6.5.1.1 Beech

Figure 6.3 shows the maximum daily predicted stomatal conductance for beech trees at 4 locations in the UK throughout the growing season (day 90-270) for 2006:

- 55.5N 3.5W near Edinburgh;
- 52.5N 2.5W, in the border area between Wales and England
- 52.5N 1.5W in the Midlands
- 52.5N 1.5E in East Anglia, near Lowestoft

The maximum daily stomatal conductance approached 4 mm s^{-1}.

The modelled maximum daily conductance for all the above locations varies quite significantly across the growing season. The range of predicted maximum daily conductance was reasonably similar for all locations. They include a period where the conductance fell sharply coinciding with a dry period in the summer.

6.5.1.2 Wheat

Figure 6.4 shows the maximum daily predicted stomatal conductance for wheat, at the same sites as above, for the accumulation period specified in the UNECE Mapping Manual. The accumulation period for wheat is based on phenological models and so the accumulation occurs much earlier in the year in southern England than it does further north.

The maximum daily stomatal conductance approached 11 mm s^{-1}. This may be compared with the species specific maximum conductance, g_{max} for wheat of 450 mmol m^{-2} PLA s^{-1} or 11 mm s^{-1}.

The range of predicted maximum daily conductance was reasonably similar for all locations, with conductance falling before the start of the dry period affecting stomatal conductance of beech.

Figure 6.3: Predicted stomatal conductance for beech trees at 4 locations in the UK for 2006

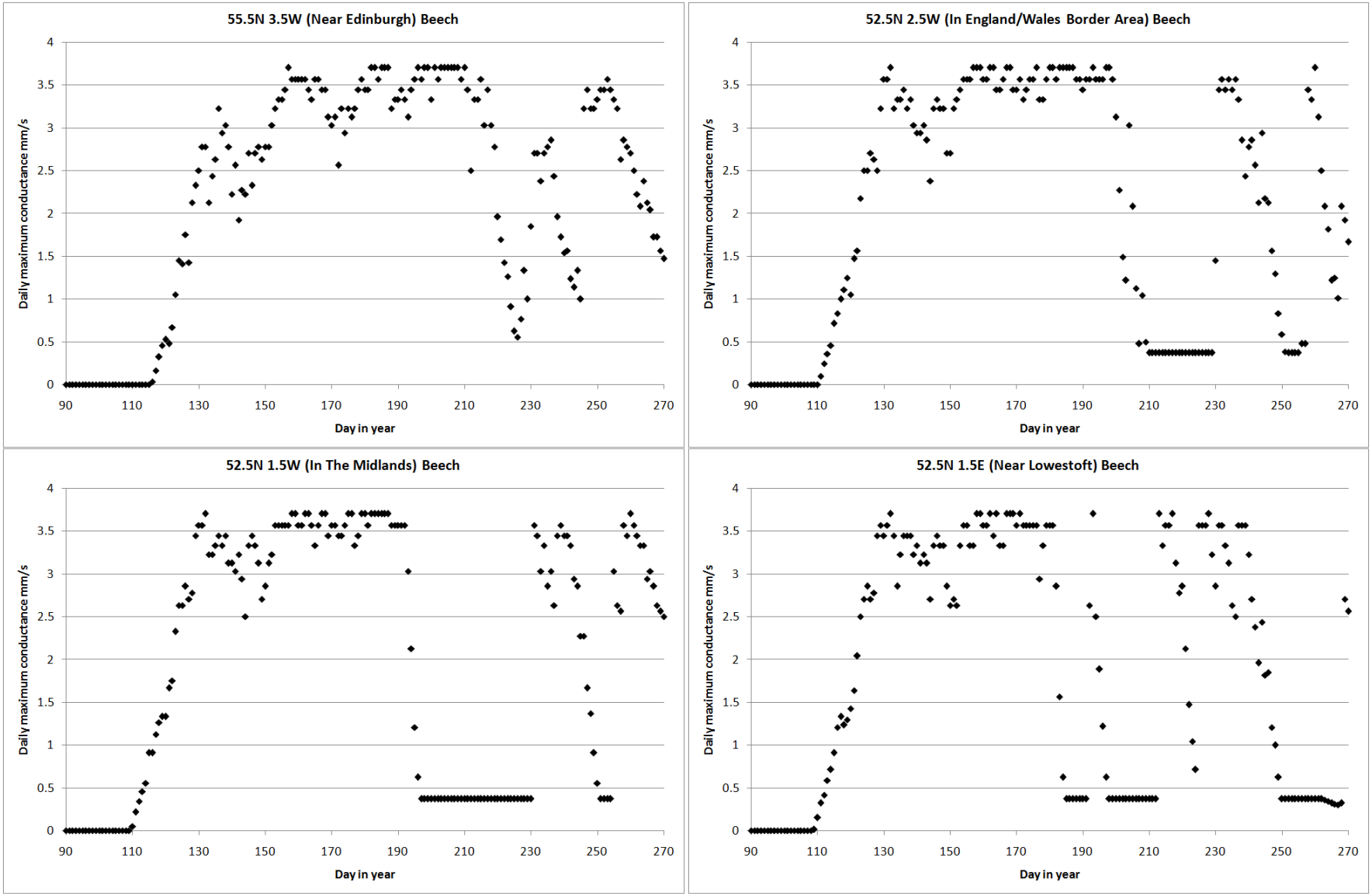

Figure 6.4: Predicted stomatal conductance for wheat at 4 locations in the UK for 2006.

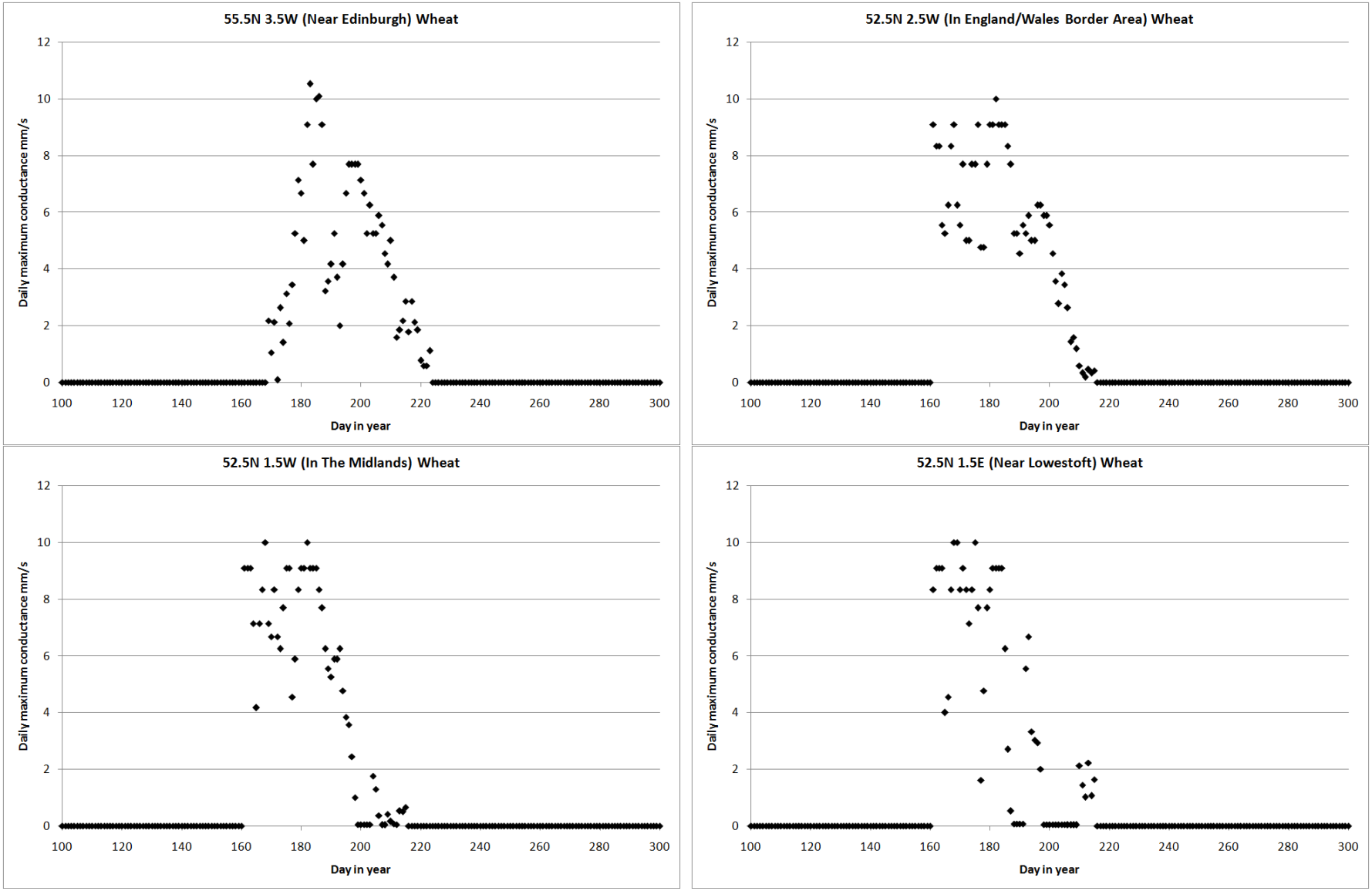

6.5.1.3 Potatoes

Figure 6.5 shows the maximum daily predicted stomatal conductance for potatoes at the same sites as above for the accumulation period specified in the UNECE Mapping Manual, based on a fixed emergence data of day 146. The accumulation period for potatoes is based on phenological models and the accumulation period is rather shorter in southern England than it is further north.

The maximum daily stomatal conductance approached 17 mm s^{-1}. This may be compared with the species specific maximum conductance, g_{max} for potatoes of 750 mmol m^{-2} PLA s^{-1} or 18.3 mm s^{-1}.

The predicted maximum daily conductance at 55.5N 3.5W near Edinburgh was generally rather less than that predicted in more southerly locations, due to the low maximum daily temperatures.

6.5.2 Accumulated flux at UK rural monitoring sites

The accumulated flux over threshold is calculated as the sum of hourly stomatal flux above threshold values over an accumulation period specified in the UNECE Mapping Manual. Table 6.2 shows the calculated stomatal flux over threshold for beech, wheat and potatoes at rural ozone monitoring sites in the UK Automatic Urban and Rural Network for 2006. The table shows the predicted accumulated fluxes calculated on the basis of modelled results from the updated OSRM and those calculated on the basis of measured ozone concentrations at these sites.

Table 6.2: Accumulated flux over threshold at UK rural monitoring sites for 2006: comparison of predictions based on OSRM ozone concentrations with predictions based on measured ozone concentrations

	Accumulated flux over threshold, mmol m^{-2} PLA					
Site	OSRM Ozone concentrations			Measured ozone concentrations		
	Beech	Wheat	Potatoes	Beech	Wheat	Potatoes
Strathvaich Dam	10.1	0.0	0.0	12.3	0.1	0.0
Aston Hill	12.9	0.0	0.3	16.2	0.8	1.2
Bush	11.8	1.0	0.8	10.1	0.6	0.9
Eskdalemuir	13.7	0.3	0.2	13.4	0.9	0.9
Great Dun Fell	11.8	1.3	1.0	11.7	2.2	2.5
Harwell	9.9	1.6	2.8	9.3	3.0	4.4
High Muffles	9.7	1.0	1.0	9.3	2.6	3.0
Ladybower	8.5	1.1	1.6	9.4	2.3	3.7
Lullington Heath	17.9	0.4	0.4	19.5	1.4	1.5
Narberth	16.7	0.1	0.1	15.4	0.2	0.4
Rochester	7.4	0.8	0.9	9.0	1.9	2.0
Sibton	10.5	2.2	3.0	11.6	4.1	5.4
Somerton	13.1	1.0	1.3	12.4	2.1	2.6
Wharley Croft	12.3	1.2	0.9	*	*	*
Wicken Fen	7.7	1.3	2.1	13.4	5.2	7.5
Wray	15.5	0.5	0.6	*	*	*
Yarner Wood	14.3	1.2	1.9	13.7	2.6	3.4
Bottesford	8.5	1.1	2.0	10.5	3.0	5.1
Glazebury	10.2	0.1	0.3	12.0	1.6	1.9
Lough Navar	12.1	0.7	1.6	8.0	0.6	1.6

*=data not available

Figure 6.5: Predicted stomatal conductance for potatoes at 4 locations in the UK for 2006

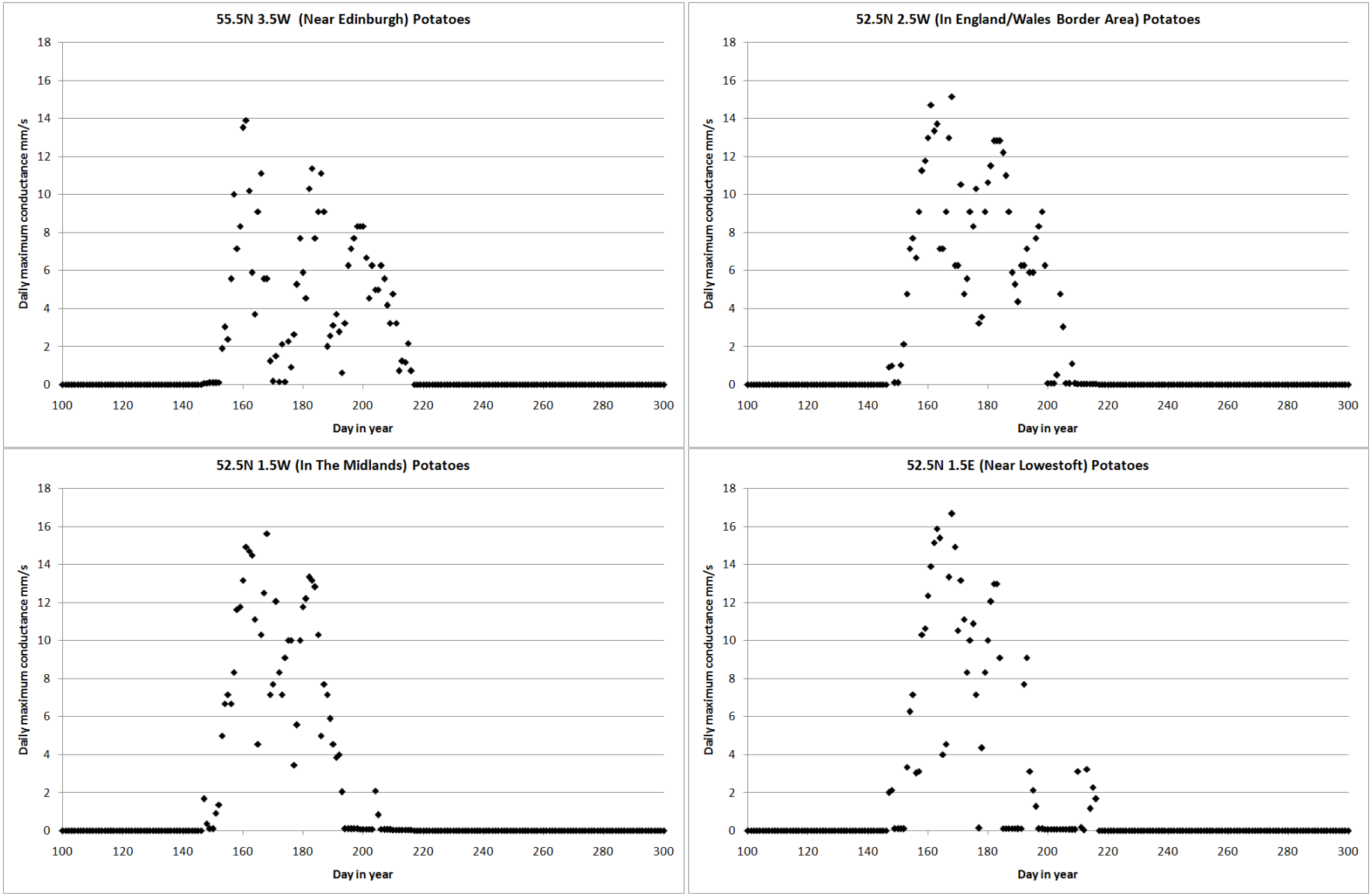

Figures 6.6, 6.7 and 6.8 show the accumulated flux over threshold in 2006 for beech, wheat and potatoes (respectively) calculated based on measured ozone concentrations plotted against the accumulated flux calculated based on predictions of ozone concentrations from the updated OSRM at these locations. The variation of the data points from the 1:1 line effectively reflects the performance of the OSRM in predicting ground-level ozone concentrations and the sensitivity of the accumulated flux over threshold calculated for each vegetation type to this level of performance.

There is fairly good agreement between the two prediction methods for beech, which suggests that OSRM can provide an effective means of predicting accumulated flux over threshold for this vegetation type. The use of the OSRM for wheat and potatoes results in under-prediction of accumulated flux over threshold typically by a factor of 2. This arises because the OSRM tends to under-estimate peak ozone concentrations and these underestimations have a more significant impact on the accumulated flux over threshold for wheat and potatoes. The under-prediction for wheat and potatoes (and not for beech) is probably due to the shorter accumulation period for these vegetation types.

Figure 6.6: Predicted accumulated flux over threshold for beech trees at UK rural ozone monitoring sites for the year 2006: comparison of predicted fluxes based on OSRM concentration predictions and measured data

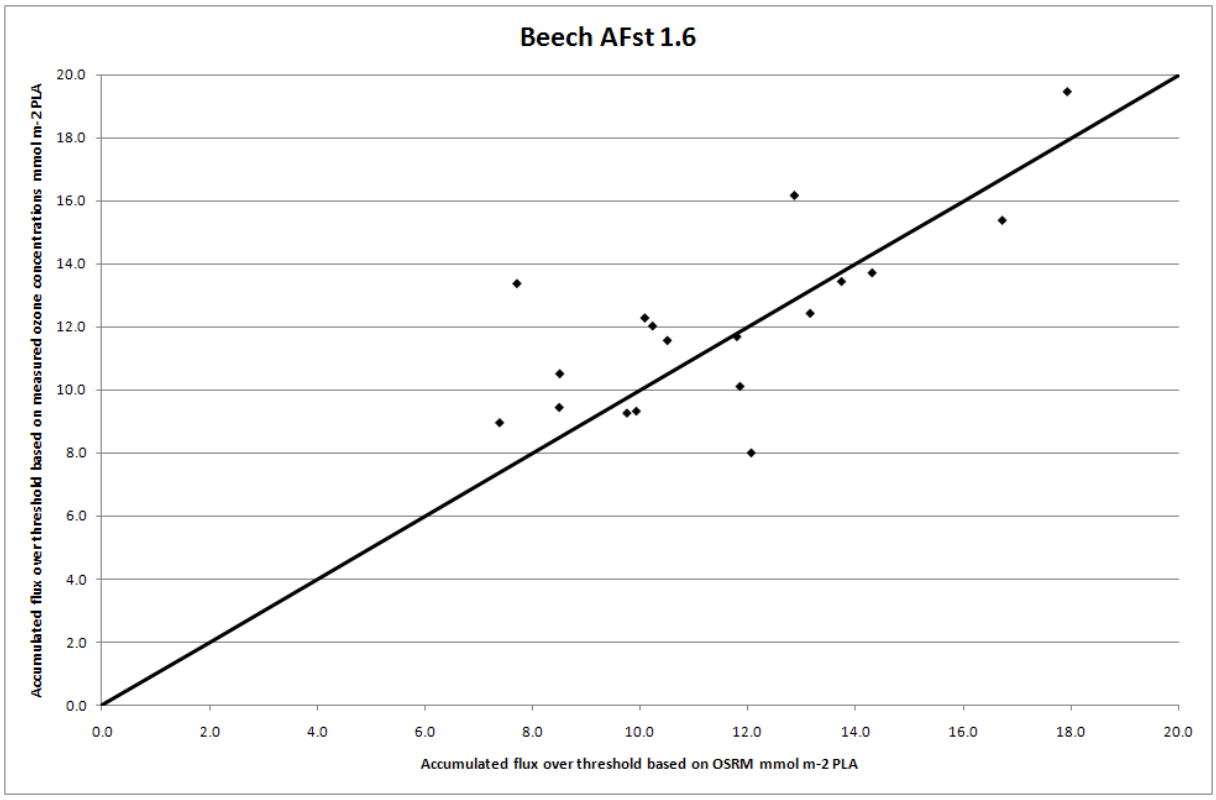

Figure 6.7: Predicted accumulated flux over threshold for wheat at UK rural ozone monitoring sites for the year 2006: comparison of predicted fluxes based on OSRM concentration predictions and measured data

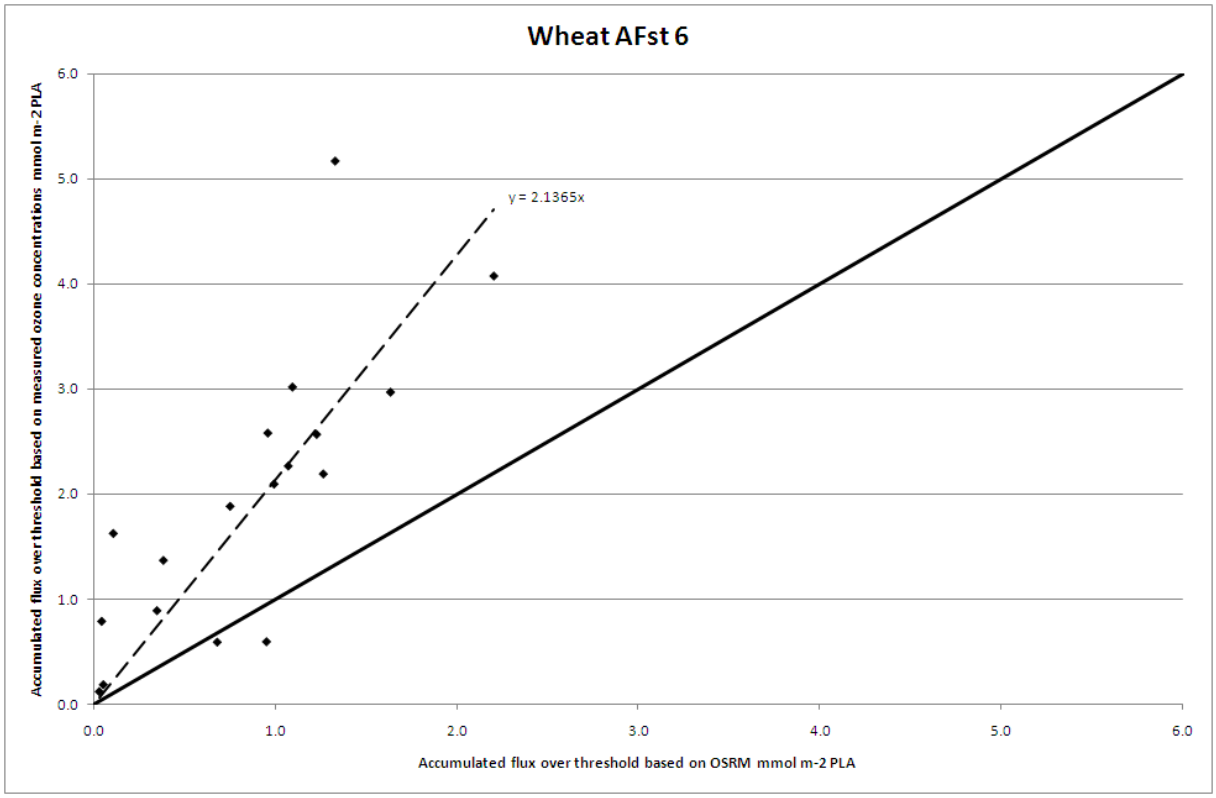

Figure 6.8: Predicted accumulated flux over threshold for potatoes at UK rural ozone monitoring sites for the year 2006: comparison of predicted fluxes based on OSRM concentration predictions and measured data

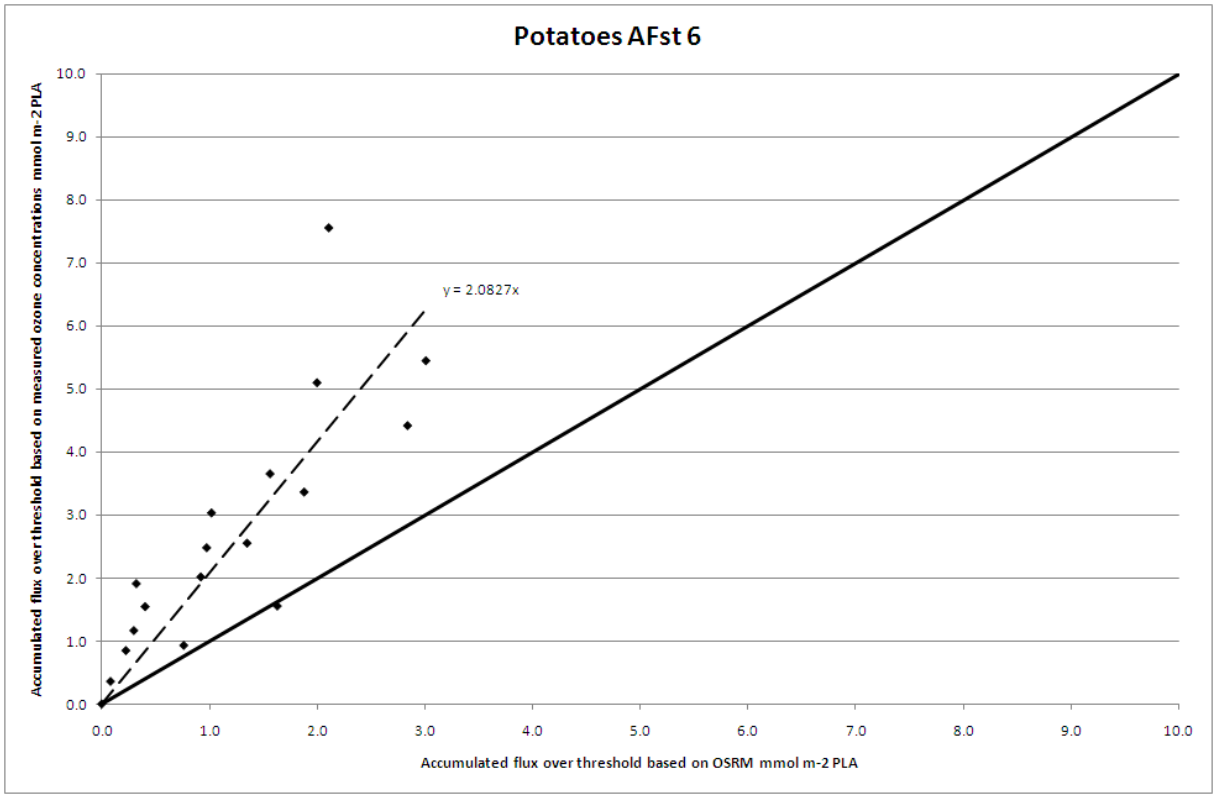

6.5.3 UK maps of accumulated flux

Figures 6.9, 6.10 and 6.11 show maps of predicted accumulated flux over threshold for beech, wheat and potatoes (respectively) for the year 2006. The maps are shown with accumulated flux calculated at 10 km resolution throughout the UK.

Figure 6.9 shows that the accumulated flux over threshold, AFst1.6 for beech exceeded the critical value of 4 mmol m^{-2} PLA (projected sunlit leaf area) over all of the UK.

Figure 6.10 shows that the accumulated flux over threshold, AFst6 for wheat exceeded the critical value of 1 mmol m^{-2} PLA over parts of England and Wales. The critical value corresponds to a 5% loss of yield. The accumulated flux was below the critical value over most of Scotland and Northern Ireland and Wales. The accumulated flux in these areas was limited to some extent by lower maximum temperatures.

Figure 6.11 shows that the accumulated flux over threshold, AFst6 for potatoes did not exceed the critical value of 5 mmol m^{-2} PLA in the UK in 2006. The critical value corresponds to a 5% loss of yield. The accumulated flux was smallest in Scotland and Wales. The accumulated flux in these areas was limited to some extent by lower maximum temperatures.

The general pattern in accumulated flux over threshold for beech is different to that for wheat and potatoes with levels lower on the eastern side of the country for beech where they are higher for the other two vegetation types. This reflects the influence of the dry summer period in this part of the country which reduces conductance to beech.

6.5.4 UK maps of crop yield

The UNECE Mapping Manual provides simple statistical relationships between the crop yield for wheat and potatoes affected by ozone uptake as a fraction of the unaffected yield and the accumulated ozone flux over threshold, $AF_{st}6$.

For wheat, the relationship is:

$$Yield = 1 - 0.048 AF_{st} 6$$

For potatoes, the relationship is:

$$Yield = 1.01 - 0.013 AF_{st} 6$$

Figures 6.12 and 6.13 show the percentage yield for wheat and potatoes (respectively) calculated for 2006 across the whole of the UK.

Figure 6.12 indicates that there was more than 10% loss in wheat yield in a small area in the north-east of England and a small area in East Anglia, and more than 5% loss in yield over much of central England. Figure 6.13 indicates that there was less than 5% loss in the yield of potatoes throughout the UK.

Figures 6.12 and 6.13 assume that wheat and potatoes are grown throughout the UK and the loss in yield has been calculated for example fields at each location. In practice, wheat and potatoes are grown to different extents in different parts of the country. The calculation of aggregate yield loss for the whole country is possible but requires additional data on crop distribution and yields.

The UNECE Mapping Manual recommends that similar maps should not be prepared for forest trees.

Figure 6.9: Map of predicted accumulated flux over threshold for beech trees for the year 2006

Figure 6.10: Map of predicted accumulated flux over threshold for wheat for the year 2006

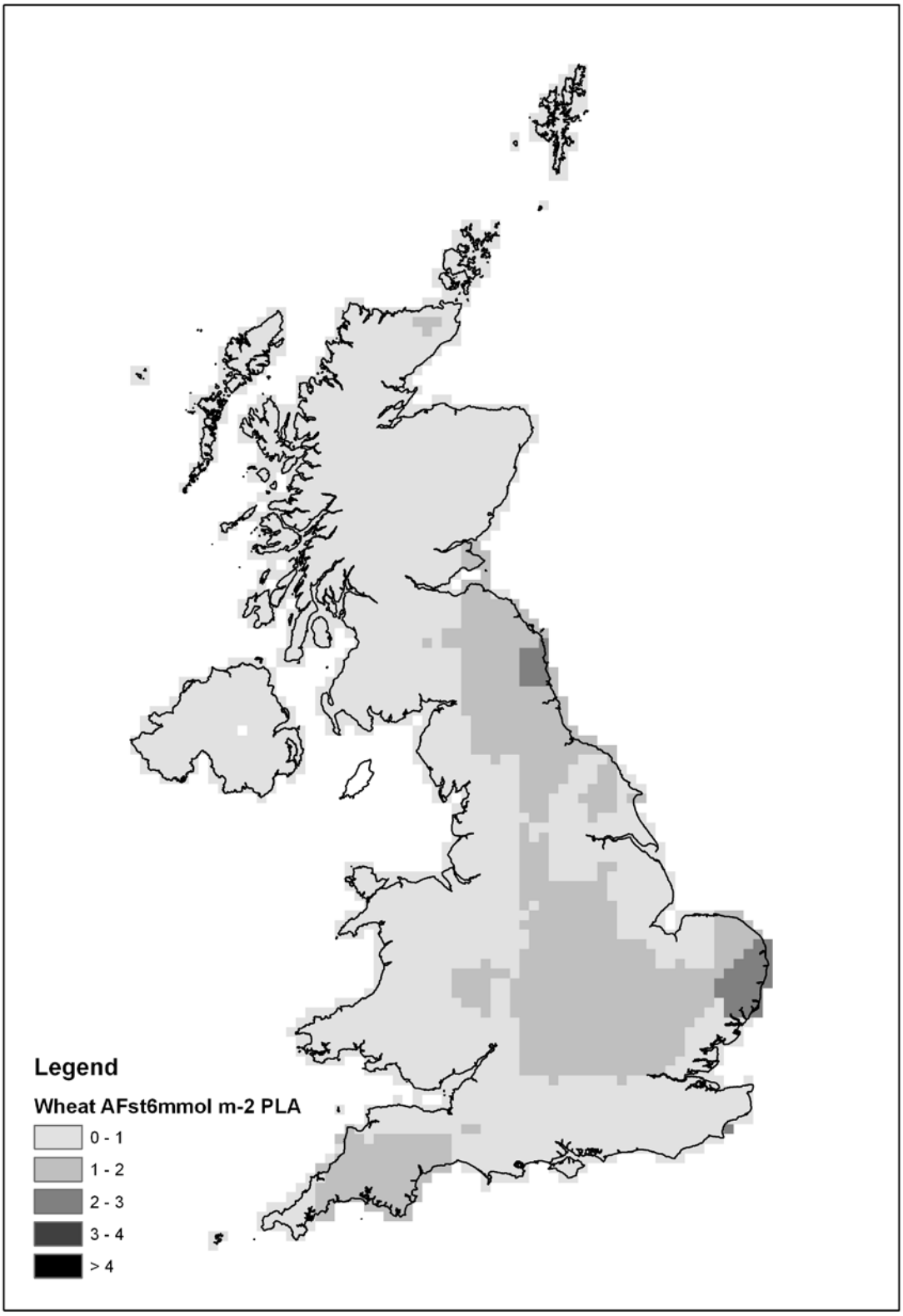

Figure 6.11: Map of predicted accumulated flux over threshold for potatoes for the year 2006

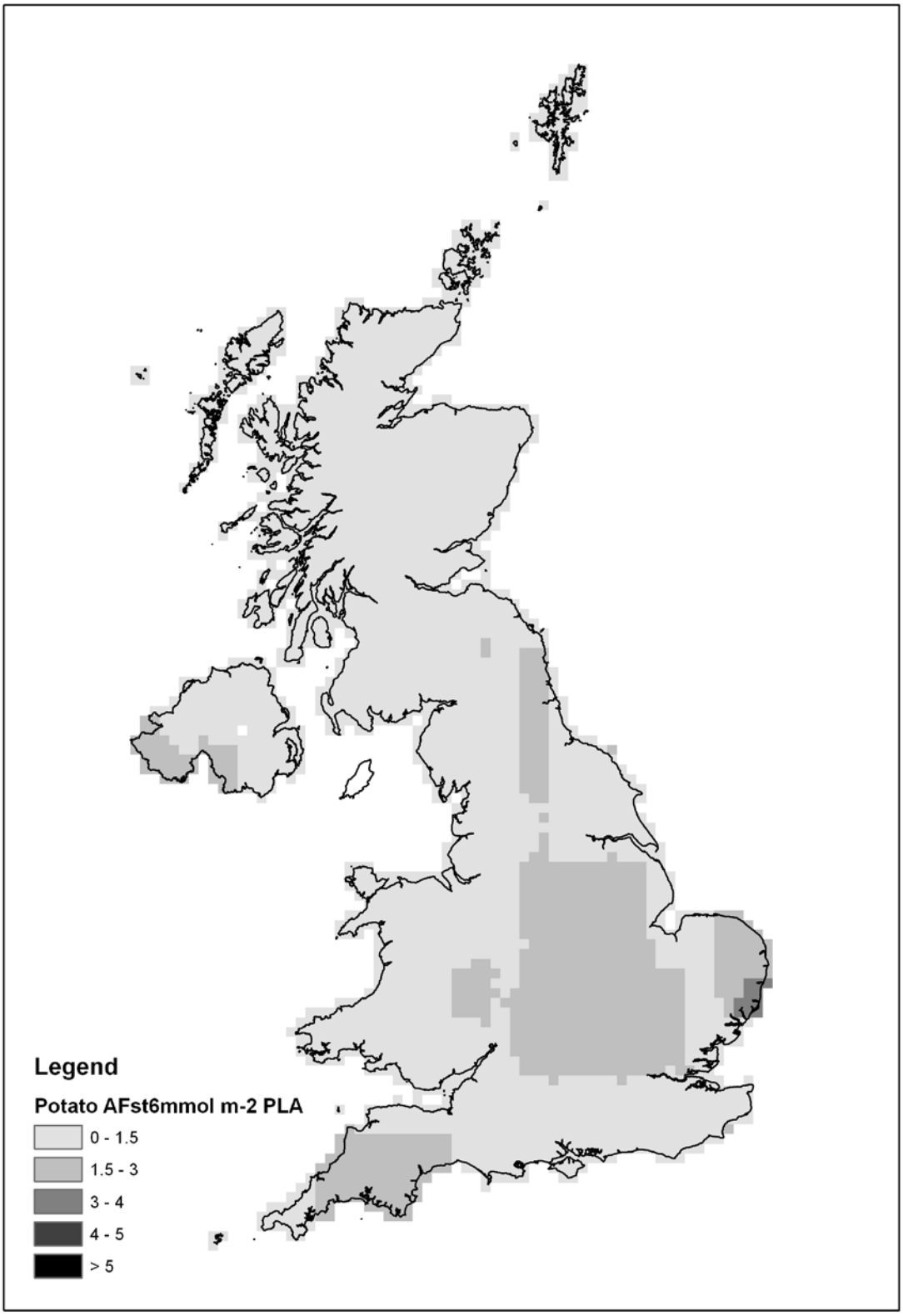

Figure 6.12: Map of predicted yield for wheat for the year 2006

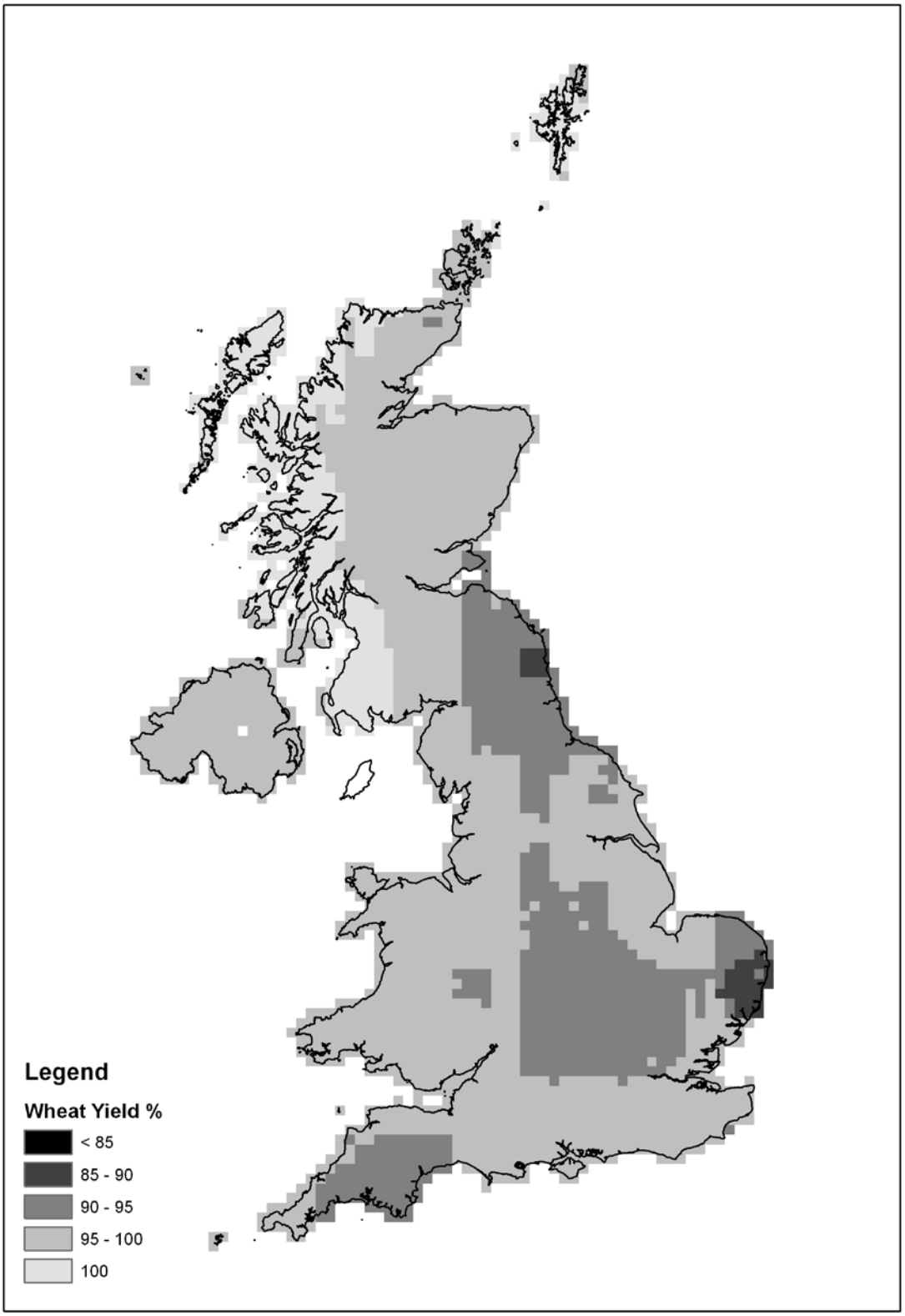

Figure 6.13: Map of predicted yield for potatoes for the year 2006

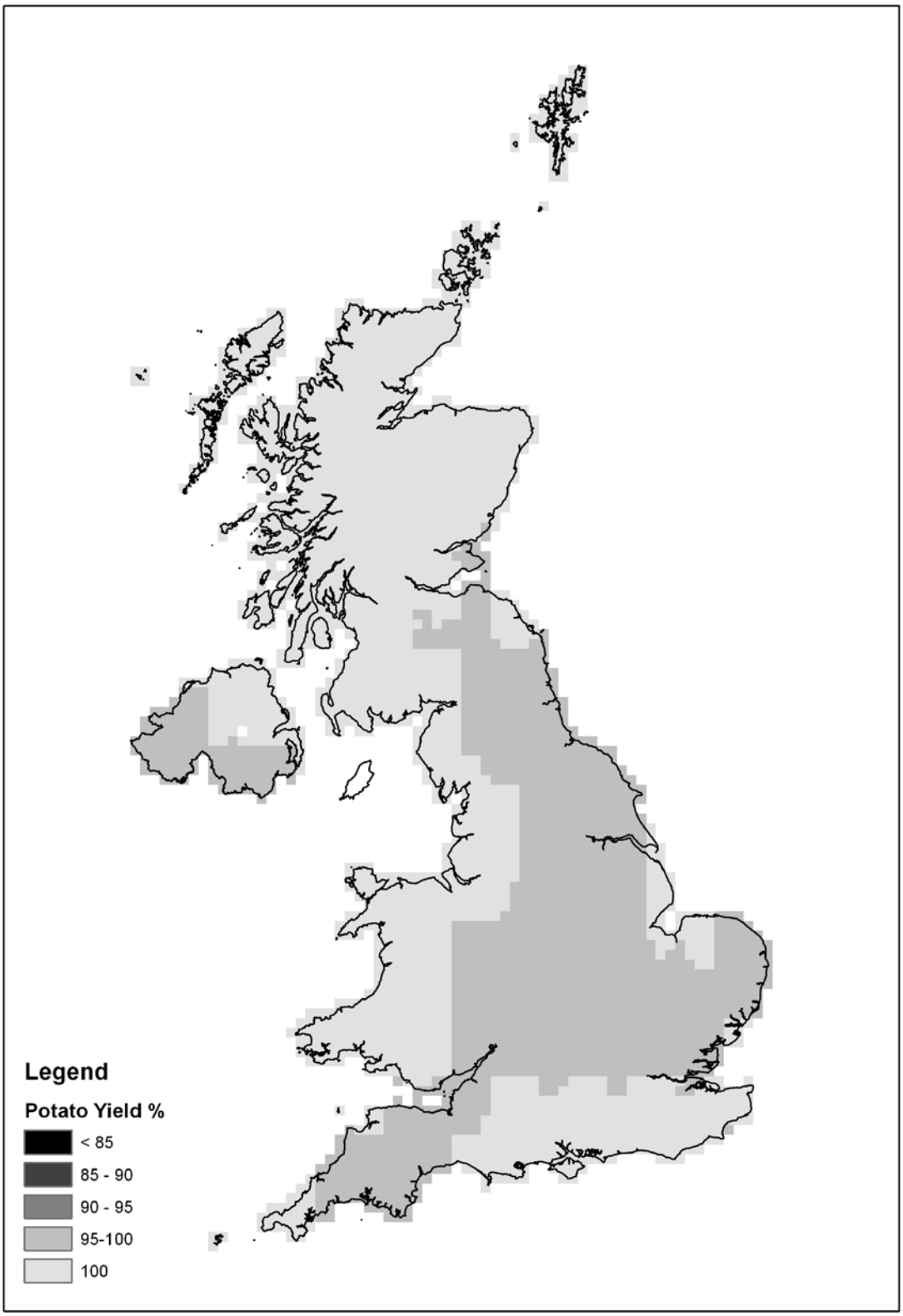

6.5.5 Ozone concentration metrics at UK rural monitoring sites

Two other ozone concentration metrics were calculated for 2006 at UK rural monitoring sites:

- The Accumulated Ozone Exposure over a threshold of 40 ppb (AOT40)
- The number of days in a year with a maximum 8-hour mean greater than 120 µg m^{-3}

The metrics calculated using the updated OSRM (taking account of reduced deposition during dry periods) were compared with those calculated using the previous version of OSRM and with those implied by measured concentrations.

Tables 6.3 and 6.4 show the predicted AOT40 and number of days with a maximum 8-hour mean greater than120 µgm^{-3} (respectively) measured at UK rural monitoring sites and modelled using the OSRM. These metrics were calculated because they are the metrics specified in the European Air Quality Directive for the protection of vegetation and human health.

Table 6.3: AOT40 at UK rural monitoring sites for 2006: comparison of values predicted by OSRM with measured values

Site	Measured AOT40 ugm-3.hours	Modelled (old OSRM with SOFM2004) AOT40 ugm-3.hours	Modelled (updated OSRM with new SOFM, 2006 fswp) AOT40 ugm-3.hours
Strathvaich Dam	6661	3045	3258
Aston Hill	11189	4717	4784
Bush	5803	3849	4382
Eskdalemuir	3729	4234	4533
Great Dun Fell	11142	4816	5058
Harwell	10834	5850	6244
High Muffles	5493	7716	7830
Ladybower	10538	3410	3642
Lullington Heath	4250	10074	10052
Narberth	8426	6876	6809
Rochester	7859	8728	9874
Sibton	11939	9557	10334
Somerton	8871	6959	6850
Wharley Croft	*	4763	5037
Wicken Fen	9222	6154	6776
Wray	*	4264	4440
Yarner Wood	12498	7617	7374
Bottesford	9896	4807	4220
Glazebury	5509	2458	2882
Lough Navar	12138	5762	5244

*=data not available

The AOT40 values predicted by the updated version of the OSRM are higher than those predicted by the old OSRM for most sites in the table above. This is due to the lower ozone deposition rates associated with the new SOFM soil moisture content model and the impact of dry conditions.

The predicted numbers of days greater than 120 µgm^{-3} from the updated version of the OSRM are higher than or the same as the numbers predicted by the old OSRM.

In general the OSRM under-predicts concentrations in a high ozone year such as 2006. The value from the updated version of the OSRM is generally closer to the measured value than the value from the old OSRM.

Table 6.4: Number of days greater than 120 µgm^{-3} at UK rural monitoring sites for 2006: comparison of values predicted by OSRM with measured values

Site	Measured number of days greater than 120 ugm-3	Modelled (old OSRM with SOFM2004) number of days greater than 120 ugm-3	Modelled (updated OSRM with new SOFM, 2006 fswp) number of days greater than 120 ugm-3
Strathvaich Dam	11	4	4
Aston Hill	21	7	7
Bush	3	2	3
Eskdalemuir	9	8	8
Great Dun Fell	13	7	7
Harwell	15	10	11
High Muffles	16	11	10
Ladybower	11	8	9
Lullington Heath	27	36	36
Narberth	8	17	16
Rochester	12	20	21
Sibton	21	25	26
Somerton	11	18	18
Wharley Croft	*	7	7
Wicken Fen	39	14	14
Wray	*	8	8
Yarner Wood	12	18	18
Bottesford	19	3	4
Glazebury	14	7	10
Lough Navar	5	12	13

*=data not available

6.5.6 UK maps of ozone concentration metrics

UK maps of two ozone concentration metrics (AOT40 and number of days with maximum 8-hour mean exceeding 120 µgm^{-3}) for 2006 were calculated using the updated OSRM.

Figure 6.14 shows the AOT40 values for 2006 predicted by the updated OSRM with the reduced deposition during dry periods.

Figure 6.15 shows the predicted number of days with maximum 8-hour mean exceeding 120 µgm^{-3} for 2006 modelled by the updated version of the OSRM with the reduced deposition during dry periods.

The general spatial patterns are similar to those calculated for the unmodified OSRM (Murrells et al, 2008)

Figure 6.14: Map of predicted AOT40 (µgm^{-3}.hours) for 2006 modelled using OSRM

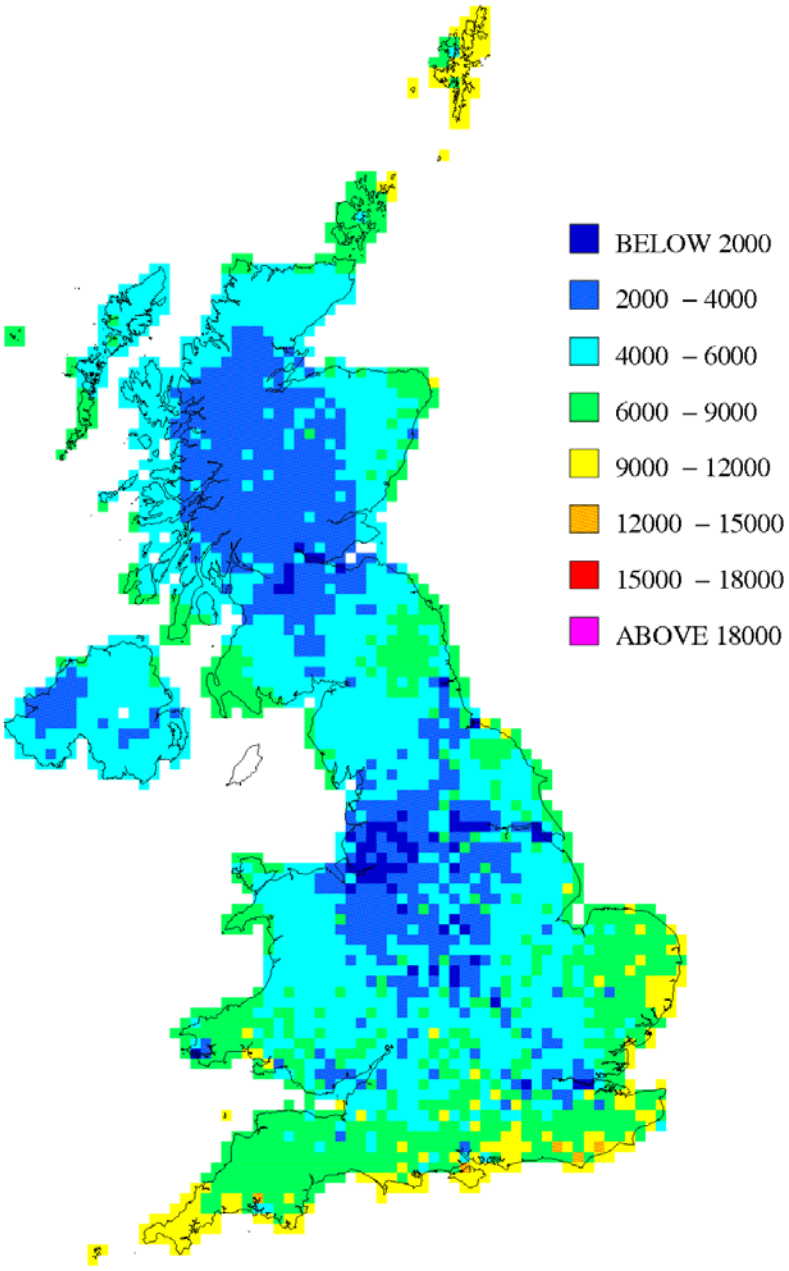

Figure 6.15: Map of predicted number of days greater than 120 µgm^{-3} for 2006 modelled using OSRM

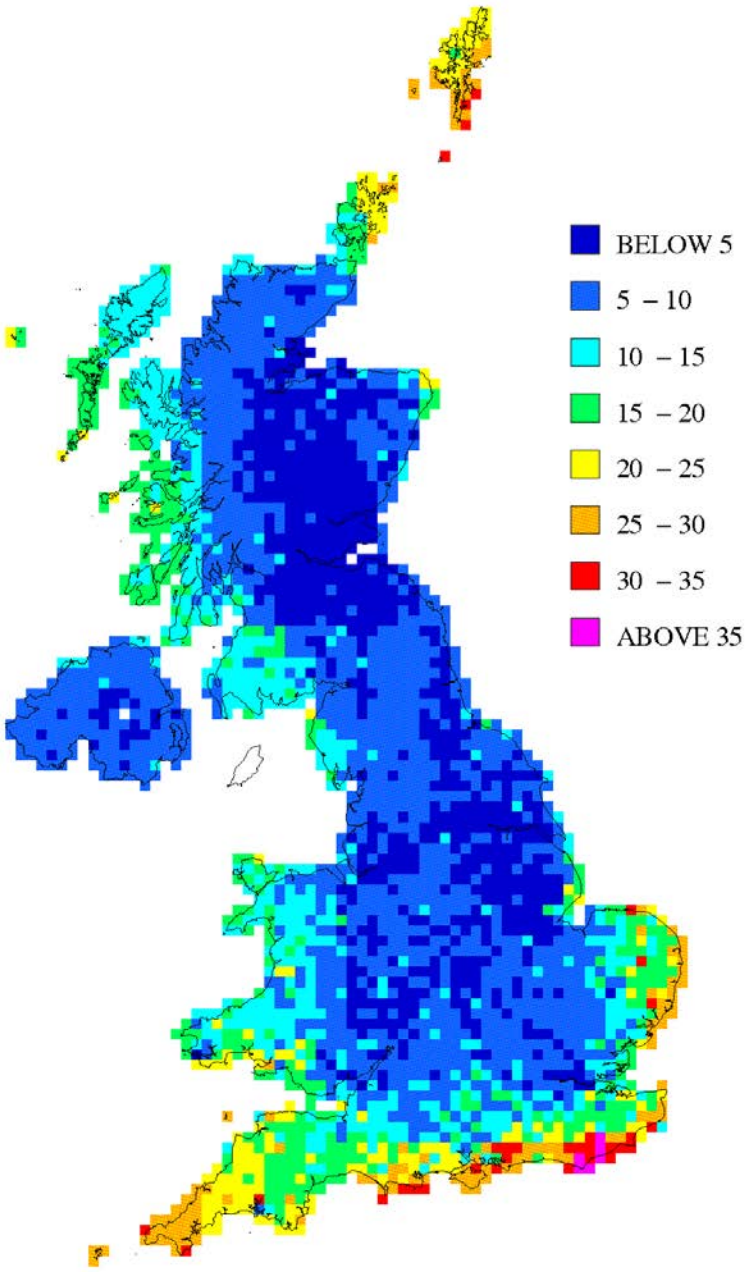

6.6 Summary and main conclusions

The main conclusions of the work of Objective 12 on the development and application of the Surface Ozone Flux Model are summarised as follows:

Summary:

- **New stomatal flux algorithms developed by SEI York have been implemented into the Surface Ozone Flux Model and used in conjunction with the OSRM to model accumulated stomatal flux conditions in the UK during 2006. The OSRM was also modified to increase surface resistance when stomatal conductivity is predicted to be low by SOFM because of dry soil conditions**
- **Modelled stomatal flux based on ozone concentrations modelled by the updated version of the OSRM were compared with stomatal flux based on measured ozone concentrations in 2006. The comparison suggested that the OSRM can provide a reasonably effective means of predicting accumulated flux over threshold to beech. The use of the OSRM for wheat and potatoes results in under-prediction of accumulated flux over threshold typically by a factor of 2. This arises because the OSRM tends to under-estimate peak ozone concentrations in years where these are particularly high**
- **The model predicted that growth of wheat across the whole of the UK was affected by ozone deposition in 2006. Ozone deposition was associated with at least a 5% loss in yield across the whole of the UK, with losses of more than 10% predicted in some areas of North-East England and East Anglia. The loss in yield was smaller in cooler areas in Scotland and Wales with lower maximum temperatures. The model also predicted that the growth of potatoes was not substantially affected by ozone deposition. Ozone deposition was associated with less than 5% loss in yield throughout the whole of the UK**
- **The predicted ozone metrics modelled for the UK rural measurement sites using the updated OSRM are higher than or the same as those predicted by the previous version of the OSRM before the modifications were made. In general the OSRM under-predicts concentrations in a high ozone year such as 2006. The value from the updated OSRM is closer to the measured value than the value from the original version of OSRM.**
- **The results from this study will be combined with those from other studies using the same stomatal flux algorithms in alternative ozone models. The results and conclusions from these assessments will then be presented in a publication for external peer review.**

7 Other Project Activities

Other project activities have been carried out in 2010 involving the project consortium members.

7.1 Model review activities

Aside from the main project objectives, the project consortium has participated in a range of activities relating to Defra's review of air quality models which was initiated in 2010.

At Defra's request, the consortium provided a review of models it uses for regional and local scale modelling outlining the modelling capacity of the OSRM, CMAQ, PTM and TRACK-ADMS. The consortium also provided information for Defra's Science Advisory Council's review of models used throughout Defra. Information was provided on the OSRM and PTM including background to the models, their development and maintenance and validation, verification and assessments undertaken on and with the models.

The other main activities carried out by members of the project team in 2010 were in relation to Defra's Model Intercomparison Protocol (MIP) and the planned model evaluation exercise. The Protocol was prepared by the project consortium in Phase I of the project and during 2010, AEA and Prof Dick Derwent carried out preparatory work in advance of the launch of the model evaluation at a meeting held in April. Dick Derwent provided an introduction to the MIP to all participants at the meeting. The group from AEA and Dick Derwent took part in the break-out groups on deposition modelling (including acidification) and regional and transboundary pollution modelling including ozone.

Following invitations to take part in the model evaluation exercise itself, questionnaires were completed providing key information on the main ozone models used in the project, namely the OSRM and PTM. Ozone modelling results from the OSRM and PTM for the defined 2006 model year were compiled and submitted in the required format to ERG/Kings' College, London to be compared with monitoring data and results from other models. AEA also submitted ozone modelling results from the CMAQ model.

7.2 Project meetings and reports

A kick-off meeting for Phase II of the project was held at Defra on 28th January. Tim Murrells (Project Manager) gave an overview of the project, followed by contributions for each contractor on the work they will be undertaking for the core objectives. Prof Derwent also gave a summary of the Model Intercomparison Protocol completed in Phase I of the project. Progress made on the core objectives was presented by the consortium members at a meeting held at Defra on 26th October.

Three quarterly progress reports were prepared for Defra providing a summary of the progress made on each of the various project objectives and project management related issues.

7.3 Technical reports and publications

The following paper covering work undertaken in this contract has been published in Atmospheric Chemistry and Physics:

Archibald A.T., Cooke M.C., Utembe S.R., Shallcross D.E., Derwent R.G. and Jenkin M.E. (2010). **Impacts of mechanistic changes on HO_x formation and recycling in the oxidation of isoprene**. Atmos. Chem. Phys., 10, 8097–8118.

The following papers have been published on work undertaken during Phase I of the contract:

Derwent, R.G. Claire S. Witham, Steven R. Utembe, Michael E. Jenkin, Neil R. Passant. **Ozone in Central England: the impact of 20 years of precursor emission controls in Europe.** Environmental Science & Policy 13 (2010) 195 – 204

Richard G. Derwent, Michael E. Jenkin, Steven R. Utembe, Dudley E. Shallcross, Tim P. Murrells, Neil R. Passant. **Secondary organic aerosol formation from a large number of reactive man-made organic compounds**. Science of the Total Environment 408 (2010) 3374–3381

The following peer-reviewed paper covering the development and testing of the OSRM was published in Atmospheric Environment:

G.D. Hayman, J. Abbott, T.J. Davies, C.L. Thomson, M.E. Jenkin, R. Thetford and P. Fitzgerald (2010). **The ozone source–receptor model – A tool for UK ozone policy**. Atmospheric Environment, 44(34), 4283-4297. http://dx.doi.org/10.1016/j.atmosenv.2010.06.013.

The following presentation was made at the “Workshop on Ozone – a regional and global pollutant, Wengen, Switzerland, 28th – 29th September 2010”:

Jenkin M.E.: **Impacts of mechanistic changes on HO_x formation and recycling in VOC oxidation.**

The following poster presentation was made at the 21st International Symposium on Gas Kinetics, Leuven , Belgium , 18th-22nd July 2010”.

Barjat, H.R., Carver, G.D., Cox, R.A., Rickard, A.R., Young, J.C. and Pascoe, S.: **Integrating Model Chemical Mechanisms with Databases of Reaction Kinetics**.

The following paper describing the original development of the MCM protocol (with support from DETR over the years) has been awarded the 2010 Haagen-Smit Prize by Atmospheric Environment:

Jenkin M.E., Saunders S.M and Pilling M.J. (1997). **The tropospheric degradation of volatile organic compounds: a protocol for mechanism development**. Atmospheric Environment, 31, 81-104.

8 Conclusions and Policy Relevance

The work carried out during 2010 in the second phase of the project has involved the further research and development of models describing the formation and removal of tropospheric ozone and secondary organic aerosol for use in Defra policy. The focus has been on further development of the chemical schemes used in models to deal with the atmospheric oxidation of VOCs emitted from biogenic sources and solvent use and the model formulations for describing the removal of ozone by vegetation. This has been supported by further analysis of monitoring data to understand spatial patterns and temporal trends in ozone and other secondary air pollutants and the contributions of hemispheric and regional components to background concentrations and the effects of locally emitted NO_x.

Current modelling tools have been used to support Defra policy on ozone and secondary PM air quality. The OSRM has been used to model the UK ozone climate in 2008 and has been used to forecast ozone concentrations in 2020 based on current projections of ozone precursor emissions. These will be used as the benchmark for further analysis of future 2020 emission scenarios.

The PTM was used for a probabilistic uncertainty analysis of modelled ozone episodes and in the model response to reductions in precursor emissions. The PTM has also been used to model SOA and the results compared with observations. The contribution of natural biogenic and anthropogenic emission sources to SOA was evaluated and the spatial distribution and seasonal cycle in SOA concentrations in the UK assessed.

To achieve the main aims of the project, the work was divided into four main objectives. The main conclusions reached so far for each objective are summarised below, taken from Sections 3-6.

Objective 9: Improvement to Photochemical Reaction Schemes for Treatment of Biogenic Emissions and Emissions of Chlorinated VOCs from Solvents

Summary:

- **A new chemical reaction scheme has been developed and successfully tested for the atmospheric degradation of a highly reactive biogenic species, β-caryophyllene, the largest VOC treated to date in the Master Chemical Mechanism and the most reactive with respect to reaction with ozone. The new mechanism has expanded the coverage of biogenic VOC chemistry and extended the reactivity range of VOC species represented in the MCM. This will help to improve the prediction of ozone and other secondary air pollutants (e.g. secondary organic aerosols) from VOCs emitted from natural sources which will become increasingly important as emissions from anthropogenic sources decrease.**
- **An initial assessment of the reactivity and mechanisms for degradation of halogenated VOCs used in solvents has been made. This has shown how the reactivity decreases with additional α-halogen substitution in the VOC. The work will form the basis for development of structure-reactivity relationships to define mechanism development protocols for the MCM.**
- **The initial steps have been taken on the implementation of a reduced secondary organic aerosol (SOA) chemistry code for the OSRM. This work will continue during 2011 and the OSRM tested for modelling of SOA.**

- A hypothesis has been developed based on independent research studies and model sensitivity tests for the OH radical-recycling under low NO_x conditions. This will help to enhance the performance of chemical mechanisms for VOC oxidation used in models which appear to be currently deficient under these conditions.
- The targeted extension and revisions to the MCM undertaken in this project are to be released as MCM v3.2 on the dedicated website facility maintained by the University of Leeds.

Objective 10.1: Modelling the UK Ozone Climate in 2008

Summary:

- When comparing the OSRM results with measured data for the two EU Air Quality Directive ozone metrics for 2008 the OSRM has generally overestimated the days greater than 120 µg m^{-3} metric and underestimated the AOT40 metric.
- Previously the OSRM overestimated these ozone metrics in low ozone years (2004, 2005 and 2007) and underestimated them in high ozone years (2003 and 2006) compared with measured data. In 2008, a moderate ozone year, a mixed effect was observed, but overall there is less of a systematic bias in the model results in the 2008 simulations than there was in the 2007 simulations.
- The UKAAQA empirical model continues to produce results that are closer to the measured concentrations than the OSRM and should continue to be used in its current capacity (contributing modelled data in fulfilment of UK reporting obligations to the European Commission).

Objective 10.2: Modelling support for Policy Development and Implementation

Summary:

- The OSRM has been used in conjunction with current UK and European emission projections to forecast the UK's ground-level ozone climate in 2020 assuming meteorology conditions representative of 2006 and 2007.
- Ozone concentrations expressed in different metrics are predicted to be higher in 2020 than in 2007 as a results of changes in emissions when the same meteorological conditions are assumed
- Concentrations are generally lower for 2020 when 2007 meteorology is assumed compared with concentrations modelled for 2020 assuming 2006 meteorology. However, the spatial pattern in concentrations and the effect of meteorological conditions are different for different metrics.
- The results from this work will form the baseline ozone concentrations for the UK against which the effects of alternative emission reduction scenarios in the UK and the rest of Europe will be modelled.
- Probabilistic uncertainty analysis using the PTM for simulating an ozone episode observed in Birmingham during the summer of 1999 showed that there was little sensitivity in the ozone model predictions to the choice of chemical mechanism used: the Carbon Bond Mechanism or CRIv2 condensed mechanism. However, this conclusion would need to be verified for other conditions to ascertain whether this conclusion had general validity.
- Probabilistic assessments of the PTM responses to 30% reductions in NO_x or

VOC emissions indicated that for simulations leading to peak ozone concentrations in the West Midlands during 1999 there was only a 10% chance that VOC emission reductions would bring predicted ozone concentrations below 60ppb. However, there was only a 5% chance with NO_x emission control indicating that VOC controls would more likely bring ozone below 60ppb than NO_x control for these specific conditions.

Objective 10.3: Specific Modelling and Assessments for Policy Development on SOA

Summary:

- Using the newly developed chemistry mechanism for SOA formation in the CRI, the PTM was able to account for organic carbon episodes observed at a site in Birmingham during 2006. However, the model showed an overall negative bias, tending to underpredict SOA concentrations
- Correlations between model predictions and observations pointed towards SOA components from anthropogenic sources as the main cause of organic PM episodes at this site.
- Model sensitivity runs showed how the performance of the PTM could be optimised by increasing precursor emissions and changing certain model parameterisations
- The optimised model was used to estimate the distribution of SOA across the UK in 2008. The results showed that the contribution of anthropogenic (ASOA) and biogenic (BSOA) sources varies across the country with the highest biogenic contributions occurring at sites in Scotland where they are 3 times higher than anthropogenic sources. At other sites, the contributions of ASOA and BSOA are comparable, but biogenic sources tend to dominate. Across the whole of the UK, about 61% of SOA was from biogenic sources, 39% from man-made sources.
- Seasonal cycles in SOA from anthropogenic sources are highly variable and driven by meteorology conditions. Seasonal cycles in BSOA at all sites showed a strong maximum in May. During May 2008, 75% of all SOA are from biogenic sources.
- Analysis of trajectories showed the varying influence of long-range transport and local emission sources to BSOA at different sites. ASOA also peaks at different times at different sites due to different contributions from precursors transported from continental Europe and UK sources.
- Based on future emissions, ASOA modelled at Aston Hill is predicted to decline by 16% between 2008 and 2020, whereas BSOA is expected to show a small increase, illustrating how SOA components respond differently to NO_x and VOC controls.
- Sensitivity studies showed that BSOA and ASOA display non-linear responses to NO_x and VOC emission reductions. It will be necessary to account for this when assessing responses of overall $PM_{2.5}$ concentrations to future emissions. Overall, SOA decreased to a greater extent in response to changes in VOC emissions than NO_x.

Objective 11: Assessments of Background and Urban-Scale Oxidant

Summary:

- A method based on the analysis of ambient data on O_3, NO_2 and NO_x has been developed to characterise the geographical variation in annual mean background oxidant concentrations over the UK at 1x1km resolution.
- The method has been used to generate optimised maps of annual mean background oxidant concentrations for each year between 2001 and 2009. The time-series has been tested by comparison with concentrations measured at 12 UK monitoring sites.
- The previously reported altitude dependence of ozone concentrations in the UK has been investigated and found to be largely due to the roughly inverse dependence of the proximity of NO_x emission sources on site altitude and the impact this has on sequestering ozone in the form of NO_2 leading to a much weaker altitude dependence of total oxidant.
- The background oxidant maps and parameterisations developed in this work are being used to inform and improve NO_2 and O_3 empirical modelling activities in the UK Ambient Air Quality Assessments programme (UKAAQA) for air quality directive reporting and further Defra policy analysis.

Objective 12: Development of the Surface Ozone Flux Model

Summary:

- New stomatal flux algorithms developed by SEI York have been implemented into the Surface Ozone Flux Model and used in conjunction with the OSRM to model accumulated stomatal flux conditions in the UK during 2006. The OSRM was also modified to increase surface resistance when stomatal conductivity is predicted to be low by SOFM because of dry soil conditions
- Modelled stomatal flux based on ozone concentrations modelled by the updated version of the OSRM were compared with stomatal flux based on measured ozone concentrations in 2006. The comparison suggested that the OSRM can provide a reasonably effective means of predicting accumulated flux over threshold to beech. The use of the OSRM for wheat and potatoes results in under-prediction of accumulated flux over threshold typically by a factor of 2. This arises because the OSRM tends to under-estimate peak ozone concentrations in years where these are particularly high
- The model predicted that growth of wheat across the whole of the UK was affected by ozone deposition in 2006. Ozone deposition was associated with at least a 5% loss in yield across the whole of the UK, with losses of more than 10% predicted in some areas of North-East England and East Anglia. The loss in yield was smaller in cooler areas in Scotland and Wales with lower maximum temperatures. The model also predicted that the growth of potatoes was not substantially affected by ozone deposition. Ozone deposition was associated with less than 5% loss in yield throughout the whole of the UK
- The predicted ozone metrics modelled for the UK rural measurement sites using the updated OSRM are higher than or the same as those predicted by the previous version of the OSRM before the modifications were made. In general the OSRM under-predicts concentrations in a high ozone year such as 2006. The value from the updated OSRM is closer to the measured value than the value from the original version of OSRM.
- The results from this study will be combined with those from other studies

using the same stomatal flux algorithms in alternative ozone models. The results and conclusions from these assessments will then be presented in a publication for external peer review.

9 Acknowledgements

The consortium partners acknowledge the support provided by the Department for Environment, Food and Rural Affairs (Defra) and the Devolved Administrations (the Welsh Assembly Government, the Scottish Executive and the Department of the Environment for Northern Ireland) under contract AQ0704. We especially acknowledge the help and support of Dr Samantha Lawrence of Atmosphere and Local Environment Programme (ALE) of Defra in facilitating the direction of the project in 2010.

We are grateful for the following collaborative contributions to this work of Objective 9 on photochemical reaction schemes: Professor Gordon McFiggans and Dr Rami Alfarra (University of Manchester) in relation to chamber evaluation of the limonene and β–caryophyllene schemes (Section 3.2); Dr Steven Utembe (University of Manchester) in relation to advice on implementation of the CRI SOA code (Section 3.4); Dr Alex Archibald and Professor Dudley Shallcross (University of Bristol) in relation to testing of the isoprene mechanism (Section 3.5).

Lisa Emberson (Stockholm Environment Institute, University of York) is thanked for providing much detailed advice on the further development of the Surface Ozone Flux Model in Objective 12 (Section 6).

10 References

Abbott, J and S Cooke (2010). Development of the Surface Ozone Flux Model. AEA Report for Defra, AEAT/ENV/R/3098 (December 2010)

Abdalmogith, S.S., Harrison, R.M., Derwent, R.G. (2006). Particulate sulphate and nitrate in southern England and Northern Ireland during 2002/3 and its formation in a photochemical trajectory model. Science of the Total Environment 368, 769–780.

AQEG (2007). Trends in primary nitrogen dioxide in the UK. Report of the UK Air Quality Expert Group, AQEG. Prepared for the Department for Environment Food and Rural Affairs, the Scottish Executive, the Welsh Assembly and the Department of the Environment in Northern Ireland. Defra publications, London, 2007. ISBN 978-0-85521-179-0.

AQEG (2009). Ozone in the United Kingdom. Report of the UK Air Quality Expert Group, AQEG. Prepared for the Department for Environment Food and Rural Affairs, the Scottish Executive, the Welsh Assembly and the Department of the Environment in Northern Ireland. Defra publications, London, 2009. ISBN 978-0-85521-184-4.

Archibald A.T., Jenkin M.E. and Shallcross D.E. (2010a). An isoprene mechanism intercomparison. Atmospheric Environment, 44, 5356–5364.

Archibald A.T., Cooke M.C., Utembe S.R., Shallcross D.E., Derwent R.G. and Jenkin M.E. (2010b) Impacts of mechanistic changes on HOx formation and recycling in the oxidation of isoprene. Atmos. Chem. Phys., 10, 8097–8118.

Boissard, C., Cao, X.-L., Juan, C.-Y., Hewitt, C.N. and Gallagher, M. (2001). Seasonal variations in VOC emission rates from gorse, Atmospheric Environment, 35, 917–927.

Bush T, I Tsagatakis, N Passant, A Griffin and B Pearson (2010). UK Emission Mapping Methodology 2007. Report for The Department for Environment, Food and Rural Affairs, Welsh Assembly Government, the Scottish Executive and the Department of the Environment for Northern Ireland. AEA Report AEAT/ENV/R/2863 (September 2010). http://www.airquality.co.uk/reports/cat07/1010011332_UKMappingMethodReport2007.pdf

Butler, T. M.; Taraborrelli, D.; Brühl; C.; Fischer, H.; Harder, H.; Martinez, M.; Williams, J. (2008). Improved simulation of isoprene oxidation chemistry with the ECHAM 5/MESSy chemistry-climate model: lessons from the GABRIEL airborne field campaign. Lawrence, M. G.; Lelieveld, J. Atmos. Chem. Phys. 8, 4529.

Calogirou, A., Kotzias, D., and Kettrup A. (1997). Products analysis of the gas phase reaction of β-caryophyllene with ozone, Atmos. Environ. 31 (2), 283–285.

Calvert, J. G., Atkinson, R., Kerr, J. A., Madronich, S., Moortgat, G. K., Wallington, T. J. and Yarwood, G (2000).: The Mechanisms of Atmospheric Oxidation of Alkenes, Oxford University Press, New York. ISBN 0195131770, 2000.

Clapp L.J. and Jenkin M.E. (2001). Analysis of the relationship between ambient levels of O_3, NO_2 and NO as a function of NOx in the UK. Atmospheric Environment, **35**, 6391-6405

Derwent, R.G., Jenkin, M.E., Saunders, S.M. (1996). Photochemical ozone creation potentials for a large number of reactive hydrocarbons under European conditions. Atmospheric Environment 30, 181–199.

Derwent, R.G., Jenkin, M.E., Saunders, S.M., Pilling, M.J. (1998). Photochemical ozone creation potentials for organic compounds in northwest Europe calculated with a Master Chemical Mechanism. Atmospheric Environment 32, 2429–2441.

Derwent, R.G., Simmonds, P.G., Manning, A.J. Spain, T.G., (2007). Trends over a 20-year period from 1987 to 2007 in surface ozone at the atmospheric research station, Mace Head, Ireland. Atmospheric Environment, **39**, 9091-9098.

Derwent, R., Witham, C., Redington, A., Jenkin, M., Stedman, J.,Yardley, R., Hayman, G., (2009). Particulate matter at a rural location in southern England during 2006: model sensitivities to precursor emissions. Atmospheric Environment 43, 689–696

Derwent, RG, M E. Jenkin, S R. Utembe, D E. Shallcross, T P. Murrells, N R. Passant (2010a). Secondary organic aerosol formation from a large number of reactive man-made organic compounds. Science of the Total Environment 408 (2010) 3374–3381

Derwent, RG, C.S. Witham, S. R. Utembe, M. E. Jenkin and N. R. Passant (2010b). Ozone in Central England: the impact of 20 years of precursor emission controls in Europe. Environmental Science & Policy 13 (2010) 195-204.

Dillon, T. J., and Crowley, J. N. (2008). Direct detection of OH formation in the reactions of HO_2 with $CH_3C(O)O_2$ and other substituted peroxy radicals, Atmos. Chem. Phys., 8(16), 4877-4889.

Emberson, L.D., D Simpson, J.-P. Tuovinen, M.R. Ashmore and H.M Cambridge (2000). Towards a model of ozone deposition and stomatal uptake over Europe. EMEP/MSC-W Note 6/00, July 2000. http://www.emep.int/index_pollutants.html

Entec (2010). UK Ship Emissions Inventory. Final Report to Defra, November 2010. http://www.airquality.co.uk/reports/cat15/1012131459_21897_Final_Report_291110.pdf

Gelencser, A., May, B., Simpson, D., Sanchez-Ochoa, A., Kasper-Giebl, A., Puxbaum, H., Caseiro, A., Pio, C., Legrand, M., 2007. Source apportionment of $PM_{2.5}$ organic aerosol over Europe: Primary/secondary, natural/anthropogenic, and fossil/biogenic origin. Journal of Geophysical Research 112, D23S04, doi:10.1029/2006JD008094.

Hasson, A. S., Tyndall, G. S. and Orlando, J. J. (2004). A product yield study of the reaction of HO_2 Radicals with ethyl peroxy ($C_2H_5O_2$), acetyl peroxy ($CH_3C(O)O_2$), and acetonyl peroxy ($CH_3C(O)CH_2O_2$) radicals, J. Phys. Chem. A, 108(28), 5979-5989.

Hayman, G.D., J. Abbott, C. Thomson, T. Bush, A. Kent, RG Derwent, ME Jenkin, MJ Pilling, A. Rickard and L. Whitehead, (2006a) "*Modelling of Tropospheric Ozone*". Final Report (AEAT/ENV/R/2100 Issue 1) produced for the Department for Environment, Food and Rural Affairs and the Devolved Administrations on Contract EPG 1/3/200

Hayman, G.D., Y Xu, J. Abbott, T. Bush, (2006b) "*Modelling of Tropospheric Ozone"*. Report on the Contract Extension produced for the Department for Environment, Food and Rural Affairs and the Devolved Administrations on Contract EPG 1/3/200, AEA Report AEAT/ENV/R/2321 Issue 1, October 2006.

Hayman, G.D., J. Abbott, T.J. Davies, C.L. Thomson, M.E. Jenkin, R. Thetford and P. Fitzgerald (2010). The ozone source–receptor model – A tool for UK ozone policy. Atmospheric Environment, 44(34), 4283-4297.

Hofzumahaus, A.; Rohrer, F.; Lu, K. D.; Bohn, B.; Brauers, T.; Chang, C. C.; Fuchs, H.; Holland, F.; Kita, K.; Kondo, Y.; Li, X.; Lou, S. R.; Shao, M.; Zeng, L. M.; Wahner, A.; Zhang, Y. H. (2009). Amplified trace gas removal in the troposphere. Science, 324, 1702.

IIASA (2010). Scope for further environmental improvements in 2020 beyond baseline projections. Background paper for the 47th Session of the Working Group on Strategies and Review of the Convention on Long-range Transboundary Air Pollution Geneva, August 30 – September 3 2010. CIAM Report 1/2010. http://www.unece.org/env/documents/2010/eb/wg5/wg47/Informal%20documents/Info.%20doc%208_CIAM%20report%201-2010_v2.pdf

Jaoui, M., Leungsakul, S. and Kamens, R.M. (2003). Gas and particle products distribution from the reaction of β-caryophyllene with ozone. Journal of Atmospheric Chemistry, 45, 261–287.

Jenkin, M.E. (2004). Analysis of sources and partitioning of oxidant in the UK-Part 1: the NOx-dependence of annual mean concentrations of nitrogen dioxide and ozone. Atmospheric Environment, **38**, 5117–5129.

Jenkin, M. E., Hurley, M. D. and Wallington, T. J. (2007). Investigation of the radical product channel of the $CH_3C(O)O_2 + HO_2$ reaction in the gas phase, Phys. Chem. Chem. Phys., 9(24), 3149-3162.

Jenkin M.E. and Clapp L.J. (2008). Spatial trends in background oxidant in the UK. Briefing note on contract AQ0704, April 2008.

Jenkin, M.E., Watson, L.A., Utembe, S.R., Shallcross, D.E. (2008a). A Common Representative Intermediates (CRI) mechanism for VOC degradation. Part 1: gas phase mechanism development. Atmospheric Environment 42, 7185–7195. doi:10.1016/j.atmosenv.2008.07.028.

Jenkin, M. E., Hurley, M. D. and Wallington, T. J. (2008b). Investigation of the radical product channel of the $CH_3C(O)CH_2O_2 + HO_2$ reaction in the gas phase, Phys. Chem. Chem. Phys, 10(29), 4274-4280.

Johnson D., Utembe S.R., Jenkin M.E., Derwent R.G., Hayman G.D, Alfarra M.R., Coe H. and McFiggans G. (2006). Simulating regional scale secondary organic aerosol formation during the TORCH 2003 campaign in the southern UK. Atmospheric Chemistry and Physics, **6**, 403-418.

Jones K.H. (2002). The determination of regionalised wind roses for the UK, for use with the HARM acid depositional model. MSc thesis, University of Edinburgh, September 2002.

Jönsson M. and Anderson P. (2007). Emission of oilseed rape volatiles after pollen beetle infestation; behavioural and electrophysiological responses in the parasitoid *Phradis morionellus*. Chemoecology, 17, 201-207.

Jorand, F., Heiss, A., Perrin, O., Sahetchian, K., Kerhoas, L. and Einhorn, J. (2003). Isomeric hexyl-ketohydroperoxides formed by reactions of hexoxy and hexylperoxy radicals in oxygen, Int. J. Chem. Kinet., 35(8), 354-366.

Kanawati, B, Herrmann, F., Joniec, S., Winterhalter, R. and Moortgat, G.K. (2008). Mass spectrometric characterization of β-□caryophyllene ozonolysis products in the aerosol studied using an electrospray triple quadrupole and time-of-flight analyzer hybrid system and density functional theory. Rapid Commun. Mass Spectrom., 22, 165–186.

Kent, A. J. and Stedman, J. R. (2008) UK air quality modelling for annual reporting 2006 on ambient air quality assessment under Council Directives 96/62/EC and 2002/3/EC relating to ozone in ambient air. AEA Report AEAT/ENV/R/2499

Lelieveld, J., Butler, T. M., Crowley, J. N., Dillon, T. J., Fischer, H., Ganzeveld, L., Harder, H., Lawrence, M. G., Martinez, M., Taraborrelli, D. and Williams, J (2008).: Atmospheric oxidation capacity sustained by a tropical forest, Nature, 452(7188), 737-740, 2008

Liu, Z.G., Berg, D.R., Vasys, V.N., Dettmann, M.E., Zielinska, B., Schauer, J.J., 2010. Analysis of C_1, C_2 and C_{10} through C_{33} particle-phase and semi-volatile organic compound emissions from heavy-duty diesel engines. Atmospheric Environment 44, 1108-1115.

Martinez, M., Harder, H., Kovacs, T. A., Simpas, J. B., Bassis, J., Lesher, R., Brune, W. H., Frost, G. J., Williams, E. J. and Stroud, C. A (2003).: OH and HO_2 concentrations, sources, and loss rates during the Southern Oxidants Study in Nashville, Tennessee, summer 1999, J. Geophys. Res, 108, 4617, 2003

Murrells, T.P., Cooke, S., Kent, A., Grice, S., Derwent, R.G., Jenkin, M., Pilling, M.J., Rickard, A. and Redington, A (2008). "*Modelling of Tropospheric Ozone. First Annual*

Report" produced for The Department for Environment, Food and Rural Affairs, Welsh Assembly Government, the Scottish Executive and the Department of the Environment for Northern Ireland under Contract AQ03508, AEA Report AEAT/ENV/R/2567, January 2008.

Murrells, TP, S Cooke, A Kent, S Grice, A Fraser, C Allen, RG Derwent, M Jenkin, A Rickard, MJ Pilling, M Holland, S Utembe (2009a). Modelling of Tropospheric Ozone - Project Summary Report: 2007-2009. Report for The Department for Environment, Food and Rural Affairs, Welsh Assembly Government, the Scottish Executive and the Department of the Environment for Northern Ireland. AEA Report AEAT/ENV/R/2899 (October 2009)

Murrells, TP, S Cooke, A Kent, S Grice, A Fraser, C Allen, RG Derwent, M Jenkin, A Rickard, M Pilling, M Holland (2009b). *Modelling of Tropospheric Ozone: Annual Report 2008*. Report for The Department for Environment, Food and Rural Affairs, Welsh Assembly Government, the Scottish Executive and the Department of the Environment for Northern Ireland. AEA Report AEAT/ENV/R/2748, February 2009.

Nguyen, T.L., Winterhalter, R., Moortgat, G.K., Kanawati, B., Peeters, J. and Vereecken, L. (2009). The gas-phase ozonolysis of β-caryophyllene ($C_{15}H_{24}$). Part II: a theoretical study. Phys. Chem. Chem. Phys., 11, 4173–4183.

Owen S.M., Boissard C. and Hewitt C.N. (2001). Volatile organic compounds (VOCs) emitted from 40 Mediterranean plant species: VOC speciation and extrapolation to habitat scale. Atmospheric Environment, **35**, 5393-5409.

Pankow J.F. (1994). An absorption model of gas/particle partitioning involved in the formation of secondary organic aerosol. Atmospheric Environment, **28**, 189–193.

Paulot, F., Crounse, J. D., Kjaergaard, H. G., Kürten, A., St. Clair, J. M., Seinfeld, J. H. and Wennberg, P. O. (2009). Unexpected epoxide formation in the gas-phase photooxidation of isoprene. Science, 325, 730-733.

Peeters, J., Nguyen, T. L. and Vereecken, L. (2009). HOx radical regeneration in the oxidation of isoprene, Phys. Chem. Chem. Phys., 28, 5935-5939.

Perrin, O., Heiss, A., Doumenc, F. and Sahetchian, K. (1998). Determination of the isomerization rate constant $HOCH_2CH_2CH_2CH(OO.)CH_3 \rightarrow HOC.HCH_2CH_2CH(OOH)CH_3$. Importance of intramolecular hydroperoxy isomerization in tropospheric chemistry. J. Chem. Soc. Faraday Trans., 94, 2323–2335.

PORG (1997). Ozone in the United Kingdom. Fourth report of the UK Photochemical Oxidants Review Group, Department of the Environment, Transport and the Regions, London. Published by Institute of Terrestrial Ecology, Bush Estate, Penicuik, Midlothian, EH26 0QB, UK. ISBN: 0-870393-30-9, and available at www.aeat.co.uk/netcen/airqual/reports/home.html.

Pugh, T. A. M., MacKenzie, A. R., Langford, B., Nemitz, E., Misztal, P. K., and Hewitt, C. N (2010).: The influence of small-scale variations in isoprene concentrations on atmospheric chemistry over a tropical rainforest, Atmos. Chem. Phys. Discuss., 10, 18197-18234, 2010

Ren, X., Olson, J. R., Crawford, J. H., Brune, W. H., Mao, J., Long, R. B., Chen, Z., Chen, G., Avery, M. A. and Sachse, G. W (2008).: HOx chemistry during INTEX-A 2004: Observation, model calculation, and comparison with previous studies, J. Geophys. Res., 113, D05310, doi:10.1029/2007JD009166, 2008

Sakulyanontvittaya, Y., Guenther, A., Hlmig, D., Milford, J., and Wiedinmeyer, C. (2008). Secondary organic aerosol from sesquiterpene and monoterpene emissions in the United States. Environmental Science and Technology 42, 8784-8790.

Saunders S.M., Jenkin M.E., Derwent R.G. and Pilling M.J (2003). Protocol for the development of the Master Chemical Mechanism, MCM v3 (Part A): tropospheric degradation of non-aromatic volatile organic compounds. Atmospheric Chemistry and Physics, **3**, 161-180.

Shu, Y. and Atkinson, R.: Rate constants for the gas-phase reactions of O_3 with a series of terpenes and OH radical formation from the O_3 reactions with sesquiterpenes at 296 ± 2 K. International Journal of Chemical Kinetics, 1994, 26, 1193–1205.

Simpson D, H. Fagerli, J.E. Jonson, S. Tsyro, P. Wind, and J. -P. Tuovinen (2003), Transboundary acidification and eutrophication and ground level ozone in Europe: Unified EMEP Model Description, EMEP Status Report 1/2003 Part I, EMEP/MSC-W Report, The Norwegian Meteorological Institute, Oslo, Norway,August 2003. http://www.emep.int/publ/reports/2003/emep_report_1_part1_2003.pdf

Stewart, H.E., Hewitt, C.N., Bunce, R.G.H., Steinbrecher, R., Smiatek, G., Schoenemeyer, T. (2003). A highly spatially and temporally resolved inventory for biogenic isoprene and monoterpene emissions: Model description and application to Great Britain. Journal of Geophysical Research 108, D20, 4644, doi:10.1029/2002JD002694.

Tan, D., Faloona, I., Simpas, J. B., Brune, W., Shepson, P. B., Couch, T. L., Sumner, A. L., Carroll, M. A., Thornberry, T. and Apel, E (2001).: HOx budgets in a deciduous forest: Results from the PROPHET summer 1998 campaign, J. Geophys. Res., 106, D20, doi:10.1029/2001JD900016, 2001

Thornton, J. A.; Wooldridge, P. J.; Cohen, R. C.; Martinez, M.; Harder, H.; Brune,W. H.; Williams, E. J.; Roberts, J. M.; Fehsenfeld, F. C.; Hall, S. R.; Shetter, R. E.; Wert, B. P.; Fried, A. J. Geophys. Res. 2002, 107(D12), 4146. doi:10.1029/2001JD000932.

Utembe, S.R., Watson, L.A., Shallcross, D.E. and Jenkin, M.E. (2009). A Common Representative Intermediates (CRI) mechanism for VOC degradation. Part 3: Development of a secondary organic aerosol module. Atmospheric Environment, 43, 1982–1990.

Walker, H.L., Derwent, R.G., Donovan, R., Baker, J., 2009. Photochemical trajectory modelling of ozone during the summer PUMA campaign in the UK West Midlands. Science of the Total Environment 407, 2012-2023.

Watson, L.A., Shallcross, D.E., Utembe, S.R., Jenkin, M.E. (2008). A Common Representative Intermediates (CRI) mechanism for VOC degradation. Part 2: gas phase mechanism reduction. Atmospheric Environment 42, 7196–7204. doi:10.1016/j.atmosenv.2008.07.034

Winterhalter, R., Herrmann, F., Kanawati, B., Nguyen, T.L., Peeters, J., Vereecken, L. and Moortgat, G.K. (2009): The gas-phase ozonolysis of β-caryophyllene ($C_{15}H_{24}$). Part I: an experimental study. Phys. Chem. Chem. Phys., 2009, 11, 4152–4172.

Yin, J., Harrison, R.M., Chen, Q., Rutter, A., Schauer, J.J., 2010. Source apportionment of fine particles at urban background and rural sites in the UK atmosphere. Atmospheric Environment 44, 841-851

The Gemini Building
Fermi Avenue
Harwell International Business Centre
Didcot
Oxfordshire
OX11 0QR

Tel: 0870 190 1900
Fax: 0870 190 6318

www.aeat.co.uk